UNIVERSITA' DEGLI STUDI DI FIRENZE

SCUOLA DI DOTTORATO IN PEDIATRIA CLINICA E PREVENTIVA

XXI CICLO

AREA DISCIPLINARE BIO/12

Dipartimento di Scienze Biochimiche

ROLE OF OXIDATIVE STRESS IN ISCHEMIA/REPERFUSION INJURY AND HUMAN HEART FAILURE

Supervisori **Prof. Paolo Antonio Nassi**

Prof.ssa Chiara Nediani

Candidato **Dr.ssa Elisabetta Borchi**

CONTENTS

CHAPTER 1 INTRODUCTION

Ai miei genitori

CHAPTER 1

INTRODUCTION

1. 1. Cardiovascular diseases and heart failure

Cardiovascular diseases (CVDs) are a group of heart and blood vessels disorders which includes coronary heart and cerebrovascular disease - or stroke - (diseases of the blood vessels supplying the heart muscle or the brain, respectively), peripheral artery disease (disease of the blood vessels supplying arms and legs), rheumatic heart disease (damage to the heart muscle and heart valves from rheumatic fever, caused by streptococcal bacteria), congenital heart disease (CHD, malformations of heart structure existing at birth), hypertension (high blood pressure), and heart failure (HF). As reported by the World Health Organization (WHO), CVDs are the leading causes of mortality in the World, occurring equally in men and women. They are no longer diseases of the developed Countries: to date, about 80% of all cardiovascular disease deaths worldwide take place in developing, low and middle-income Countries. It is has been estimated by the WHO that by 2015, CVDs will be the leading cause of death in developing Countries, interesting almost 20 million people.

The most relevant causes of cardiovascular diseases are known as “modifiable risk factors” and include unhealthy diet, physical inactivity and tobacco use. The consequences of unhealthy diet and physical inactivity, called “intermediate risk factors”, are increases in blood lipid and glucose contents and obesity.

The major biological risk factors for CVDs are high blood pressure, high blood cholesterol, overweight and obesity, and the chronic disease of type 2 diabetes. A condition of great importance, among cardiovascular diseases, is represented by heart failure. Common causes of HF include myocardial infarction and other forms of ischemic heart disease, hypertension, valvular heart disease and cardiomyopathies[1]. A

failing heart is characterised by a pathological structure or function which reduces its ability to supply the body with a sufficient blood flow. Heart failure can be categorised taking into account different aspects of the disease, for example:

1) the myocardial portion interested (left heart failure or right heart failure);
2) whether the abnormality is due to a myocardial contraction (systolic dysfunction) or relaxation (diastolic dysfunction);
3) whether the problem is primarily an increased venous back pressure to the heart (backward failure), or a failure to supply adequate arterial perfusion from the heart (forward failure);
4) the degree of functional impairment conferred by the failure.

The main functional classification is the New York Heart Association (NYHA) Functional Classification[2], which takes into account the following four classes of HF:

Class I: no limitation is experienced in any activities; there are no symptoms from ordinary activities;

Class II: slight, mild limitation of activity; the patient is comfortable at rest or with mild exertion;

Class III: marked limitation of any activity; the patient is comfortable only at rest;

Class IV: any physical activity brings on discomfort and symptoms occur at rest.

This score documents severity of symptoms, and can be used to assess response to treatment. The American College of Cardiology (ACC)/American Heart Association (AHA) working group in 2005 introduced a new classification of HF[3], based on four failure stages:

Stage A: Patients at high risk for developing HF in the future but no functional or structural heart disorder;

Stage B: a structural heart disorder but no symptoms at any stage;

Stage C: previous or current symptoms of heart failure in the context of an underlying structural heart problem, but managed with medical treatment;

Stage D: advanced disease requiring hospital-based support, a heart transplant or palliative care.

The Stage A, which describes a pre-heart failure condition when treatments presumably prevent the progression to effective symptoms, lacks a corresponding NYHA class; ACC Stage B would correspond to NYHA Class I, ACC Stage C

corresponds to NYHA Class II and III and ACC Stage D overlaps with NYHA Class IV.

In the present study we have pointed out attention on two of the principal causes leading to the onset of heart failure: the presence of cardiomyopathies and the ischemic damage due to post-ischemic reperfusion injury.

1. 1. 1. Dilated cardiomyopathy

Dilated cardiomyopathy (DCM), also known as congestive cardiomyopathy, is the most common form of cardiomyopathy and it is more frequent in men, occurring also in children. It is a condition in which the heart becomes weakened and enlarged, and can not pump blood efficiently. The decreased heart function can affect the lungs, the liver, and other body systems. In DCM a portion of myocardium is dilated and the left and/or right systolic pump function of the heart is impaired. This leads to a progressive hypertrophy and to the complex process known as cardiac remodelling, a whole of structural and functional alterations in the heart which arises also from chronic pressure overload, chronic volume overload or myocardial infarction (MI).

It has been estimated that about one in tree cases of congestive heart failure (CHF) is due to dilated cardiomyopathies. The causes leading to the onset of DCM are different, for example it can be due to fibrous change of the myocardium from a previous myocardial infarction, or it can be the late phase of acute viral myocarditis, possibly mediated through an immunologic mechanism[4]. Moreover, alcohol abuse, pregnancy or thyroid disease may lead to a reversible form of DCM. Whenever the causes of DCM remain unknown, this cardiomyopathy is indicated as “idiopathic”. Frequently (in the 20-40% of cases) patients have a familiar form of DCM, showing mutations of gene encoding for cytoskeletal or contractile proteins[5]. In the case of gene mutations, the most common form of transmission of the disease is with an autosomal dominant pattern. The progression of heart failure is associated with left ventricular remodelling, which manifests as gradual increases in end-diastolic and end-systolic volumes, wall thinning, and a change in chamber geometry to a more spherical, less elongated shape. This process is usually associated with a continuous decline in ejection fraction. The concept of cardiac remodelling was initially developed to describe changes which occur in the days and months following myocardial infarction, but it has been

extended to cardiomyopathies of non-ischemic origin, such as idiopathic dilated cardiomyopathy or chronic myocarditis, suggesting common mechanisms for the progression of cardiac dysfunction.

1. 1. 2. Maternally inherited mitochondrial cardiomyopathy

Over the last years, mutations in human mitochondrial deoxyribonucleic acid (mtDNA) have become increasingly recognised as causes of diseases[6,7]. An increasing number of maternally inherited mtDNA point mutations have been described, affecting protein coding, ribosomal ribonucleic acid (mt-rRNA) or, more frequently, transfer ribonucleic acid (mt-tRNA) genes[8]. The majority of reported pathogenic mtDNA mutations are heteroplasmic, a situation in which both the mutated and the wild-type forms of mtDNA are present within the same cell. Homoplasmic mtDNA mutations (in which all copies of the genome are affected) have been reported in association with tissue-specific disease, such as Leber's hereditary optic neuropathy (LHON) and sensorineural hearing loss, affecting protein-encoding[9,10], 12S mt-rRNA[11] and the mt-tRNA$^{Ser(UCN)}$[12] genes. A number of mtDNA point mutations have been described in patients with cardiomyopathy[13,14]. In a recent study of Taylor and colleagues[15], two unrelated families with isolated maternally inherited cardiomyopathy (MIC) with a hypertrophic phenotype due to a homoplasmic point mutation (4300A>G) in the mitochondrial transfer ribonucleic acid isoleucine (mt-tRNA^{Ile}) gene were identified. In both families, the clinical features and associated histochemical and biochemical abnormalities were confined to the heart. Heart tissue from affected family members showed a severe defect in respiratory chain enzyme activity and low steady-state levels of the mature mt-tRNA^{Ile}. Of note, comparably low levels of tRNA^{Ile} were present in skeletal muscle, which failed to show either a biochemical or a clinical defect. The illness had an early onset and an adverse clinical course in both families, with rapid progression of left ventricular hypertrophy to dilation and cardiac failure, necessitating heart transplant in two patients.

Mutations in human mtDNA cause a large variety of multi-system disorders whose main unifying feature is the altered energy homeostasis (for example a reduced adenosine triphosphate [ATP] production). Highly energy-dependent tissues, such as the central nervous system and skeletal and cardiac muscle, are commonly involved[7].

Cardiac dysfunction can occur as the sole or predominant symptom and often takes the form of hypertrophic cardiomyopathy[14]. The molecular events linking mtDNA defects to cardiac hypertrophy are unknown. Studies of experimental models suggest that both energy derangements and increase of mitochondrial-derived reactive oxygen species (ROS) could play a role in the development of cardiac dysfunction in MICs[16,17]. In addition, mitochondrial proliferation, a well recognized compensatory mechanism in mitochondrial disease, could contribute to cardiomyopathic remodelling through mechanical dysfunction[18].

1.1.3. Ischemic heart disease

Ischemic heart disease (IHD) is a pathological condition arising from a myocardial ischemia, due to a reduced blood supply to the heart muscle. Generally IHD is a consequence of coronary artery disease (CAD, imputable to coronary atherosclerosis). Like the others CVDs, it is principally due to smoke, hypercholesterolemia, diabetes and hypertension and its risk increase with age. IHD is more frequent in people who have close relatives with ischemic heart diseases. It is the most common cause of death in Western Countries, and a major cause of hospital admissions.

1. 1. 4. Ischemia/reperfusion injury and cardiac myocytes homeostasis

When the heart undergoes a pathophysiological stress, such as during the ischemic phase of acute myocardial infarction (AMI), a part of cardiac myocytes, the contractile cells of the heart, can die, leading to a reduction in cardiac activity. Though restoration of coronary blood flow to ischemic myocardium (reperfusion phase) clearly represents a prerequisite for myocardial salvage, reperfusion is also able to emphasize ischemic injury, leading to cardiac myocytes irreversible damage and consequent death. As cardiac myocytes are terminally differentiated cells that withdraw from the cell cycle in the perinatal period, the only way the survival myocytes have to redress this condition is to increase cellular size and myofibrillar content by a process known as hypertrophy. Ventricular hypertrophic growth is an adaptation occurring in response to heart dysfunction and it is realized by both a regulation of existing proteins (through phosphorylation or dephosphorylation) and a modification in gene expression with a

subsequent change in new proteins synthesis. In the short term such hypertrophy is beneficial and facilitates survival, but this "compensated" hypertrophy may degenerate, leading to heart failure with its associated morbidity and mortality. A common marker of cardiac myocytes hypertrophy is the increased expression of immediate early genes (IEGs), such as c-*fos*, c-*jun* and *egr1*, and of genes typically expressed in the early development (e.g. genes for myosin heavy chain, MHC, and atrial natriuretic factor, ANF, or B-type natriuretic peptide, BNP)[19]. Moreover, a modification in gene expression pattern is also observed during cardiac myocytes apoptosis.

A range of stimuli promote hypertrophy including Gq protein-coupled receptor (GPCR) agonists (e.g. endothelin-1, ET-1; -adrenergic agonists), receptor protein tyrosine kinase (RPTK) ligands or mechanical stretch/strain[20,21]. Other pathophysiological stimuli promote apoptosis/necrosis, particularly those associated with increase oxidative stress (e. g. in the case of ischemia/reperfusion) but also, for example, death receptor ligands (e.g. Fas ligand) or pro-inflammatory cytokines (e.g. interleukin-1, IL1; tumor necrosis factor, TNF)[22]. However, the effects of specific stimuli are not always well defined and the response of a particular cardiac myocyte to any stimulus, whether apoptosis/necrosis or cell survival with/without hypertrophy, depends on the degree of stress and on the balance of cytoprotective *Vs* pro-death signals/proteins within the cell. Thus, high levels of oxidative stress promote cardiac myocyte necrosis, lower levels induce apoptosis and sub-toxic levels may be cytoprotective or even pro-hypertrophic[23]. Furthermore, healthy cardiac myocytes appear to be resistant to death-inducing signals (e.g. via the death receptor Fas) unless they have been previously compromised (e.g. by ischemia/reperfusion)[24,25]. Moreover, stimuli which promote cardiac myocyte hypertrophy (e.g. phenylephrine, an -adrenergic agonist[19]) or are associated with physiological growth (e.g. insulin[26]) are also cytoprotective[27-29].

The various hypertrophic, survival or death stimuli activate intracellular signalling pathways in cardiac myocytes, leading to changes in protein phosphorylation which elicit the phenotypic changes. For example, GqPCRs (signalling through protein kinase C, PKC) or RPTKs potently activate the extracellular signal-regulated kinases 1 and 2, members of the mitogen-activated protein kinases (MAPKs) family, which are particularly implicated in hypertrophy and/or cytoprotection[19,30,31]. Other MAPKs (e.g.

JNKs; p38-MAPKs, ERK5) are also implicated in cardiac hypertrophy, although JNKs and p38-MAPKs may regulate apoptosis and ERK5 is specifically implicated in the response to gp130 receptor ligands. The calcineurin/NFAT signalling pathway may be a specific hypertrophic signal responding to changes in intracellular Ca^{2+}[30,32]. As in other cells, activation of phosphoinositide 3-kinase (PI3K) and protein kinase B (PKB) in cardiac myocytes (e.g. in response to insulin) is potently cytoprotective[33]. Notably, many of these same signalling pathways are activated by pro-apoptotic stresses. For example, oxidative stresses (including ischemia/reperfusion) or pro-inflammatory cytokines activate ERK1/2, JNKs, p38-MAPKs and PKB in cardiac myocytes and the heart[34-37]. Presumably, the precise phenotypic outcome depends on the relative activation and integration of these signals.

Acute insults, such as an ischemic event, are associated with an inflammatory response and alterations in cardiac myocytes gene expression. This condition results in functional, structural and molecular changes that lead to ventricular remodelling[38]. During early inflammatory phase, a rapid induction of interleukin 6 (IL-6) gene has been reported[39,40]. IL-6 is required for the activation of the JAK-STAT pathway and its serum levels have been found increased in a pathological hypertrophic condition. In a very recent study, Sen and co-workers have explored the early and the late inflammatory phase of ischemic-reperfused rat hearts by DNA microarrays[40]. Through such an exhaustive technique, they have evaluated the pattern of some candidate genes implicated in the response against I/R and they have pointed out the necessity of global gene analysis regarding a complex disease such as myocardial infarction. Moreover, Sen and colleagues have documented a rapid induction of IL-18 gene in the early inflammatory phase of reperfusion[40]; IL-18 serum levels have been identified as strong predictors of cardiac mortality in patients affected by coronary artery disease[41]. An increase in endothelial type $gp91^{phox}$ gene (*Cybb*), the catalytic subunit of NADPH oxidase, has been also detected. This observation contributes to explain the well documented increase in ROS production during reperfusion. Caspases-2 (initiator), -3 (effector) and -8 (initiator) are induced after myocardial infarction[40,42]; despite caspase-8 is thought to be required for the growth and development of myocardial cells[43], it has not yet been fully clarified if it plays also a role in post-infarction myocardial remodelling. Collagen type I and III is found to be increased after post-ischemic

reperfusion[40,44]. Collagen, the major extra-cellular matrix protein in the heart, is organized in a complex structure of fibres and represents a crucial target for anti-remodelling and cardioprotective therapy. A great number of both basic research laboratories and clinicians in the World are focusing on the molecular mechanisms leading to heart failure but despite increasing studies on this field, there is still lack of effective protective strategies.

1. 2. Oxidative stress: the balance between reactive oxygen species production and degradation

The mechanisms responsible for the gradual development of CHF in response to MI, sustained pressure overload or other diseases are undoubtedly multifactorial and are the subject of intense investigation[45] performed by many research groups. Over the past 20 years, significant evidence has suggested a role for increased oxidative stress in the pathophysiology of CHF[46]. As a matter of fact, it is well established that patients with CHF show an enhance in oxidative stress (e.g., elevated plasma markers of oxidative stress), which correlates with myocardial dysfunction and the overall severity of heart failure[47,48]. Not only CHF but also its precursors are associated with evidence of increased oxidants production, which appears to contribute to disease pathophysiology. For example, the development of experimental pressure overload LVH or the transition of compensated LVH to failure in rodents are inhibited by antioxidants, supporting a role for reactive oxygen species production in cardiac hypertrophy *in vivo*[49,50]. Similarly, increased oxidants production is implicated in the development of adverse LV remodelling following experimental MI[51,52] and in the onset of heart failure following ischemic and non ischemic cardiomyopathies[53,54].

Reactive oxygen species (ROS) are oxygen-based chemical species characterised by their high reactivity. They include free radicals (species with one or more unpaired electrons), such as superoxide ($O_2^{\cdot -}$) and hydroxyl ($OH^{\cdot}$), and non-radicals capable of generating free radicals, for example hydrogen peroxide (H_2O_2). The balance between ROS production and their removal by antioxidant enzymatic and non enzymatic systems

is responsible of the ‘‘redox state’’ of a cell; a pathological imbalance in favour of a ROS excess is termed oxidative stress.

ROS are normally produced in the cell: a small amount of $O_2^{-\cdot}$ derives as a byproduct from molecular oxygen during mitochondrial oxidative phosphorylation. A family of superoxide dismutase enzymes rapidly converts $O_2^{-\cdot}$ to H_2O_2, which is itself broken down by glutathione peroxidase and catalase to H_2O. However, under pathological conditions, the single-electron reduction of H_2O_2 may lead to the formation of highly reactive OH radicals.

The pathophysiological effects of ROS depend on the type, the concentration and the specific site of production of oxidants. Moreover, the effects exerted in the cardiovascular system may be clustered into the following three types (Fig.1.1):

1) When the local levels of ROS are high, they tend to react with numerous protein centres, DNA, cell membranes and other molecules, causing considerable cellular damage as well as generating other more reactive radicals.
2) At lower concentrations, however, local targeted production of ROS serves as a second-messenger system that transmits biological information through the highly specific modulation of intracellular signalling molecules, enzymes and proteins. This action is known as “redox signalling” function and it is principally performed by H_2O_2, which is more stable and diffusible than superoxide, and by nitric oxide. Redox signalling pathways involve the activation of many signal transduction protein kinases and transcription factors, the stimulation of DNA synthesis and expression of growth-related genes[55,56], and the regulation of myocardial excitation–contraction coupling[57].
3) Finally, the superoxide radical can interact with nitric oxide leading to the formation of peroxynitrite ($ONOO^-$) and to the inactivation of nitric oxide and its biological role in vascular homeostasis and cardiac function modulation. The reaction is especially likely to occur when both $O_2^{-\cdot}$ and nitric oxide levels are high and antioxidant activity is low. Interestingly, although high levels of $ONOO^-$ may induce non-specific toxic effects, at lower levels this species is itself capable of modulating signalling events *in vivo*, thus indicating an additional level of complexity.

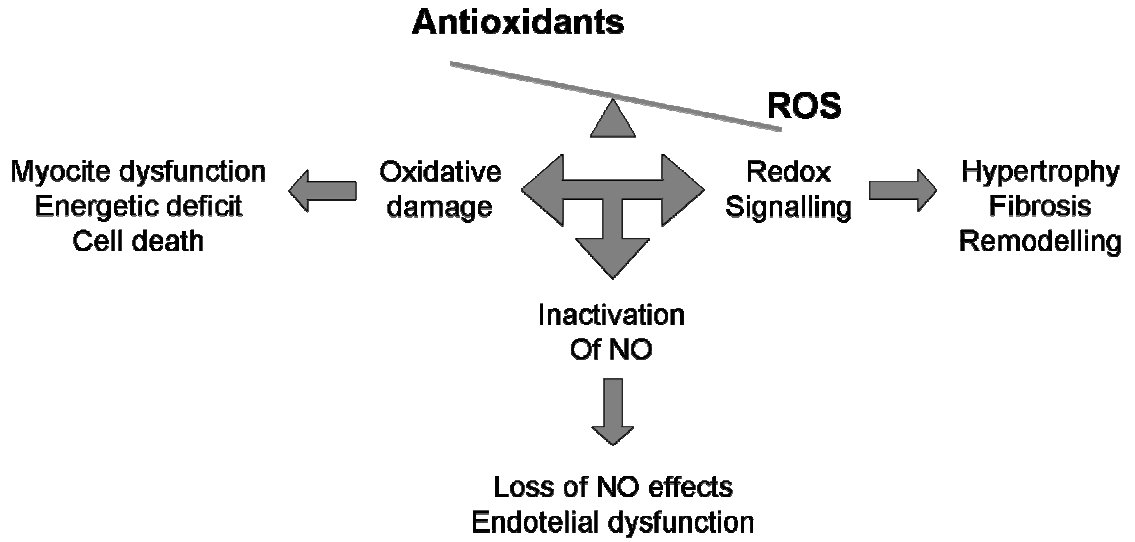

Figure 1.1. The three principal consequences of oxidative stress increase. Effects are reported with regard to the cardiovascular system (modified figure from a review of Seddon M. and colleagues[58]).

There are many potential sources of ROS in CHF, which have varying effects on pathophysiology. Excessive ROS derived from mitochondria have been shown in cardiomyocytes from experimental models of myocardial infarction and rapid pacing-induced heart failure[59]. Xanthine oxidase also produces $O_2^{-\cdot}$ as a byproduct of the terminal steps of purine catabolism and its expression and activity are increased in experimental models of CHF as well as in human end-stage CHF[60]. Nitric oxide synthase enzymes (NOS) normally produce nitric oxide, but they may instead generate $O_2^{-\cdot}$ if they become ‘‘uncoupled’’, a state that is especially likely to occur in the setting of deficiency of the NOS cofactor BH4 or the NOS substrate L-arginine[61]. NOS uncoupling and subsequent $O_2^{-\cdot}$ production are implicated in the genesis of vascular endothelial dysfunction in patients with heart failure[62]. Another important source of ROS and consequent oxidative stress are infiltrating inflammatory cells, especially in conditions such as myocarditis and in the early stages after myocardial infarction. Recent studies have suggested that multimeric enzymes called NADPH oxidases are especially important with regard to redox signalling in CHF and its antecedent conditions[63,64]. These enzymes catalyse electron transfer from NADPH to molecular oxygen, resulting in the formation of $O_2^{-\cdot}$. NADPH oxidase activity has been found

increased in experimental models of LVH and CHF as well as in end-stage failing human myocardium[53,65-67] and in isolated cardiomyocytes subjected to ischemia/reperfusion injury[68]. Interestingly, ROS produced by NADPH oxidases can promote ROS generation by other sources, thereby amplifying their effect. For example, superoxide radical deriving from NADPH oxidase may oxidise and degrade BH4, thereby leading to NOS uncoupling, and this mechanism has been shown in diabetes and experimental hypertension[61]. Similarly, NADPH oxidase-derived ROS may also activate xanthine oxidase[56]. For more detailed elucidations about the NADPH oxidase enzyme structure and role in cardiac disease, see § 1. 3.

In non pathological conditions, cells have a large variety of both enzymatic and non enzymatic antioxidant defences. Briefly, non enzymatic antioxidants are scavenger molecules which can react with radicals leading to less reactive products. Differently from antioxidant enzymes, which have specificity for particular radical compounds (for a more exhaustive description of antioxidant enzymes, see § 1. 4.), non enzymatic antioxidants show a wide range of activity. They may be clustered into water-soluble and liposoluble compounds[69]. Liposoluble antioxidants are vitamin E (α-tocopherol), vitamin A (retinol), β-carotene and ubichinol. Water-soluble antioxidants are vitamin C (ascorbic acid) and thiol compounds like cysteine and glutathione. Moreover, bilirubin and uric acid are important scavengers against radicals. Other important oxidants are proteins like transferrin, ceruloplasmin, and ferritin.

Growing evidence implicates redox-sensitive pathways in the development of cardiac hypertrophy either in response to neurohumoral stimuli or chronic pressure overload. In cultured cardiomyocytes, hypertrophy induced by angiotensin II, endothelin 1, norepinephrine, tumour necrosis factor α or pulsatile mechanical stretch has been shown to involve intracellular ROS production and to be inhibited by antioxidants[64]. *In vivo*, the development of experimental pressure overload LVH in mice or guinea pigs is attenuated by antioxidants, thus implying a role for ROS. Recently, NADPH oxidases have been suggested to be key sources of these ROS. In experimental pressure overload LVH, an increase in NADPH oxidase activity and MAPK activation have been observed[65].

In vitro studies have shown that an increase in ROS production may be responsible of myocyte contractile function impairment, a central feature of CHF.

Contractile dysfunction has a multifactorial basis, involving changes in cardiomyocyte function as well as altered chamber structure and properties. Oxidative stress can act in this context through several mechanisms, including disruption of calcium cycling, altered myofilament responsiveness to calcium, and deleterious effects on cellular metabolism and energetics[57,59,64]. In some cases, xanthine oxidase[60] and NADPH oxidase[70,71] have been suggested to play an important role in this field.

Excessive interstitial fibrosis is another important detrimental aspect of chronic LVH and CHF. Oxidative stress is well known to be profibrotic in many organs and this seems to be also true in the heart, where NADPH oxidase-derived ROS play a central role in this process[70,72]. Multiple underlying mechanisms are likely to be involved in the NOX2-dependent pro-fibrotic effects, including increased expression of pro-fibrotic growth factors and genes, increased activation of NF-kB, activation of matrix metalloproteinases, and inflammatory cell infiltration.

Finally, growing evidence suggests an important role for increased oxidative stress in adverse left ventricular remodelling after myocardial infarction[46]. An increase in oxidative stress after myocardial infarction is well recognised, and in experimental models various antioxidant approaches (e.g., probucol, dimethylthiourea or genetic manipulation) have been shown to ameliorate the adverse remodelling. A significant factor for the detrimental effect of ROS in this setting is the activation of matrix metalloproteinases, which drive matrix turnover and promote left ventricle dilatation. The increase in ROS may be driven by stimuli such as activation of the renin angiotensin system, cytokine activation, local inflammation and mechanical stimuli. The main enzymatic complexes responsible for ROS generation in this context are NADPH oxidase[73] and xanthine oxidase[74].

1. 3. The NADPH oxidase of cardiovascular system

1. 3. 1. Generalities and history

Reduced nicotinamide adenine dinucleotide phosphate (NADPH) oxidase is an enzyme which catalyses the production of superoxide radical ($O_2^{\cdot -}$) from oxygen, using NADPH or NADH - that is why the expression “NAD(P)H” is frequently used - as

electron donor. The enzyme was first identified in professional phagocytes (neutrophils[75], eosinophils, monocytes and macrophages[76]) where it is involved in non-specific host defence against microbes. In the phagocytes the oxidase is normally quiescent but becomes activated during phagocytosis, when it generates high levels of ROS and protons that are involved in the microbicidal process. Among the oxidising agents derived from NADPH oxidase, H_2O_2 is also included as a product of superoxide dismutation[77]. Unlike other sources of ROS, the NADPH oxidases clearly appear to have ROS generation as their primary function.

Historically, a respiratory burst by cells was supposed to exist since the first half of the 20th century, even if the NADPH oxidase was not yet identified. These observations were done in sea urchin eggs, in phagocytes (in 1933)[78], and in spermatocytes (in 1943)[79]. In 1961, Quastel and collaborators[80] showed that the phagocyte respiratory burst led to the generation of hydrogen peroxide. There was a major controversy with regard to the main substrate for the enzyme system, as it could be NADPH or NADH. In 1964, Rossi and Zatti[81] correctly proposed that a NADPH oxidase was responsible for the respiratory burst. Finally, in 1973 and in 1975 respectively, Babior and co-workers reported that the initial product of the respiratory burst oxidase was superoxide and not hydrogen peroxide[82] and that the enzyme was selective for NADPH over NADH by a factor of 100[83].

An important line of study that led to the discovery of the phagocyte NADPH oxidase came in 1957, from a clinical study of Berendes and colleagues[84] who recognized a new and relatively rare syndrome in young boys who suffered from recurrent pyogenic infections that were accompanied with granulomatous reaction, lymphadenopathy, and hypergammaglobulinemia. The genetic disorder is now known as Chronic Granulomatous Disease (CGD). The significance of NADPH oxidase system is now well exemplified by this pathology. CGD causes recurrent and life-threatening infection since the phagocytes are deficient in the superoxide producing activity[85,86]. The lack in superoxide producing activity is due to the deficiency of one of the four phox (phagocytic oxidase) subunits, the components of NADPH oxidase. The disease is characterized by infections which begin very early in life and are frequently fatal[87], although their severity tends to decrease when the patient is over twenty.

In 1978 Segal, Jones, and colleagues[88,89] identified the cytochrome b_{558}, which was missing in the leukocytes of many CGD patients. In the late 1980s, the gene coding for the catalytic subunit of the phagocyte NADPH oxidase, commonly referred to as gp91^{phox}, was cloned by two distinct groups: Royer-Pokora and colleagues[90] and Teahan and colleagues[91]. In the last decade, several homologues of this enzyme have been discovered in numerous other cell types, where they are involved in many different non-phagocytic functions[63,92]. The discovery that non-phagocytic cells also contain superoxide-producing enzymes similar to the phagocyte NADPH oxidase has been accompanied by the observation that several gp91^{phox} homologues are expressed in a variety of tissues. In 1999, on the basis of a BLAST (basic local alignment search tool) search using the protein sequence of gp91^{phox} as a query, Prof. Lambeth and co-workers cloned the cDNA encoding a homologue of gp91^{phox}, initially designated as MOX1 but presently termed NOX1 (NADPH oxidase), which is abundantly expressed in the colon[93]. Afterwards, using a similar strategy, additional homologues were identified by several other groups[94-99]. In particular, a phagocytic-like NADPH oxidase, NOX2 (also known as gp91^{phox}, the core of the classical phagocyte NADPH oxidase) have been found in the cardiovascular system, were it markedly contributes to the ROS production process. NOX2 is expressed in several cell types, like endothelial cells[100-103], cardiomyocytes[72,104], and fibroblasts[105]. The other main isoforms that appear to be important in the cardiovascular system are NOX1, which is expressed in vascular smooth muscle cells (VSMC)[106], and NOX4 which is expressed in endothelial cells[107], cardiomyocytes[108,109], VSMC[110], and fibroblasts[111].

1. 3. 2. Membrane subunits

The structure of the phagocytic NADPH oxidase is quite complex, as this is a multimeric enzymes with two membrane subunits, gp91^{phox} (or NOX2) and p22^{phox}, three cytosolic components, p67^{phox}, p47^{phox} and p40^{phox}, and a low-molecular-weight G protein, either Rac1 or Rac2. The catalytic core of the phagocytic oxidase is the cytochrome b_{558}, which comprises the two membrane subunits. gp91^{phox} is considered to be directly involved in the superoxide production, since it contains binding sites for NADPH, flavine adenine dinucleotide (FAD) and two hemes, which constitute the complete electron-transferring apparatus from NADPH to molecular oxygen. The two

hemes have very low redox potentials and are both hexacoordinate. There are currently five human members identified in the NOX family (NOX1-5), where the founder member gp91^{phox} has been renamed NOX2. Additionally, in humans, two thyroid NADPH oxidases, probably involved in thyroid hormone synthesis, were identified[112-114]. Since the two enzymes contain not only a NADPH oxidase-homology region at the C-terminus but also a peroxidase domain at the N-teminal extracellular region, they have been designated as dual oxidases 1 and 2 (DUOX1 and DUOX2, respectively).

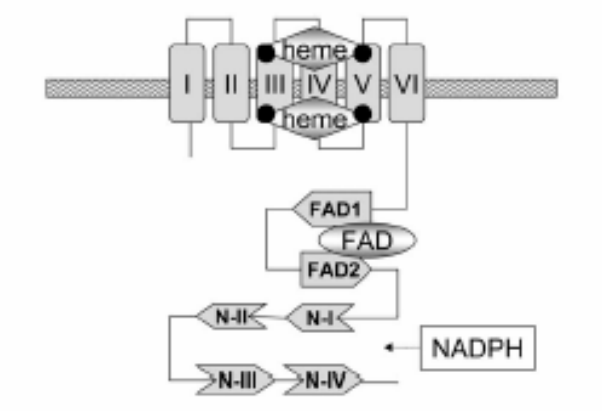

Figure 1.2. The NOX domain (figure from Kawahara T. *et al.*[115]).

The structure of gp91^{phox}/NOX2 has been extensively studied. This protein has four conserved histidines, which ligate two hemes between the 3rd and 5th of six transmembrane (TM) α-helices, and six subregions that fold to provide binding cavities for FAD and NADPH. These canonical regions occupy about 35% of the gp91^{phox}/NOX2 sequence and are grouped together under the definition of NOX domain. However, little is known about essential roles for the other regions. As shown in fig.1.2, all the members of the NOX family expressed a NOX domain containing, from the N-terminal to the C-terminal NOX region, a cluster of six transmembrane α-helices (I through VI, represented with boxes in the figure), two hemes (represented with rhombi in the figure), and six predicted sub-regions that provide binding cavities for a co-enzyme FAD (FAD1 and FAD2) and for the substrate NAD(P)H (N-I, N-II, N-III, and N-IV). In addition, NOX5 and Duoxes present an EF hand-containing calcium-binding domain. Duoxes also show the peroxidase homology domain, as described

above (fig. 1.3). The NOX proteins are expressed in most eukaryotes including vertebrates, urochordates, echinodermates, nematodes, insects, fungi, plants amoeba, and red alga, but not in prokaryotes (from a study of Prof. Lambeth and co-workers[115]).

Figure 1.3. Homology between some NOX/DUOX isoforms (figure from Kawahara T. *et al*.[115]).

The catalytic subunit gp91^{phox}/ NOX2 alone is inactive and must associate with p22^{phox}, whose tail is in the cytosol, to form a non-covalent heterodimer known as flavocytochrome b_{558}. The association between the p22^{phox} subunit and the NOX subunit seems to be important for the stability of the complex as well as for the interactions with other protein-binding partners to assemble the active oxidase.

All NOX/DUOX family members are transmembrane proteins that transport electrons across biological membranes to reduce oxygen to superoxide. The molecular mechanism at the basis of NOX-dependent superoxide production is quite different among all components of the NOX/DUOX family. In particular, tacking into account only mammalian NOX members, there are conserved structural properties of NOX enzymes that are common to all family members (the NADPH-binding site at the C-terminus, the FAD-binding region, six conserved transmembrane domains and four highly conserved heme-binding histidines, two in the third and two in the fifth

transmembrane domain. Given the additional NH_2-terminal transmembrane domain, the histidines are in the fourth and sixth transmembrane domains in DUOX proteins) and most data suggest that all NOX family members must be selective for NADPH over NADH. The following part is a brief description of NOX1-5 and of DUOX1-2.

NOX1

NOX1 was the first homolog of gp91^{phox}/NOX2 to be described[93,116]. NOX1 and NOX2 genes appear to be the result of a relatively recent gene duplication, as the number and the length of the exons is virtually identical between the two genes[116]. Similarly, at the protein level, there is a high degree of sequence identity (of about 60%) between NOX1 and NOX2[93,117,118]. The human and mouse NOX1 genes are located on the X chromosome. Most studies suggest a molecular mass of NOX1 in the range of 55–60 kDa[119-121]. If these values are correct, NOX1 is most likely not *N*-glycosylated, despite the presence of two NXT/S consensus glycosylation sites in the extracellular domains. NOX1 is most highly expressed in colon epithelium[116]; however, it is also expressed in a variety of other cell types, including VSMC[106], endothelial cells[122], uterus[93], placenta[120], prostate[93], osteoclasts[123], retinal pericytes[124], as well as in several cell lines, such as the colon tumor cell lines Caco-2, DLD-1 and HT-29 and the pulmonary epithelial cell line A549 (for a review see Bedard K. and Krause K. H.[125]). In addition to its constitutive expression in a variety of tissues, the NOX1 mRNA is induced under many circumstances. In vascular smooth muscle, platelet-derived growth factor (PDGF), prostaglandin $F_{2\alpha}$, and angiotensin II induce NOX1 expression[106]. Data on the subcellular localization of NOX1 are scarce, mainly because the generation of high quality antibodies against NOX1 (as well as for other NOX isoforms) turned out to be a challenge and some of the antibodies used were not subjected to rigorous validation protocols. Despite this limitation, several studies report a subcellular localization of NOX1; in keratinocytes, there were a weak cytoplasmic and a strong nuclear staining[126]. One study in vascular smooth muscle suggests an endoplasmic reticulum (ER) pattern, while another describes punctuate patches along cell surface membranes, possibly corresponding to a caveolar localization. In studies using a cell-free system, NOX1 is selective for NADPH over NADH as a substrate (for a review see Bedard K. and Krause K. H.[125]). The cytosolic subunits required for NOX1 activation are named

p41^{nox}/NOXO1 (NOX organizer 1, a p47^{phox} homolog) and p51^{nox}/NOXA1 (NOX activator 1, a p67^{phox} homolog)[116,127]. The proteins NOXO1 and NOXA1 exhibit almost the same domain arrangement as the classical p47^{phox} and p67^{phox} (fig. 1.4), and can interact with the target proteins thus-far identified for p47^{phox} or p67^{phox}, except that NOXA1 fails to bind to p40^{phox}.

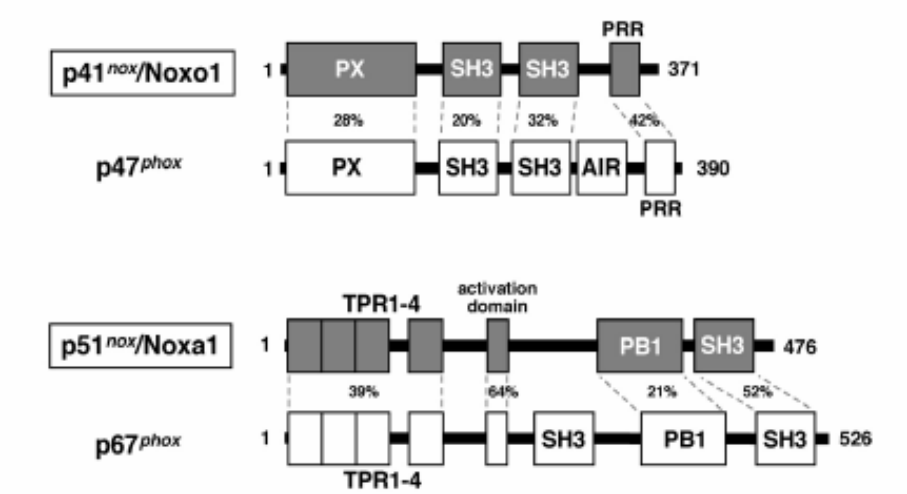

Figure 1.4. Differences and homologies between p47^{phox}/p67^{phox} and NOXO1/NOXA1 subunits (figure from Takeya R. and Sumimoto H.[128]).

NOXO1 interacts via its SH3 domains with p22^{phox}, as p47^{phox} does. In addition, NOXA1 binds, via the N-terminal domain composed of four tetratrico-peptide repeat (TPR) motif, to Rac in a GTP-bound state (fig. 1.5).

Although both novel and classical homologues are capable of activating NOX1 and gp91^{phox}/NOX2, NOXO1 and NOXA1 appear to prefer NOX1; p47^{phox} and p67^{phox}, on the other hand, likely activate gp91^{phox}/NOX2 more efficiently. Consistent with the preference, colon epithelial cells, abundant in NOX1, exclusively express NOXO1 and NOXA1, whereas phagocytes that express large amounts of gp91^{phox}/NOX2 contains solely p47^{phox} and p67^{phox}[116,127]. Differently from what happens in the phagocyte NADPH oxidase, where p47^{phox} and p67^{phox} are able to activate gp91^{phox}/NOX2 only after specific stimuli, NOXO1 and NOXA1 are capable of activating NOX1 and gp91^{phox}/NOX2 without cell stimulation under certain conditions.

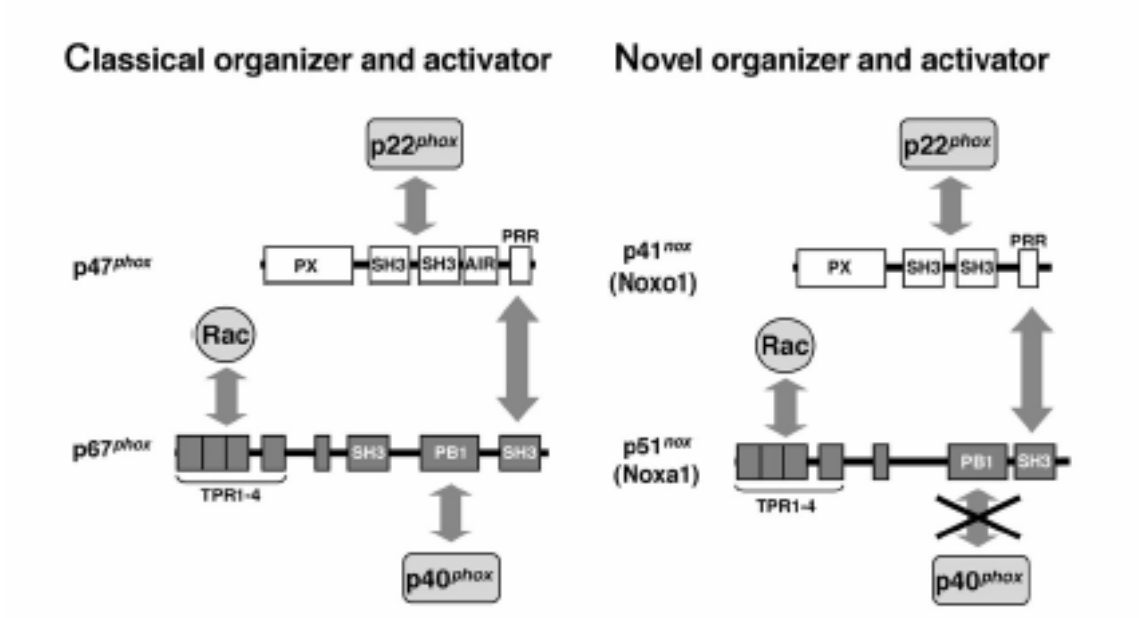

Figure 1.5. Interactions between either p47^{phox}/p67^{phox} or NOXO1/NOXA1 and the other cytosolic subunits (figure from Takeya R. and Sumimoto H.[128]).

Endogenous NOX1 in the colon epithelial adenocarcinoma Caco2 cells spontaneously generate superoxide, when NOXO1 and NOXA1 are co-expressed[129] and both NOX1 and gp91^{phox}/NOX2 are constitutively active in COS-7 or HEK293 cells, which ectopically express a pair of NOXO1 and NOXA1 or a pair of NOXO1 and p67^{phox}[116,127]. On the other hand, when p47^{phox} is expressed instead of NOXO1 in these cells, a stimulus such as phorbol 12-myristate 13-acetate (PMA) is absolutely required for activation of the oxidases. Thus, stimulus-independent activation of NOX1 and gp91^{phox}/NOX2 seems to require NOXO1. In this context, it should be noted that NOXO1does not present a sequence homologous to the AIR region that prevents the SH3 domains of p47^{phox} from interacting with p22^{phox} (for details on the AIR region see § 1. 3. 3.). Indeed the SH3 domains of NOXO1 are considered to be always in an accessible state to its target p22^{phox}, hence the full-length of NOXO1 can bind to p22^{phox}[127], while the full-length of p47^{phox}, in a resting state, can not.

In addition the regulation mechanism of NOX oxidases by NOXA1 is not the same as that by its homologue p67^{phox}. For instance, NOXA1 can not interact with p40^{phox}, a dispensable but significant regulator of the phagocyte oxidase[130]. Hence the regulation mediated via p40^{phox} is not expected in an activation system that uses

NOXA1. The N-terminal SH3 domain of p67*phox* is the most conserved module in this protein[131], albeit its target protein remains unidentified. The absence of this SH3 domain in NOXA1 may suggest a difference between the homologues in oxidase activation.

Moreover, in transfected cells, NOX1 is also able to use the p47*phox* and p67*phox* subunits, suggesting that cytosolic subunits are not specific for a given NOX protein[116]. In addition to its dependence on cytosolic subunits, NOX1 requires the membrane subunit p22*phox*[119], even if this dependence is less forced than that observed for gp91*phox*/NOX2 and NOX3[132]. There is now also evidence for an involvement of the small GTPase Rac in the regulation of NOX1 activity[132]. Rac binds to the TPR domain of the activator subunit NOXA1[133], but in analogy with gp91*phox*/NOX2, Rac activation of NOX1 might be a two step process that also includes a direct binding to NOX1.

NOX2

Most of what is known about the structure of the NOX isoforms is derived from studies on NOX2. Antibody mapping studies demonstrate a cytoplasmic localization of the C-terminus[134]. Sequencing data and antibody mapping confirm a cytoplasmic N-terminus[91]; taken together, the available data suggest that NOX2 has six transmembrane domains and that its COOH-terminus and its NH2-terminus are facing the cytoplasm. Human NOX2 is a highly glycosylated protein (the carbohydrate chains are composed of *N*-acetylglucosamine and galactose and, to a lesser extent, frucose, mannose, and glucose[135]) that appears as a broad smear on SDS-PAGE reflecting the heterogeneity of glycosylation. The fully glycosylated form runs with an apparent molecular mass of 70–90 kDa. Removal of the carbohydrates by endoglycosidase F leaves a protein that runs at 55 kDa, demonstrating the extent of glycosylation[135]. NOX2 constitutively associates with p22*phox*, a subunit which stabilises NOX2 as demonstrated by the observation that phagocytes from p22*phox*-deficient patients have no detectable NOX2 protein (for a review see Bedard K. and Krause K. H.[125]). Activation of NOX2 requires translocation of cytosolic factors to the NOX2/p22phox complex. Once assembled, the complex is active and generates superoxide by transferring an electron from NADPH in the cytosol to oxygen on the luminal or extracellular space. NOX2 can be regarded as a transmembrane redox chain that connects the electron donor, NADPH on the cytosolic side of the membrane with the electron acceptor, oxygen on the outer side of the

membrane. It transfers electrons through a series of steps involving a FAD and two assymetrical hemes, with the inner heme binding to histidines H101 and H209 and the outer heme binding to histidine H115 and H222[136]. In the first step, electrons are transferred from NADPH to FAD, a process that is regulated by the activation domain of p67*phox*. NOX2 is selective for NADPH over NADH as a substrate, with *K*m values of 40–45 μM versus 2.5 mM, respectively[137]. In the second step, a single electron is transferred from the reduced flavin FADH2 to the iron center of the inner heme. Since the iron of the heme can only accept one electron, the inner heme must donate its electron to the outer heme before the second electron can be accepted from the now partially reduced flavin, FADH. The force for the transfer of the second electron, while smaller (31 vs. 79 mV), is still energetically favourable. However, the transfer of the electron from the inner to the outer heme is actually against the electromotive force between these two groups. To create an energetically favourable state, oxygen must be bound to the outer heme to accept the electron[138]. When tissue distribution of total mRNA from various organs is investigated, NOX2 appears to be the most widely distributed among the NOX isoforms. It has been described in a large number of tissues, including thymus, small intestine, colon, spleen, pancreas, ovary, placenta, prostate, and testis (for a review see Bedard K. and Krause K. H.[125]). The message and the protein level for expression of NOX2 have been found in neurons, cardiomyocytes, skeletal muscle myocytes, hepatocytes, endothelial cells, and hematopoietic stem cells (for a review see Bedard K. and Krause K. H.[125]). In phagocytes, NOX2 localizes to both intracellular and plasma membranes in close association with the membrane protein p22*phox*[139]. In resting neutrophils, most of the NOX2 localizes to intracellular compartments, in particular secondary (i.e., specific) granules[139] and tertiary (i.e., gelatinase-containing) granules[140]. Upon phagocyte stimulation, there is a translocation of NOX2 to the surface as the granules fuse with the phagosomal or the plasma membrane[139]. This fusion is thought to be a key event for the microbicidal activity of NOX2. In cells other than phagocytes, the subcellular distribution varies depending on the specific cell type. For example, in smooth muscle cells, NOX2 is found to co-localize with the perinuclear cytoskeleton[141].

The human and mouse NOX2 gene is located on the X chromosome. NOX2 gene expression is inducible. This has been demonstrated in phagocytes in response to

interferon-γ (mRNA), in myofibroblasts after carotid artery injury (mRNA), and in cardiomyocytes after acute myocardial infarction (protein) (for a review see Bedard K. and Krause K. H.[125]). NOX2 expression is also increased in response to angiotensin II in adipose tissue (mRNA), aorta (mRNA), heart (mRNA), resistance artery vascular smooth muscle cells (mRNA and protein), and pancreatic islets (protein) (for a review see Bedard K. and Krause K. H.[125]). An increase in NOX2 levels is not invariably due to transcriptional activation. In the case of resistance arteries, the angiotensin II-induced NOX2 elevation may be due to increased de novo protein synthesis, regulated at a post-transcriptional level[142].

NOX3

NOX3 was described in the very last years[143]. NOX3 shares of about 56% amino acid identity with NOX2. The gene for human NOX3 is located on chromosome 6. NOX3 is a $p22^{phox}$-dependent enzyme; its expression stabilises the $p22^{phox}$ protein[144] and leads to $p22^{phox}$ translocation to the plasma membrane[133]. In functional studies, $p22^{phox}$ is required for NOX3 activation[144], and truncated $p22^{phox}$ inhibits ROS generation by NOX3[145]. In the absence of cytosolic subunits, heterologously expressed NOX3 was found to be inactive[146], weakly active[143], or substantially active[144]. An enhanced activation of NOX3 in the presence of NOXO1 was found in all studies[143]. *In vivo* studies have demonstrated that inactivation of NOXO1 mimics the phenotype of NOX3-deficient mice[147]. The results on the requirement for NOXA1 are contradictory: while some studies found enhancement of NOX3 activity through NOXA1[143], others did not[144]. Thus the results of heterologous expression studies depend on the experimental conditions, and *in vivo* data with NOXA1-deficient animals will be necessary to clarify the issue. In heterologous expression studies, $p47^{phox}$ and $p67^{phox}$ are capable of activating NOX3[143]. The Rac dependence of NOX3 is also still unclear. Two studies suggest a Rac independence[144], while the results of a third study suggest an effect[133]. The differences in the findings may be due to a less strict requirement for Rac in NOX3 activation, or to the presence of endogenous Rac in the cells in which Rac independence was found. Biochemical evidence suggest a constitutive activation of the NOX3 superoxide-generating system, infact NOXO1, the key subunit for NOX3 activation, constitutively activates NOX3 in reconstituted systems. However, the reason of such a

constitutively active ROS-generating system is much less clear from a physiological point of view and *in vivo* studies will be necessary to clarify the point.

NOX4

NOX4 was originally identified as a NADPH oxidase homolog highly expressed in the kidney[98]. NOX4 shares only about the 39% identity to NOX2. The gene for human NOX4 is located on chromosome 11. NOX4 antibodies recognise two bands, one of 75–80 kDa and a second of 65 kDa from both endogenous NOX4-expressing cells (smooth muscle and endothelium) and NOX4-transfected Cos7 cells[98]. The subcellular distribution of the two bands is distinct[148]. The fact that two molecular masses are detected and that NOX4 contains four putative *N*-glycosylation sites might suggest that NOX4 is glycosylated, although treatment with *N*-glycosidase F failed to reduce the protein to a single band[98]. In addition to its strong expression in the kidney, NOX4 mRNA is also found in osteoclasts, endothelial cells, smooth muscle cells, hematopoietic stem cells, fibroblasts, keratinocytes, melanoma cells, and neurons (for a review see bedard K. and Krause K. H.[125]). Moreover, Nox4 protein appears to be the most widely expressed isoform, being found in endothelial cells[107], cardiomyocytes[149] and fibroblasts[150,151].

Induction of NOX4 mRNA expression is observed in response to endoplasmic reticulum stress, shear stress, carotid artery injury, hypoxia and ischemia, and transforming growth factor (TGF)-β1 and TNF-α stimulation of smooth muscle (for a review see bedard K. and Krause K. H.[125]). Up-regulation of NOX4 (mRNA and protein) has been reported in response to angiotensin II[152]. The angiotensin II-induced up regulation of NOX4 mRNA was prevented by pigment epithelium-derived factor (PEDF)[152]. Down regulation of NOX4 mRNA and protein is observed in response to PPAR-γ ligands[153]. In vascular smooth muscle, NOX4 is described in proximity to focal adhesions[148], while in transfected cells, NOX4 localization is mostly observed in the ER. While a functional role for NOX4 in the ER is entirely possible, this localization may also represent an accumulation at its site of synthesis. In vascular smooth muscle and endothelial cells NOX4 expression in the nucleus is suggested by several lines of arguments (immunofluorescence, electron microscopy, nuclear Western blots, and nuclear ROS generation)[148]. It is however difficult to understand how a protein that

spans the membrane six times can be found in a presumably membrane-free space, such as the interior of the nucleus. NOX4 need $p22^{phox}$ for its ROS generation process[154] (it co-localizes and co-immunoprecipitates with $p22^{phox}$) and it is also able to stabilises the $p22^{phox}$ subunit[119]. $p22^{phox}$ mutants lacking the PRR in the C-terminus are still fully active in supporting NOX4 activity, while such mutants are not sufficient for NOX1, -2, and -3 activation.

Moreover, NOX4 does not require cytosolic subunits for its activity, and upon heterologous expression, it is active without cell stimulation[154]. Yet, at least in some endogenously NOX4-expressing cells, a Rac requirement has been documented[155]. Whether the Rac requirement reflects a direct Rac/NOX4 interaction or is rather indirect remains to be established. NOX4 might be a constitutively active enzyme, but not all available data agree with this hypothesis. The mechanisms responsible for regulating the NOX4 activity remain poorly understood, but it is thought that the enzyme may be constitutively active and that increased activity may be related to an increased protein expression. NOX4 activation is observed in lipopolysaccharide (LPS)-stimulated HEK293 cells[156], in insulin-stimulated adipocytes (569), in angiotensin II- or high glucose-stimulated mesangial cells[155], and in PMA-stimulated vascular endothelial cells (494). Mechanisms of NOX4 activation might include a direct binding of TLR4 to NOX4[156].

NOX5

NOX5 was discovered in 2001 by Cheng and colleagues[95] and Banfi and co-workers[94], separately. The human NOX5 gene is located on chromosome 15. Differently from the other NOX1–4 enzymes, the NOX5 isoforms described by Banfi (NOX5α, -β, -γ, and -δ) showed a long intracellular N-terminus containing two cassettes of EF-hand calcium-binding motif[94,157]. The NOX4 described by Cheng (NOX5ε or NOX5-S) lacks the EF-hand region and therefore has an overall structure more similar to NOX1-4[95]. NOX5 protein gives a band of about 85-kDa on SDS-PAGE. This would be consistent with its predicted molecular mass and suggests that the protein is not glycosylated. As seen for NOX2, NADH cannot replace NADPH as a cytoplasmic electron donor for NOX5[157].
NOX5 mRNA expression is described in testis, spleen, lymph nodes, vascular smooth muscle, bone marrow, pancreas, placenta, ovary, uterus, stomach, and in various fetal

tissues[94,95]. Interestingly, NOX5 mRNA could not be detected within circulating lymphocytes[94]. No data on the tissue distribution or subcellular distribution of the NOX5 protein are available.

Nothing is known about the activation of the EF hand deficient NOX5 ε; thus the activation mechanisms are based on studies using EF hand-containing NOX5 isoforms. NOX5 does not require $p22^{phox}$ for activity, as demonstrated by siRNA suppression of $p22^{phox}$ leading to a decrease in the activity of NOX1 to NOX4, but not of NOX5[145], and it does not require cytosolic organizer or activator subunits[94]. As predicted by the presence of EF hands, activation of NOX5 is mediated by an increase in the cytoplasmic Ca^{2+} concentration[157]. The Ca^{2+}-binding domain of NOX5 behaves as an independent folding unit and undergoes conformational changes in response to Ca^{2+} increase[157]. This is thought to activate the enzyme through an intramolecular protein-protein interaction between the Ca^{2+}-binding region and the catalytic C- terminus of the enzyme[94,157]. Finally, the binding of Ca^{2+} to the N-terminal region may induce a conformational change of Nox5, which allows electron transport from NADPH to molecular oxygen.

DUOX1 and DUOX2

For several novel NOX isoforms, the identification of the protein preceded the definition of its function. In the case of DUOX1 and DUOX2, the situation was reversed. It had been known for a long time that thyroid epithelial cells produce H_2O_2 at the apical plasma membrane in a Ca^{2+}- and NADPH-dependent manner[158]. Researchers in the thyroid field were actively looking for an NADPH oxidase. It took 15 years from the discovery of this function to the identification of DUOX proteins (originally called thyroid oxidase), which were identified from thyroid gland by two groups[112,113]. The genes for both human DUOX isoforms are located on chromosome 15. In addition to a NOX homology domain and two EF-hand regions, DUOX proteins have a seventh transmembrane domain at the N-terminus with an ectofacing peroxidase like domain. Within the NOX backbone, DUOX isoforms share about 50% identity with NOX2[112]. DUOX enzymes are glycosylated. Both DUOX1 and DUOX2 have two *N*-glycosylation states: the high mannose glycosylated form found in the ER, which runs by gel electrophoresis at 180 kDa, and a fully glycosylated form found at the plasma membrane that runs at 190 kDa[159,160]. Carbohydrate content analysis of plasma

membrane DUOX revealed specific oligosaccharides indicative of a Golgi apparatus processing. When totally deglycosylated, the molecular mass of both DUOX1 and DUOX2 drops to 160 kDa[159]. It is not clear whether the peroxidase homology domain of DUOX enzymes functions as a peroxidase. One study suggests that DUOX peroxidase homology domains, when expressed as recombinant proteins, have a peroxidase function[114]. However, the DUOX peroxidase homology domains lack many amino acid residues identified as essential for peroxidase function (for a review see Bedard K. and Krause K. H.[125]). The fact that a peroxidase is usually co-expressed in DUOX expressing systems, e.g., thyroid peroxidase in the thyroid gland and lactoperoxidase in salivary glands, also questions the peroxidase function of DUOX. This is particularly well documented for the thyroid, where thyroid peroxidase deficiency leads to severe hypothyroidism, due to a lack of peroxidase-dependent hormone synthesis[161]. Still, the peroxidase homology region of DUOX2 seems to be of functional importance, as hypothyroidism in patients with mutations in the extracellular domain has been reported[162]. Based on its homology with NOX2 and the fact that heme enzymes are monoelectron transporters, DUOX enzymes should generate superoxide. The substrate selectivity for human DUOX has not been defined; however, the GXGXXPF sequence typical of NADPH over NADH substrate selectivity is conserved. Both DUOX1 and DUOX2 are highly expressed in the thyroid[112,113]. In addition, DUOX1 has been described in airway epithelia and in the prostate (for a review, see Bedard K. and Krause K. H.[125]). DUOX2 is found in the ducts of the salivary gland, in rectal mucosa, all along the gastrointestinal tract including duodenum, colon, and cecum, in airway epithelia, and in prostate (for a review, see Bedard K. and Krause K. H.[125]). Induction of DUOX enzymes has been described; DUOX1 is induced in response to interleukin (IL)-4 and IL-13 in respiratory tract epithelium, while DUOX2 expression was induced in response to interferon-γ in respiratory tract epithelium, in response to insulin in thyroid cell lines, and during spontaneous differentiation of postconfluent Caco-2 cells (for a review see Bedard K. and Krause K. H.[125]). In thyrocytes, DUOX enzymes localize to the apical membrane[112,113], although it appears that substantial amounts are found intracellularly, presumably in the ER[159]. When heterologously expressed, DUOX enzymes tend to be retained in the ER, and superoxide generation can be measured only in broken cell preparations[163]. This

observation led to the discovery of DUOX maturation factors, which are ER proteins termed DUOXA1 and DUOXA2[164]. DUOX maturation factors seem to be crucial in overcoming ER retention of DUOX enzymes. Studies on the activation of heterologously expressed DUOX2 in membrane fractions indicated that the enzyme does not require cytosolic activator or organizer subunits and can be directly activated by Ca^{2+}, suggesting that its EF-hand Ca^{2+}-binding domains are functional[163]; however, the $p22^{phox}$ requirement is still a matter of debate.

A schematic representation of the activation mechanism of all the NOX/DUOX family members is reported in fig. 1.6.

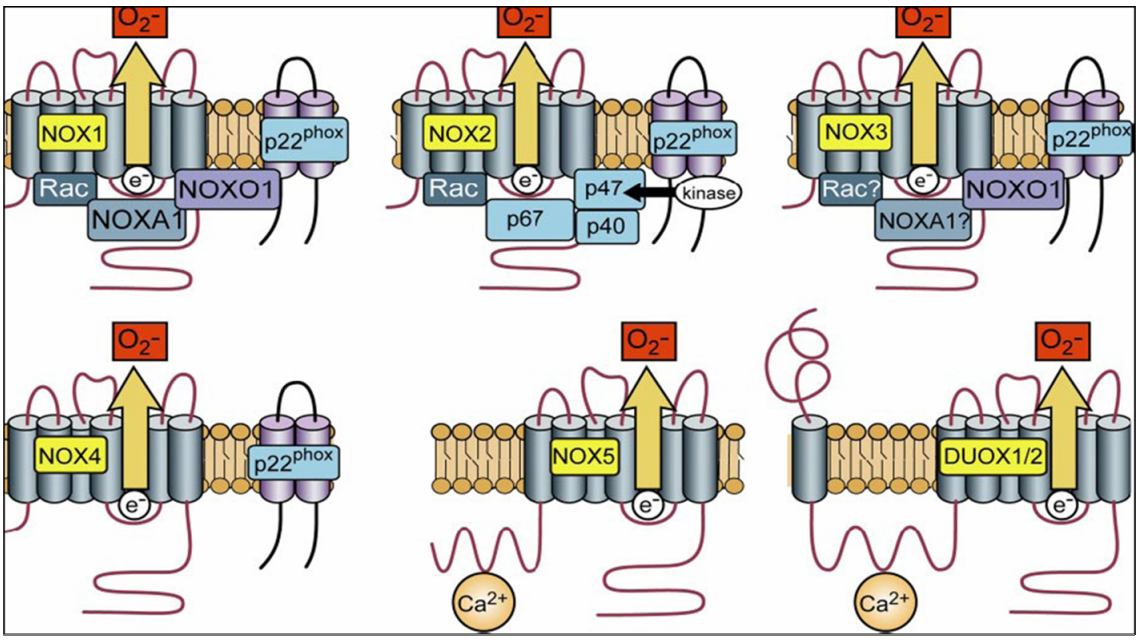

Figure 1.6. Different regulation mechanisms of the members of the NOX/DUOX family (figure from Bedard K. and Krause K. H.[125]).

1. 3. 3. Cytosolic subunits

The oxidase activity must be strictly regulated, since inappropriate or excessive production of superoxide results in inflammatory disorders of surrounding tissues. Indeed $gp91^{phox}$/NOX2 never generates superoxide in resting cells; its activation requires interactions with the cytoplasmic factors Rac and the SH3 domain-containing proteins $p47^{phox}$ and $p67^{phox}$ [85,165]. In stimulated phagocytes these proteins translocate

from the cytosol to the membrane, where they interact with cytochrome b_{558} and thus activate gp91^{phox}/NOX2 (fig. 1.7). p67^{phox} contains two Src homology 3 domains (SH3), one in the middle of the protein and one near the C-terminus; p47^{phox} is the protein that carries all the cytosolic subunits to the membrane. In this process, p47^{phox} translocates to the membrane by itself, whereas p67^{phox} is recruited via p47^{phox}[166,167]: they constitutively associates through the interaction between the C-terminal SH3 domain of p67^{phox} and the C-terminal proline rich region (PRR) of p47^{phox}[168]. p47^{phox} binds the PRR domain of p22^{phox} through its SH3 domains and this interaction is crucial for the oxidase assembly and, consequently, activation[169].

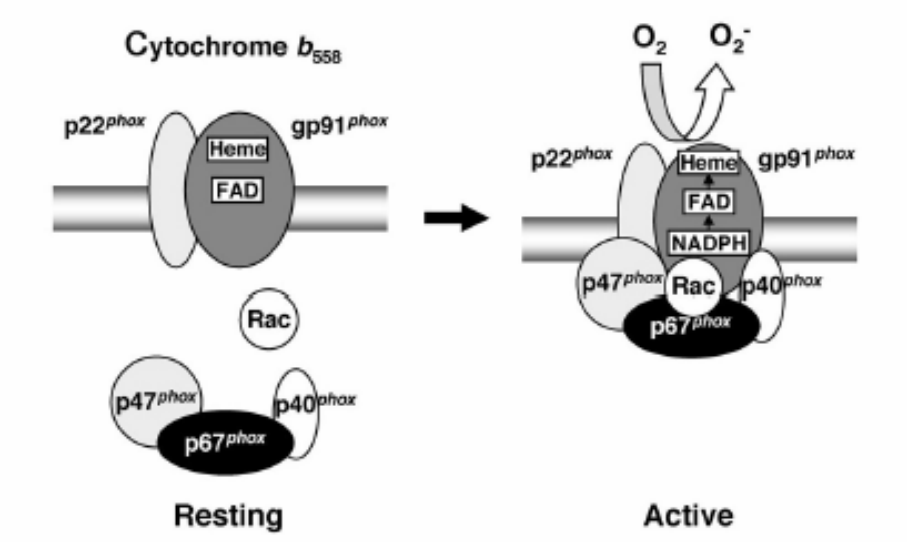

Figure 1.7. Activation mechanism of NOX2/gp91^{phox} (figure from Takeya R. and Sumimoto H.[128])

In the resting state, to avoid superxide production, the SH3 domains of p47^{phox} are normally masked via an intramolecular interaction with an autoinhibitory region (AIR)[170]. In addition to the two SH3 domains, p47^{phox} contains a PX domain in the N-terminus (fig. 1.8): the PX domain is capable of binding to phosphoinositides but the lipid-binding activity is also negatively regulated in resting cells[170]. Upon cell stimulation, p47^{phox} becomes phosphorylated at multiple serines by different protein kinases (including protein kinases B and C). Several of these serines are located in the AIR sequence[171,172]. The phosphorylation induces a conformational change in the

protein structure which allows both the SH3 and the PX domains to be in an accessible state to their membrane targets, $p22^{phox}$ and phosphoinositides, respectively[170,173]. Cooperation of these two interactions, each being indispensable, leads to activation of the phagocyte NADPH oxidase[170]. The main $p67^{phox}$ and $p47^{phox}$ domains are shown in fig. 1.8.

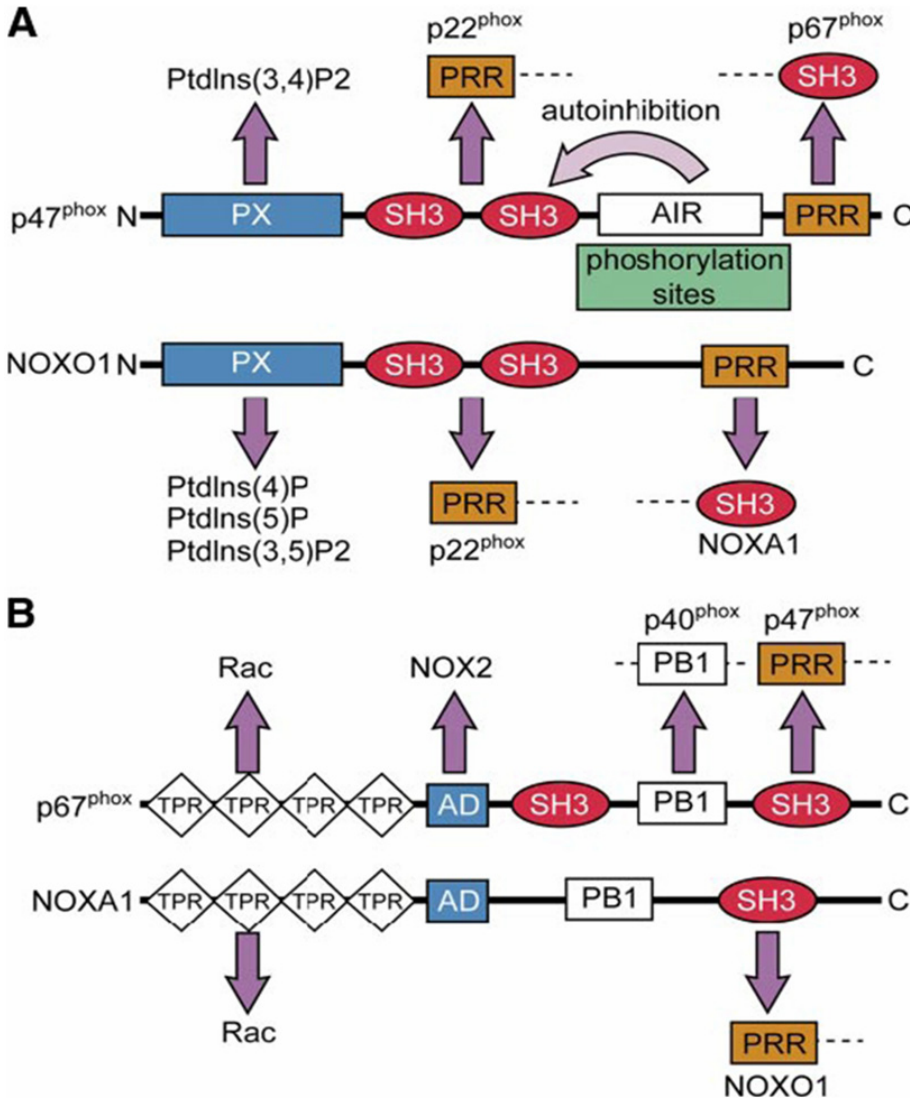

Figure 1.8. The main domains of $p67^{phox}$ and $p47^{phox}$ (figure from Bedard K. and Krause K. H.[125]).

Moreover, Rac is recruited upon cell simulation to the membrane independently of $p47^{phox}$ or $p67^{phox}$[174]. A crucial event for NOX2 activation is the conversion of Rac from

the GDP- to the GTP-binding state. At the membrane, Rac in the GTP-binding state directly interacts with p67^{phox} through the binding to the N-terminal domain which harbors four TPR motifs and thus the Rac/p67^{phox} complex is probably targeted to gp91^{phox}/NOX2 (for a review see Takeya R. and Sumimoto H.[128]), leading to the oxidase activation. In resting cells, this switch is kept "off", preventing the oxidase from producing superoxide. Furthermore, p67^{phox} is known to catalyse the transfer of electrons from NADPH to electron acceptor dyes (but not to oxygen)[175], so it could be directly involved in the electrons transfer process operated by the NADPH oxidase.

The active oxidase can be formed in a cell-free system reconstituted with the purified proteins described above and anionic amphiphiles such as arachidonic acid[85]. In the presence of excess amounts of p67^{phox} and Rac, however, p47^{phox} is not essential for the cell-free activation of the oxidase (for a review see Takeya R. and Sumimoto H.[128]). However, p47^{phox} is essential in neutrophils, since its deficiency in patients leads to CGD, as it occurs in patients who lacks in p67^{phox}, p22^{phox} or gp91^{phox}/NOX2.

There is another factor in the oxidase complex, p40^{phox}, which contains PX, SH3, and PB1 domains[176] and whose function is still unclear. p40^{phox} is supposed to act as an adaptor protein which constitutively associates with p67^{phox} in the cytosol of resting phagocytes, and enhances superoxide production in stimulated cells[130]. Differently from the other NADPH oxidase subunits, p40^{phox} does not seem to be absolutely essential for the oxidase activity, since there is no form of CGD in which it is lacking. Some researcher even suggest an inhibitory function of p40^{phox}[177]. Since p40^{phox} facilitates membrane translocation of both p67^{phox} and p47^{phox,} but not that of Rac[130], it is likely to participate in the activation of the oxidase by regulating membrane recruitment of p67^{phox} and p47^{phox}. This stimulatory effect of p40^{phox} is totally dependent on its binding to p67^{phox}[130], and the binding is mediated through the interaction between the PB1 domains of both proteins[176]. It appears that p67^{phox} should function as an oxidase activator by using its TPR, PB1, and C-terminal SH3 domains to interact with Rac, p40^{phox} and p47^{phox}, respectively.

1. 3. 4. Downstream effects of NADPH oxidase and activating stimuli

NADPH-oxidase-derived ROS exert many downstream effects in the cellular system, which include:

1) alterations in the activity of redox-sensitive protein kinases, such as mitogen-activated protein kinases (MAPKs) and protein kinases B,C, and D, which may occur indirectly following inactivation of tyrosine phosphatases or through direct activation;
2) modifications in the activity of transcription factors, including nuclear factor-kappa B (NF-κB), activating protein-1 (AP-1), hypoxia-inducible factor-1 (HIF-1), and STATs;
3) direct effects on enzymes like matrix metalloproteinases (MMPs), receptors, or ion channels.

NADPH oxidases are specifically activated by diverse agonists that evoke the activation of cellular signal transduction pathways. Agonists and stimuli relevant to myocardial remodelling and heart failure that are also known to activate NADPH oxidases include:

1) G-protein-coupled receptor agonists, e.g. angiotensin II, endothelin-1, and α-adrenergic agonists[100,104,178];
2) growth factors (for example vascular endothelial growth factor (VEGF)[179] and plateled-derived growth factor (PDGF)[180,181]) and insulin[182];
3) cytokines, for example TNF-α [101,183];
4) mechanical forces[184];
5) hypoxia-reoxygenation[185].

Interestingly, since activation of Rac is inhibited by the HMG-CoA reductase inhibitors (for example, statins), inhibition of Rac-requiring NADPH oxidases may be one of the many pleiotropic actions of these drugs.

1. 3. 5. NADPH oxidase in hypertrophy and heart failure

When the heart is subjected to systemic workload, it undergoes structural and functional changes which lead to myocytes size increase and wall-thickness and are described as left ventricular hypertrophy (LVH). This process can be initially considered as an

adaptative response to stress, but if the overload persists, LVH progresses to chronic heart failure, with the well known consequences of interstitial fibrosis, chamber stiffness, LV dilatation, contractile depression and arrhythmia. Similarly, the heart adapts to myocardial infarction by alteration in myocytes, extracellular matrix and chamber properties, in a process known as ventricular remodelling. Also in this case, the process leads to fibrosis, impaired contraction and arrhythmia. In both the processes, an increased activation of the renin-angiotensin-aldosterone system (RAAS) and β-adrenergic system is involved.

Reactive oxygen species production has been demonstrated to play a crucial role in the onset of both LVH and adverse remodelling post-MI[46,186]. Moreover, the hyperetrophy of isolated cardiomyocytes induced by Angiotensin II, endotelin-1 or mechanical forces is reported to involve increased ROS production[46]. Taking into account the role of NADPH oxidase as a ROS-generating system, it is clear the involvement of this enzyme in such heart diseases.

An increasing body of data indicates important roles for NADPH oxidase in LVH and CHF, and well established evidence shows that this enzyme is involved in the pathophysiology of VSM proliferation, angiotensin II-dependent and low renin hypertension, atherosclerosis and angiogenesis, largely through the modulation of redox-sensitive signalling pathways[187-189]. Furthermore, end-stage failing myocardium from human CHF patients exhibits increased NADPH oxidase subunit expression and activity[53,66,67] and, recently, polymorphisms in components of NADPH oxidase were reported to be associated with an increased risk of CHF occurring in response to cytotoxic therapy[190].

NADPH oxidase subunit expression and activity were found to be increased in both cardiomyocytes and endothelial cells in experimental pressure overload LVH in guinea-pigs[65] and in mice[149,191]. The role of NADPH oxidases has recently been investigated more directly by studies employing NOX2 knock out mice. In a model of *in vivo* cardiac hypertrophy induced by short-term (7-14 days) subpressor infusion of angiotensin II, Bendall and colleagues[72] found that increases in heart/body weight ratio, myocytes area and mRNA expression of ANF and hMHC were all markedly inhibited in $NOX2^{-/-}$ mice compared to wild-type controls. This was associated with an absence of Angiotensin II-induced increases in LV NADPH oxidase activity in $NOX2^{-/-}$ mice.

These data suggest an essential role for the NOX2 oxidase in short-term angiotensin II induced cardiac hypertrophy. In keeping with this, angiotensin II-induced signalling and hypertrophy of isolated cardiomyocytes were found to be dependent upon NOX2[192,193] while the small GTP-binding protein Rac1 was reported to be involved in isolated myocyte hypertrophy induced by endothelin1, angiotensin II or phenylephrine.

Byrne and co-workers[149] studied the effects of aortic constriction, as a model of pressure overload, on wild-type and $NOX2^{-/-}$ mice. They found that, in contrast to angiotensin II infusion, both morphological LVH and the associated rises in mRNA expression of molecular markers such as ANF were similar in $NOX2^{-/-}$ and wild-type mice. Interestingly, however, LV NADPH oxidase activity was significantly increased by aortic banding not only in wild-type but also in $NOX2^{-/-}$ mice, which was attributed to an increased expression of the NOX4 isoform in banded $NOX2^{-/-}$ animals. These data suggest that NOX4-derived ROS could contribute to the development of pressure overload-induced LVH whereas NOX2 appears indispensable for the response to short-term angiotensin II infusion.

Nevertheless, further studies suggest that NOX2 has an important role in the development of other aspects of the cardiac phenotype in response to pressure overload. Detailed analyses of LV contractile function by echocardiography and LV conductance pressure–volume measurements in wild-type and $NOX2^{-/-}$ mice subjected to aortic banding showed that $NOX2^{-/-}$ mice were significantly protected against the LV systolic and diastolic dysfunction observed in wild-type animals[70]. This protection against contractile dysfunction was also evident in isolated cardiomyocytes. The signal transduction pathways through which the above effects of NADPH oxidase may be mediated remain to be fully elucidated. Potential redox-sensitive downstream targets that have been shown to be activated by NADPH oxidase-derived ROS in other tissues include RAS, c-src, the MAPKs, the PI3 kinase (PI3K)/Akt pathway, NF-κB, AP-1, HIF-1 and others. Taken together, these data suggest several potential redox-sensitive signalling pathways that may be modulated by NADPH oxidase. However, the precise pathways activated or inhibited in a NOX isoform-specific manner remain the subject of ongoing investigation.

Another well known effect of ROS its their role in fibrosis, a process which involves several aspects such as an increase in fibroblast proliferation, their

transformation into matrix-generating myofibroblasts, the expression of pro-fibrotic genes and alterations in the balance between the activities of MMPs and tissue inhibitors of MMPs (TIMPs). Furthermore, NADPH oxidase has been shown to be involved in MMP activation in the vasculature, e.g., in response to mechanical stretch[194] or angiotensin II[195]. Interestingly, NOX2 also appears to have a pro-fibrotic role in pressure overload LVH since NOX2-deficient mice subjected to aortic banding were found to have reduced interstitial fibrosis compared to banded wild-type animals[70]. The above results suggest an important role for NOX2-containing NADPH oxidase in the development of interstitial cardiac fibrosis. However, the relevant NOX2-expressing cell type that is involved remains unclear. NOX4 is also known to be expressed in cardiac fibroblasts, but its role in mediating *in vivo* cardiac fibrosis has not been addressed to date.

An important role for increased oxidative stress in adverse LV remodelling post-MI is also well recognized. Markers of oxidative stress are elevated post-MI[196] and, in experimental models, various antioxidant approaches (e.g., probucol, dimethylthiourea or genetic manipulation) have been found to ameliorate the adverse remodelling. Post-MI remodelling was also prevented in mice overexpressing glutathione peroxidase[197]. The benefits of these antioxidant approaches extended to an improvement in contractile function and lower mortality. Recently, a role for NOX2 oxidase as a specific source of ROS involved in the above effects has been suggested. The expression of the NADPH oxidase subunits, NOX2 and p22^{phox}, was found to be increased after experimental MI in rats and it was also suggested that the increases correlated with the inflammatory phase of tissue repair[73]. Human myocardium from patients who had died for acute MI was also found to exhibit increases in the expression of cardiomyocitic NOX2 and p22^{phox}[198]. Taking into account the great body of studies present in literature, the implications of NADPH oxidase in many aspects of cardiovascular disease appear evident. The NADPH oxidase-related redox pathways should be completely clarified in order to find out new possible therapies for such complex diseases.

1. 4. Antioxidant enzymes

As reported in the § 1. 2., an important line of defence against ROS is represented by antioxidant enzymes. In mammalian cells, there are three principal enzymes responsible for ROS degradation: superoxide dismutase, which catalyses the dismutation of superoxide radical to hydrogen peroxide, and both the glutathione peroxidase and the catalase, which catalyse the reduction of H_2O_2 to water.

1. 4. 1. Cytosolic and mitochondrial superoxide dismutase

Superoxide dismutases (SODs) are metalloenzymes that catalyse the dismutation of superoxide anion to molecular oxygen and hydrogen peroxide[199,200]. They represent a crucial part of the cellular antioxidant defence mechanism.

Three types of SODs have been described with regard to their metal content: copper/zinc (Cu-Zn), manganese (Mn) and iron (Fe) SODs. In humans, the three form of SODs are differently distributed in the cytosol (Cu-ZnSOD, also named SOD1), in mitochondria (MnSOD, also named SOD2) and in the extracellular space (FeSOD, also named SOD3)[201]. SOD1 is a citosolic homodimeric enzyme of 32 kDa. SOD2 is a homotetrameric enzyme of 25 kDa located in the mitochondrial matrix. The Mn2+ ion is coordinated to three histidine and one aspartate residues. SOD3 is an extracellular homotetrameric enzyme. Extracellular SOD is localised both in the interstitial spaces of tissues and in extracellular fluids, accounting for the majority of the SOD activity in plasma, lymph and synovial fluid[202,203]. Sodium cyanide is usually used as an inhibitor of cytosolic and extracellular SOD[204,205], since it is able to interact with their specific metals. The genes for SO1, SOD2 and SOD3 are located in the chromosomes 21, 6 and 4, respectively.

The amount of SOD in cellular and extracellular environments is crucial for the protection against diseases linked to oxidative stress. Mutation in SOD account for approximately 20% of familiar amyotrophic lateral sclerosis (ALS) cases. SOD appears to be also a key enzyme in the prevention of other neurodegenerative disorders such as Alzheimer's, Parkinson's and Huntington's disease[206,207].

The reaction catalysed by SODs is extremely fast, with a turn over of 2×10^9 M^{-1} sec^{-1} and the presence of sufficient enzymes amounts in cells and tissues typically keeps

the concentration of superoxide very low[208]. When either SOD activity is decreased or absent (i.e. SOD mutations) or NO concentration is increased (i.e. iNOS upregulation), NO outcompetes SOD for superoxide, resulting in the formation of peroxynitrite. The presence of nitrotyrosyne as a "footprint" for peroxynitrite, and hence the prior co-existence of both superoxide and nitric oxide, has been observed in a variety of mediacal conditions, including atherosclerosis, sepsis and ALS[208].

In the heart, MnSOD accounts for about 70% of total SOD activity; this value reach the 90% in cardiac myocytes[209]. Few data are present in literature on SOD activity during the progression to heart failure. The behaviour of SOD had been evaluated in rodent hearts subjected to hemodynamic overload induced by myocardial infarction or aortic constriction. Early after these stimuli, an increase in oxidative stress was followed by enhances in GPx1 and SOD activity. Interestingly, when the hearts of these animals showed sighs of transition to failure, the activity of SOD was decreased allowing a progress to severe heart failure[49,196]. Unlike these animal models, studies in pathologic samples of patients with end-stage heart failure gave conflicting data, showing either unchanged myocardial SOD and GPx1 activities [204,205] or a decreased SOD activity[210].

1. 4. 2. Catalase

Catalase is a tetrameric enzyme which catalyses the reduction of one molecule of H_2O_2 to H_2O (two molecules) and oxidizes a second H_2O_2 to O_2. Being exclusively localized in the peroxisomes in mammalian cells, a major role of catalase is likely to remove H_2O_2 produced during α-oxidation of fatty acids in peroxisomes. With the exception of rat myocardial cells, catalase is not detectable in the mitochondria[211]. Catalase effects on cytosolic H_2O_2 must rely on the diffusion of H_2O_2 into these organelles. Furthermore, despite its high turnover number, catalase is not efficient in eliminating low levels of H_2O_2 because it is difficult to saturate with H_2O_2 and its catalytic cycle requires the interaction of two H_2O_2 molecules with a single active site, which is less likely at low H_2O_2 concentrations[212]. Therefore, catalase is not expected to play a significant role in eliminating low levels of H_2O_2 produced in response to receptor engagement. Nevertheless, recently Kufe and colleagues have shown recently that catalase is extensively regulated in responses to H_2O_2[213-217] concentration through the Abelson (Abl) family of non receptor tyrosine kinases. The Abl family members are c-Abl and

Arg (the product of c-Abl-related gene)[218] and they are activated in response to oxidative stress. Treatment of cells with H_2O_2 induces the binding between the protein kinase Cδ and c-Abl, followed by phosphorylation and activation of c-Abl[217]. As a matter of fact, activation of c-Abl by H_2O_2 is attenuated by the protein kinase Cδ inhibitor, rottlerlin, and by overexpression of the regulatory domain of protein kinase Cδ. Activated c-Abl and Arg appear to regulate catalase. In cells treated with H_2O_2, c-Abl and Arg form heterodimers trough a mechanisms which involves the SH3 domain of one kinase and the PXXP motif of the other kinase. The resulting dimeric kinases then associate with catalase through interaction involving the SH3 domain of the kinase and the P^{293}FNP motif of catalase[214,215]. The binding is independent of the c-Abl kinase function as c-Abl (K→R) or Arg (K→R) mutants, which have an inactive kinase, also associates with catalase. The bound kinases then phosphorylate catalase at Tyr231 and Tyr386 and enhance the catalytic activity of catalase by four- to five fold. The treatment with c-Abl inhibitor STI571 is able to attenuate tyrosine phosphorylation of catalase in response to H_2O_2 in MCF-7 cells[214]. However, mutations on Tyr231 and Tyr386 failed to completely abrogate phosphorylation, thus indicating the potential involvement of other tyrosines. The significance of the physical interaction between c-Abl/Arg and catalase and the subsequent phosphorylation of catalase is supported by the demonstration that cells deficient in either c-Abl or Arg exhibit increased H_2O_2 levels[214].

The mechanism of catalase regulation by c-Abl and Arg is biphasic in response to H_2O_2 concentrations[214]: at lower H_2O_2 levels, c-Abl and Arg phosphorylate and activate catalase. If H_2O_2 concentration increases, c-Abl and Arg dissociate from catalase and render catalase susceptible to dephosphorylation by tyrosine phosphatases, resulting in decrease of catalase activity.

Moreover, in another study, Kufe and colleagues showed that catalase is degraded through an ubiquitination-dependent processes and that the rate of catalase ubiquitination is dependent on c-Abl- and Arg mediated tyrosine phosphorylation[216]. As a matter of fact, Tyr→Phe catalase mutants (Y231F and Y386F) showed a substantially decreased ubiquitination level compared with that of wild-type catalase. In concert with these results, human 293 cells expressing Y231F or Y386F exhibit attenuated levels of reactive oxygen species when exposed to H_2O_2[216]. Based on the observations described

above, Kufe and colleagues proposed a dual roles model of c-Abl and Arg in catalase regulation (fig. 1.9).

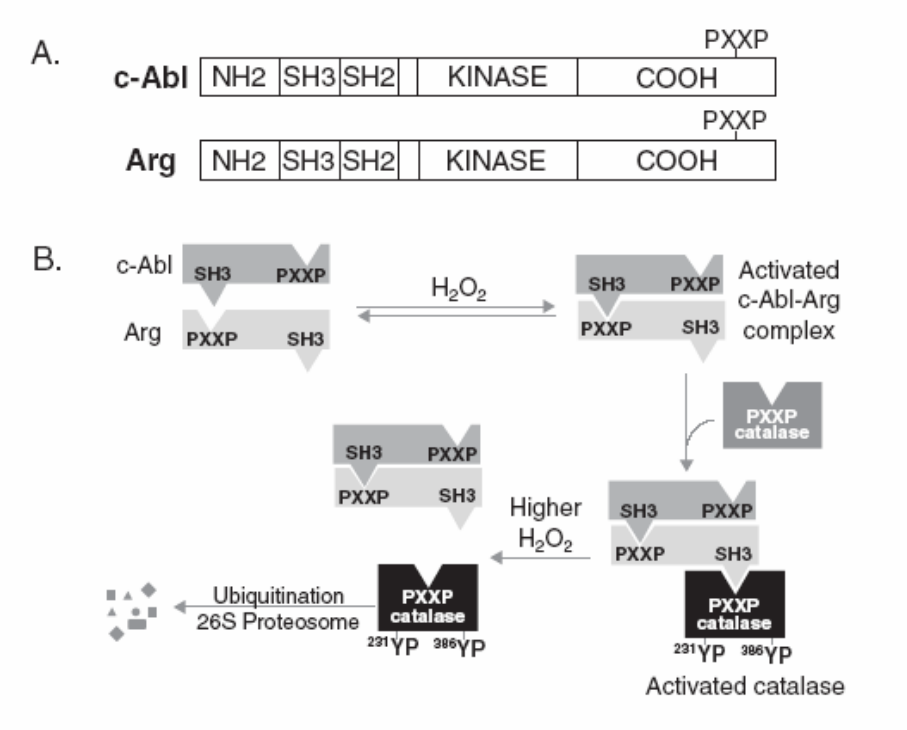

Figure 1.9. The structure of c-Abl and Arg and the regulation mechanism of catalase activity. (A) Domain structure of c-Abl and Arg. The N-terminal region, the SH3, the SH2 and the SH1 (kinase) domains share about 90% identity. Both the proteins present a PXXP domain in the c-terminus, which serves as binding site for the SH3 domains. (B) Proposed model for H_2O_2 concentration-dependent mechanism of catalase activity regulation.

In the model, in addition to stimulating catalase activity by inducing catalase phosphorylation at lower H_2O_2 levels, c-Abl and Arg promote catalase degradation in the event of uncontrollable H_2O_2 levels. Thus, at lethal concentrations of H_2O_2, c-Abl and Arg function as pro-apoptotic effectors, as indicated by the fact that cells deficient in both the kinases exhibit an attenuated apoptotic response[216].

1. 4. 3. Glutathione peroxidase

Glutathione peroxidase (GPx) reduces hydrogen peroxide to H_2O through the oxidation of reduced glutathione to its disulfide form. GPxs are obligatory tetramers, each containing one selenocysteine (Cys-SeH) in its active site. During the catalytic mechanism of GPx, the Cys-SeH residue reacts with H_2O_2 to produce cysteine selenenic acid (Cys-SeOH). GSH then binds to the Cys-SeOH and reduces it to Cys- SeH.
There are at least five types of GPx in mammalian cells. The classical GPx1 is a more abundant ubiquitous protein[219] and found mainly in the cytosol and in the matrix of mitochondria; the gastrointestinal GPx2; the plasma GPx3; the phospholipids hydroperoxide GPx4, and the epididymal secretory GPx5[220]. Mice deficient in GPx1 develop normally, but exhibit sensitivity to H_2O_2[219,221].

Kufe and colleagues extended their studies on the role of c-Abl and Arg on antioxidant enzymes activation also to GPx1. They found that c-Abl and Arg bind to GPx1 through interaction between their SH3 domains and a proline rich region in GPx present in the aminoacidic sequence 132–145[222]. This leads to the GPx1 phosphorylation at Tyr96 by the kinase complex and to its consequent activation. In concert with these findings, inhibition of c-Abl with STI571 in SH-SY5Y cells decreases GPx activity; expression of kinase active c-Abl increases GPx activity, whereas the dominant negative c-Abl (K→R mutant) has an inhibitory effect. Moreover, GPx activity is decreased in *c-abl*$^{-/-}$ *arg*$^{-/-}$ mouse embryo fibroblasts (MEF) cells compared with wild-type cells[222].

1. 5. Mitogen activated protein kinases

The mitogen-activated protein kinase (MAPK) superfamily is a widely distributed group of enzymes that has been highly conserved through evolution. There are at least three subfamilies of the MAPKs: the extracellular signal-regulated kinases (ERKs), the c-Jun N-terminal kinases (JNKs), which are also known as stress-activated protein kinases (SAPKs), and the p38- MAPKs[223-225]. While the ERKs appear to be principally involved in anabolic processes (cell growth, division and differentiation), the JNKs and p38 MAPKs- related pathways are primarily activated by various environmental

stresses: osmotic shock, UV radiation, heat shock, oxidative stress, protein synthesis inhibitors, stimulation of FAS, and proinflammatory cytokines such as TNFα and interleukin-1 (IL-1)[226]. Recently, ERK5/big MAPK 1 (BMK1) was identified as the novel class of stress activated MAPK. ERK5 is also activated in response to oxidative stress and osmotic shock[227].

All MAPKs are proline-directed protein kinases and preferentially phosphorylate Ser/Thr residues within a Pro-Xaa-(Ser/Thr)-Pro motif or minimally a Ser/Thr-Pro motif. However, such sequences are relatively common within proteins, and other determinants of substrate specificity undoubtedly exist. The MAPKs are final components of a three-members MAPKs cascade (fig. 1.10).

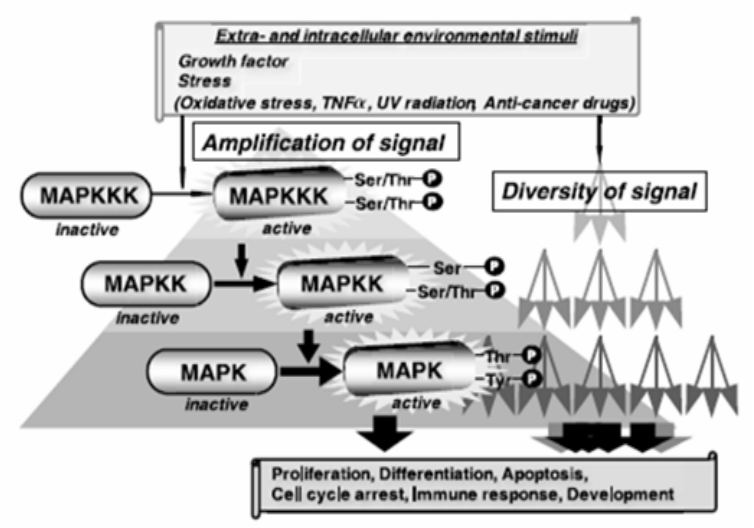

Figure 1.10. MAPKs cascade (from Matsuzawa A. and Ichijo H.[228])

As shown in the figure, MAPKs are activated by MAPK kinases (MAPKKs, or MKKs) which catalyse the ordered dual phosphorylation of a Tyr and a Thr residue lying within a Thr-Xaa-Tyr motif of the MAPKs. The identity of the variable (Xaa) amino acid helps to define MAPK subfamily membership. Activation of MAPKKs involves their phosphorylation on Ser/Thr residues by MAPKK kinases (MAPKKKs). The MAPKs cascade is evolutionarily well conserved in all eukaryotic cells.

ERK, JNK, and p38 have all been shown to be activated in response to oxidant injury and therefore they may potentially contribute to influencing cell survival or cell

death. In neuron- like PC12 pheochromocytoma cells, nerve growth factor (NGF) withdrawal leads to sustained activation of the JNK and p38 MAPK and inhibition of ERK, and both effects are required for the induction of apoptosis[229].

Although the idea that ERK and JNK/p38 have opposing functions is still generally accepted, recent studies suggest that activations of SAPKs appear to be important for cell survival and differentiation. The dynamic balance between the magnitude and the duration of both ERK and JNK/p38 activations is a key to determining whether a cell will survive or undergo apoptosis. The following is a brief description of the three principal members of the MAPKs family, which have been particularly implicated in the present study.

ERK

The best studied MAPK pathway is the ERK1/2 pathway. ERK1/2 is generally phosphorylated in response to growth factors and cytokines, and its activation is related to the stimulation of tyrosine kinase receptors, which elicits a signalling cascade involving Ras activation, recruitment of Raf-1 MAPKKK to the plasma membrane, and sequential activation/phosphorylation of MEK1/2 and ERK1/2[230]. Activated ERK1 and -2 phosphorylate various transcription factors and other protein kinases, thereby influencing a large variety of cellular processes, such as cell survival, differentiation, and cell-cycle regulation. Moreover, oxidative stress leads to substantial activation of ERK1/2. Many growth factor (e.g. epidermal growth factor (EGF) and PDGF) receptors, which have been shown to undergo phosphorylation in response to oxidative insults such as H_2O_2 and UV irradiation[231,232], play an important role in mediating this effect. The activation of the growth factor receptor-ERK1/2 pathway by oxidative stress is consistent with the observation that low and adequate concentrations of ROS are mitogenic[233]. Although it has been reported that the ERK1/2 pathway contributes to cisplatin-induced apoptosis[234], ERK1/2 generally can function as a survival and antiapoptotic factor following oxidative injury[235].

ERK5, a putative MEK5 target, was cloned as part of a two-hybrid screening that used MEK5 as bait[227]. It is about 90-kDa and it has the specific sequence Thr-Glu-Tyr in its phosphorylation loop, like ERK1/2. ERK5/BMK1 can be activated by stress stimuli such as oxidative stress, UV irradiation, ischemia, and hyperosmolarity. Several

studies have shown that a non receptor tyrosine kinase, c-Src, is redox-sensitive and required for activation of ERK5/BMK1[236,237]. It has been demonstrated that ERK5/BMK1 activation contributes to cell proliferation, although its physiological role remains to be fully characterized.

JNK and p38 MAPK

Both JNK and p38, which are stress-activated MAPK family members, are regulated by environmental stress and proinflammatory cytokines such as IL-1 and TNFα. JNK is activated by various oxidant compounds, such as H_2O_2, arsenite, cadmium chloride, and UV-B radiation[235,238,239]. Differently from ERK, JNK and p38 have Thr-Pro-Tyr and Thr- Gly-Tyr motifs, respectively, as phosphorylation consensus sequence. The p38 MAPKs are activated by various types of oxidative stress, like JNK-activating oxidants, as well as other cellular stress such as osmotic shock, heat shock, and lipopolysaccharide[235,240,241]. Singlet oxygen and NO contribute to activate the p38 MAPK pathway, which is required for oxidant-induced apoptosis[242,243]. Specific inhibitors of JNK and p38 pathways or expression of dominant-negative mutants for JNK and p38 suppressed apoptosis induced by various stresses[226]. A cell-penetrating peptide inhibitor of JNK is an extremely potent neuronal protector *in vivo* against cerebral ischemia and excitotoxicity[244]. Many studies have show that JNK and p38 have a critical role in signal transduction of oxidative stress-induced apoptotic cell death. Recent data offer some mechanisms linking ROS and SAPK. Antioxidants and thiol reductants, such as *N*-acetylcysteine and dithiothreitol, and overexpression of antioxidative enzymes, such as MnSOD and glutathione *S*-transferase π (GSTp), can block or delay apoptosis. GSTp can interact with JNK to suppress its activation. ROS trigger the detachment of JNK from GSTp, and thereby facilitate JNK activation[245].

Hsp70 can inhibit JNK activity and JNK-mediated apoptosis[246]. JNK- and p38-mediated phosphorylation of p53, which augments the p53 response, may also play a role in their proapoptotic actions[247,248]. However, the mechanisms by which MAPK signalling molecules regulate oxidative stress-induced apoptosis have not yet been clearly understood.

1. 6. Aim of the study

The NADPH oxidase is known to play an important role in many cardiovascular pathologies such as atherosclerosis, hypertension, hypertrophy and failure[187-189]. Moreover, no convincing data had been reported on the role of the enzyme and its activation mechanism in cardiomyocytes undergoing post-ischemic reperfusion injury. The aim of the first part of this study was to investigate the level and the activation mechanism of NADPH oxidase during post-ischemic reperfusion and to find a link between its related ROS production and the switch of a specific redox-sensitive pathway. To this purpose, a cellular line of rat embryonic cardiaomyocytes was used for simulated ischemia/reperfusion injury experiments to:

1) investigate the role and the activation mechanism of NADPH oxidase in I/R conditions and assess whether NADPH oxidase-derived ROS may be involved in the activation of oxidative stress-sensitive MAPKs;
2) describe the possible role performed by the different members of the MAPK family in cell death;
3) check whether cardiomyocytes damage could be prevented by the use of NADPH oxidase (and MAPKs) inhibitor(s).

As extensively documented in literature, oxidative stress plays a key role in the onset of heart failure[46-48] and cardiac remodelling[51,52]. The role of NADPH oxidase in ROS production has been documented in human and animal models of cardiac failure and myocytes hypertrophy. Moreover, the complete NADPH oxidase-dependent redox signalling cascade during heart failure had been incompletely clarified and the behaviour of antioxidant enzymes in this condition is still a topic of discussion.

Notwithstanding these studies, the main data are focused on the left ventricle, which is considered the most compromised during heart failure and cardiac remodelling. Given that RV function is a predictor of survival in heart failure patients[249-251], the characterisation of its specific redox-signalling pathway can contribute to a broaden insight into the pathophysiological processes involved in the progression toward end-stage heart failure. Based on these observations, human left and right ventricular biopsies from end-stage non-failing and failing donor hearts affected by ischemic, dilated and mitochondrial cardiomyopathies were examined with the aims to:

1) evaluate the activity status and the activation mechanism of NOX2-containing NADPH oxidase in both the heart chambers;
2) assess the cascade of events triggered by increased NADPH oxidase activity in human heart failure;
3) investigate the mutual relationship between the two ventricles;
4) describe the activity status of antioxidant enzymes (superoxide dismutase, glutathione peroxidase, and catalase) in response to the increased oxidative stress and assess whether these changes were equally coordinated in the left and right ventricles.

CHAPTER 2

EXPERIMENTAL PROCEDURES

2. 1. Experimental model PART I: simulated ischemia/reperfusion injury on H9c2 rat cardiac myoblasts

2. 1. 1. H9c2 rat cardiac myoblast cells culture

A cellular line of embryonic rat cardiac myoblasts (line H9c2 (2-1), n° 88092904) with skeletal muscle properties was used. H9c2 cells were provided from European Collection of Cell Cultures (ECACC, Salisbury, UK). Cells were plated at a density of 5 x 10^5/ 100 mm plate dishes (Barloworld Scientific Italia s. r. l., Italy) and cultured at 37° C in 5% CO_2 humidified atmosphere in Dulbecco's Modified Eagles Medium (DMEM, Sigma, Italy) supplemented with 10% heat-inactivated fetal bovine serum (FBS, Sigma, Italy), 1% L-glutamine, 1% streptomycin and 1% penicillin (Sigma, Italy). Cells were passaged regularly at sub-confluence (70-80%) and re-cloned periodically, to maintain differentiated characteristics, before experimental procedures.

2. 1. 2. Ischemia/reperfusion simulation

H9c2 cells were seeded the day before the experiment, at an established concentration, into 35 mm culture dishes for fluorometric measurements of ROS production, into 96-well plates, for LDH release and MTT assays, or into *petri* dishes, for all the other procedures (Barloworld Scientific Italia s.r.l., Italy). Cells were maintained in normoxic condition till the beginning of the experiment. Simulated ischemia was obtained as previously reported[252] with minor modifications. Briefly, at the time of experiment, cells were washed with PBS (Sigma, Italy) and the culture medium was replaced with a

low volume of substrate-free medium (serum-free, glucose-free and sodium pyruvate-free DMEM, DME base, Sigma, Italy), supplemented with 4.3 g/L $NaHCO_3$, 1% L-glutamine, 1% streptomycin and 1% penicillin. Cells were incubated in an anaerobic Plexiglas box (Billups-Rothenberg Inc., CA, USA), hermetically sealed, which was saturated with 95% N_2 and 5% CO_2, and incubated at 37° C for 24 h. The volume of hypoxic medium used was the minimum volume required to coat the cellular monolayer for the prevention of cellular dehydration during the ischemic period. Simulated ischemia was followed by a simulated "reperfusion" period, during which the cells were exposed to normoxic fresh culture medium at 37° C for 60 min in the absence and in the presence of the following drugs: 10 μM diphenyleneiodonium chloride (DPI, Sigma, Italy), a flavoprotein inhibitor, and 100 μM apocynin (Sigma, Italy), both used as NADPH oxidase inhibitors, 10 μM rotenone (Sigma, Italy), a mitochondrial oxidase complex I inhibitor, 100 μM oxypurinol (Sigma, Italy), a xanthine oxidase inhibitor, 20 μM SP600125 (Sigma, Italy), a selective JNK inhibitor compound, and 10 mM 4,5-dihydroxy-1,3-benzene-disulfonic acid (tiron, Sigma, Germany), a superoxide scavenger. For each experiment, control H9c2 cardiac cells were incubated at 37° C in 5% CO_2 humidified atmosphere in complete culture medium for the time of simulated ischemia and reperfusion.

2. 2. Sample preparation

2. 2. 1. Cell lysis

At the end of "reperfusion" cells were washed twice with ice-cold PBS, harvested with a 0.25% Trypsin-EDTA solution and lysed in an ice-cold lysis buffer (10 mM Tris-HCl, pH 7.4 containing 150 mM NaCl, 2 mM EGTA, 2 mM DTT), supplemented with fresh 10 mg/L leupeptin(Sigma, Italy), 10 mg/L aprotinin(Sigma, Italy), 1 mM PMSF (Sigma, Italy) and phosphatase inhibitor cocktail (Sigma, Italy). Cells were maintained on ice for 30 min and then sonicated with a Vibra Cell sonicator (Sonics & Materials Inc., Danbury, CT, USA) three times on ice, for an overall 15 sec time period. Samples were centrifuged using an Eppendorf Centrifuge 5804 R (Eppendorf, Italy) for 5 min at 960 x g (4° C) and the supernatants (homogenates) were assayed for superoxide production,

and lipid peroxidation. To evaluate NOX2/gp91^{phox} protein expression and p47^{phox} translocation, membrane and cytosolic fractions of the homogenates were separated by ultracentrifugation with an L8-70M Ultracentrifuge (Beckman Coulter Inc., Fullerton; CA, USA) for 60 min at 100000 x g (4° C) and used for immunoblotting. The "purity" of membrane and cytosolic fractions were confirmed by markers of enzyme activities as previously described. Western blotting for MAP kinases was performed on homogenates centrifuged for 10 min at 20800 x g (4° C) on the Eppendorf Centrifuge 5804 R (Eppendorf, Italy).

2. 2. 2. Protein content evaluation

Protein concentration was measured by bicinchoninic acid (BCA) protein assay (Pierce, Italy). The assay is based on the reduction of Cu^{2+} to Cu^{1+} by proteins in an alkaline medium (Biuret reaction) and the colorimetric detection of Cu^{1+} cations by bicinchoninic acid. The purple-coloured product is formed by the chelation of two molecules of BCA with one cuprous ion and absorbs at 562 nm (absorbance can be measured between 550 and 570 nm). The reaction is also strongly influenced by the presence of any of cysteine, tyrosine or tryptophan residues in the amino acid sequence of the protein.

Every assay was performed on a 96 wells multiwell and the 570 nm absorbance of the samples was read on a Microplate Reader model 550 (Bio-RAD Laboratories, Italy) spectrophotometer. For each assay, protein concentration of the samples was extrapolated from a standard curve obtained with different concentrations of bovine serum albumin (BSA, Sigma, Italy).

2. 3. Fluorometric measurements of intracellular ROS production in adherent H9c2 cells

Intracellular ROS content in H9c2 cells was evaluated measuring the oxidation of 10 μM 2', 7'-dihydrodichlorofluorescein diacetate (H_2DCF-DA, Invitrogen, Italy) to fluorescent dichlorofluorescein, as described previously[253]. Dichlorofluorescein diacetate is a cell permeable non fluorescent compound whose acetate groups are

removed by intracellular esterases once it has entered the cell. The product of de-acetylation, known as dichlorofluorescein (DCF), is a charged form of the dye, not able to pass the plasma membrane. Oxidation of DCF by hydrogen peroxide occurs within the cell and leads to the formation of a fluorescent probe which absorbs at 438 nm and emits at 535 nm (fig. 2.1).

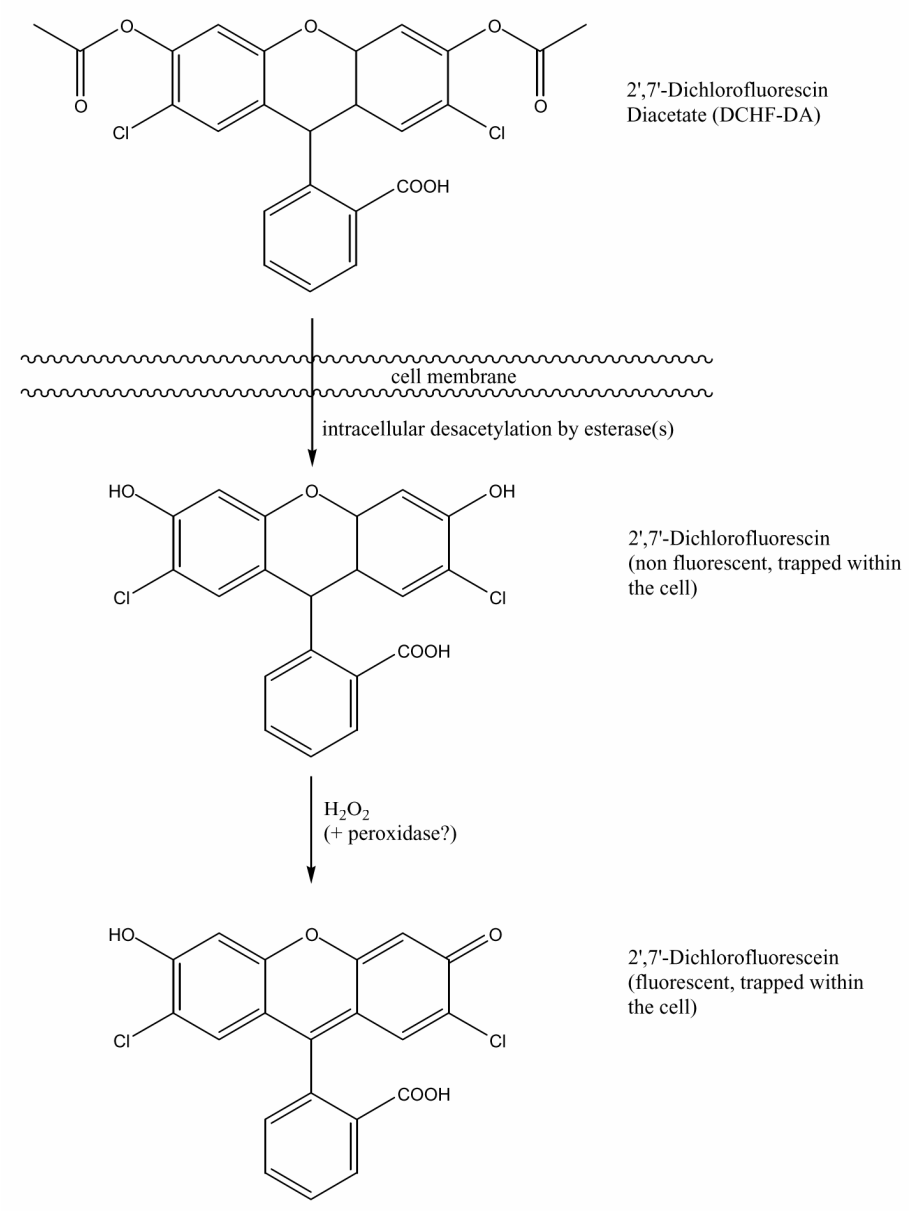

Figure 2.1. Mechanism of action of H_2DCFDA.

For this analysis, cells were plated on 6-well plates and exposed to simulated ischemia/reperfusion as previously described. 10 min before the end of reperfusion, cells were washed in PBS and re-suspended in a 2 ml/well of PBS containing 10 μM H_2DCF-DA. After 10 min of incubation at 37° C in the dark, cells were washed with PBS, lysed in RIPA buffer (50 mM Tris-HCl pH 7.5, containing 150 mM NaCl, 1% Triton X-100 and 2mM EGTA) and fluorescence of samples was immediately analyzed with Fluoroskan Ascent Fluorometer (Thermo Electron Corporation, Finland). Positive and negative controls were also evaluated. The positive control consisted of cells treated for 30 min with 200 μM H_2O_2 (to allow a significantly high ROS production) which did not undergo to simulated ischemia/reperfusion. The negative controls consisted of RIPA buffer with 10 μM H_2DCFDA in the absence/presence of oxidase inhibitors and tiron (to avoid autofluorescence phenomena). DCF fluorescence was expressed as arbitrary units (A.U.) and normalized to total protein content.

2. 4. Luminometric evaluation of superoxide production in cell lysates

Superoxide production was assessed by lucigenin-enhanced chemiluminescence. Experiments were performed on a luminometer (Lumat LB 9507 EG&G Berthold) in 20mM Tris-HCl, pH 7.2, with 100 μg of cell lysate/tube and a non redox–cycling 5 μM lucigenin.

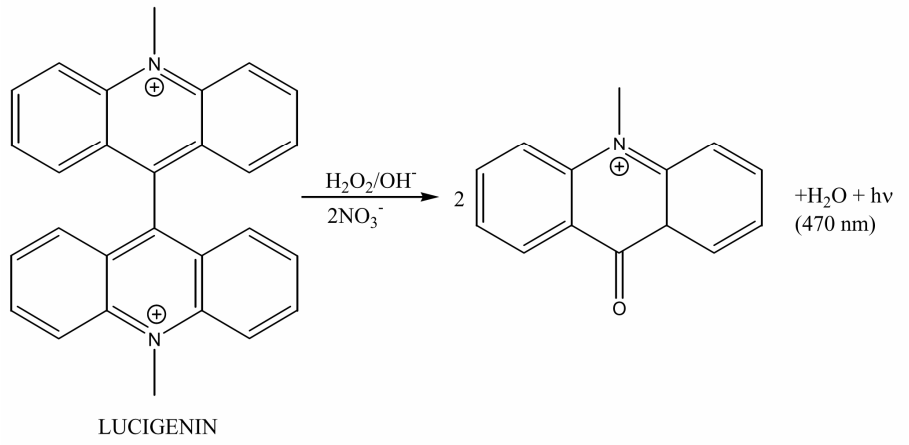

Figure 2.2. Lucigenin oxidation and its chemiluminescent product.

In the presence of superoxide radical lucigenin is oxidized to a chemiluminescent product which emits light at 470 nm (fig. 2.2).
Superoxide generation was measured at room temperature in the absence or in the presence of substrates of the most important oxidase complexes: 300 μM NADPH (Sigma, Italy), 5 mM succinate (Sigma, Italy) or 1 mM xanthine (Sigma, Italy), substrates, respectively, of NADPH oxidase, mitochondrial oxidase complex I and xanthine oxidase. Measurements were also taken after a 10 min pre-incubation with the oxidase inhibitors: 10 μM DPI, 50 μM rotenone and 100 μM oxypurinol. Moreover, 20 mM tiron was also used as negative control. The signal of a blank buffer (consisting of the reaction mixture without oxidases substrates) was subtracted from each reading.

Superoxide production was expressed as mean arbitrary light units (MLU) per mg protein per sec over a 10 min period.

2. 5. Lipid peroxidation assay on cell lysates

Lipid peroxidation is a well-established marker of oxidative stress injury. The peroxidation of polyunsaturated fatty acid leads to the production of a series of instable compounds, and eventually to the formation of malondialdehyde (MDA) and 4-hydroxyalkenals. Hence, MDA content can be assessed as a marker of oxidative stress.

MDA content was determined using a "Biooxytech LPO-586 Assay" kit (Oxis International Inc, Prodotti Gianni, Italy). The assay is based on the reaction between one molecule of MDA and two molecules of the chromogenic reagent N-methyl-2-phenylindole (R1), provided by the manufacturer, at 45° C in the presence of HCl (fig. 2.3). HCl allows the condition to selectively measure MDA, without 4-hydroxyalkenals. The reaction product absorbs at 586 nm.

In particular, 100 μg of samples, reagent R1 and 37% HCl were mixed and incubated at 45° C for 60 min. After this step (acid hydrolysis), samples were centrifuged at 950 x g for 10 min (4° C), transferred into spectrophotometric cuvettes with a 1 cm optical path length and their 586 nm absorbance was measured on a Ultrospec 2000 spectrophotometer (Pharmacia Biotech, NJ, USA). MDA concentration for each sample was extrapolated from a standard curve obtained with a 10 mM standard MDA, provided as an acetal by the kit and freshly diluted in H_2O to a 20 μM

solution before each experiment. Sample blanks were also assessed to subtract the sample background. MDA concentration was expressed as nmol/mg protein.

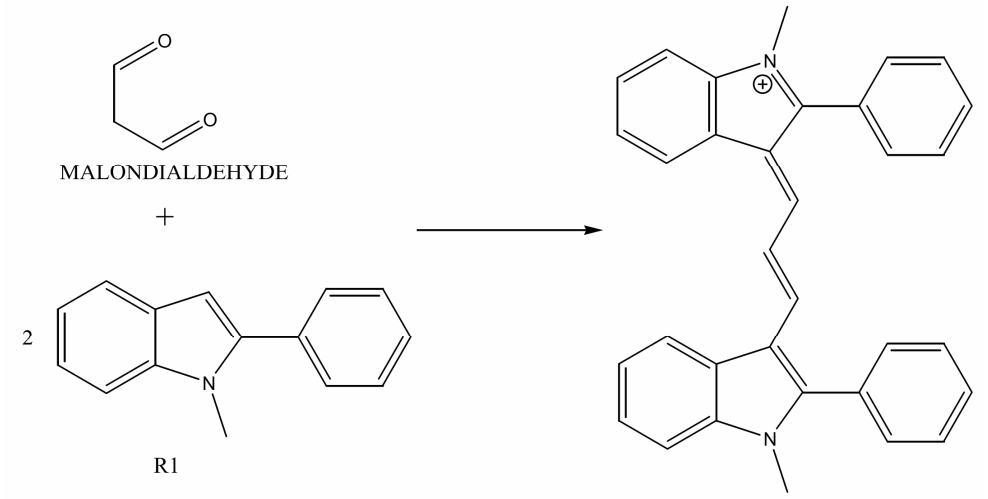

Figure 2.3. Scheme of the reaction between MDA and reagent R1.

2. 6. Western blotting on cell lysates

Equal protein amounts of cellular homogenates or membrane and cytosolic fractions (35 µg) for every sample were diluted in 2X reducing Laemmli buffer (0.5 M Tris-HCl, pH 6.8, glycerol, 10% SDS, 2-β-mercaptoethanol, bromophenol blue) and boiled at 90° C for 5 min. A HL-60 cell lysate (sc-2209, Santa Cruz Biotechnology, Santa Cruz, CA, USA) was used as a positive control for the detection of NOX2. Samples were separated on 12% SDS-PAGE using a Tris/Glycine/SDS running buffer (BioRad, Italy) in the presence of a Precision Plus Protein Prestained Dual Colour molecular weight marker (BioRad, Italy). Samples were transferred to Immobilion-P transfer membranes (Millipore, MA, USA), pre-equilibrated in Tris/Glycine buffer (BioRad, Italy), using a transferring apparatus (Biorad, Italy). After blocking with 5% (w/v) BSA in 0.1% (v/v) TBS-Tween, membranes were incubated overnight at 4° C with one the following antibodies:

1) goat polyclonal anti-gp91^{phox} (1:1000, sc-5827), and anti-p47^{phox} antibodies (1:1000, sc-7660) (Santa Cruz Biotechnology, Santa Cruz, CA, USA), for NADPH oxidase subunities detection;
2) rabbit monoclonal antibodies that specifically recognize the phosphorylated active forms of MAP kinases (1:1000, #9938 Phospho- MAPK family kit, Cell Signaling Technology, MA, USA);

To ensure equal protein loading, membranes were washed 3 times with 0.1% (v/v) TBS-Tween and then stripped with a Restore Western blotting Stripping buffer (Pierce, Italy) for 40 min at 37° C. After a blocking with 5% (w/v) BSA in 0.1% (v/v) TBS-Tween, membranes were incubated with one the following antibodies:

1) mouse monoclonal anti-α-actin antibody (1:1000, sc-32251, Santa Cruz Biotechnology, Santa Cruz, CA, USA), for NOX2;
2) anti-β-tubulin antibody (1:1000, sc-5274, Santa Cruz Biotechnology, Santa Cruz, CA, USA), for p47^{phox};
3) rabbit polyclonal anti-JNK (1:1000, sc-571), anti-ERK (1:1000, sc-93) and anti-p-38 (1:1000, sc-535) antibodies (Santa Cruz Biotechnology, Santa Cruz, CA, USA), for phospho-MAP kinases;

After washing in 0.1% (v/v) TBS-Tween, membranes were incubated for 60 min at room temperature with anti-goat (1: 3000, sc-2020), anti-rabbit (1:10000, sc-2004) or anti-mouse (1:5000, sc-2005) peroxidase-conjugated antibodies (Santa Cruz Biotechnology, Santa Cruz, CA, USA), diluted in 1% (w/v) BSA in 0.1% (v/v) TBS-Tween, were used. Immunoreactive bands were detected by chemiluminescence Immobilion Western ERP Substrate (Millipore, MA, USA) and quantified by densitometric analysis using a Gel Logic 2200 Imaging System and a Kodak Molecular Imaging Software (Kodak, CT, USA). MAP kinases activation was expressed relative to their total protein content. NOX2 and p47^{phox} protein expression were expressed relative to α-actin and β-tubulin protein content, respectively. p47^{phox} membrane translocation was expressed relative to its cytosolic content

2. 7. Immunocytochemical localization of NOX2 protein expression and p47^{phox} membrane translocation in H9c2 adherent cells

In order to perform immunofluorescence staining, H9c2 cardiac muscle cells were grown on coverslips (VWR, Strasbourg, France) in 35 mm culture dishes (Barloworld Scientific Italia s.r.l., Italy). After ischemia and reperfusion, cells were washed with PBS, fixed with 3% (v/v) paraformaldheyde/PBS and incubated for 20 min at 4° C. Cells were permeabilized with 0.1% (v/v) Triton-X-100/TBS and blocked with PBS containing 1% BSA and 10% horse serum for 60 min at room temperature. The coverslips were incubated overnight at 4° C with 100 µl of a 1:50 goat-anti-gp91^{phox} or a goat-anti-p47^{phox} antibody (sc-5827 and sc-7660, respectively, Santa Cruz Biotechnology, Santa Cruz, CA, USA), dissolved in TBS containing 3 % BSA. To avoid evaporation of TBS, the multiwell was sealed up with parafilm. Coverslips were washed three times in 0.1% Triton-X-100/TBS and once with 0.1% BSA in 0.1% Triton-X-100/TBS, and then a 1:400 fluorescein-isothiocyanate (FITC)-conjugated anti-goat secondary antibody (green fluorescence, Fluka, Switzerland) diluted in 0.1% (v/v) Triton-X-100/TBS containing 1% BSA was added for 60 min at room temperature.

After several washes in 0.1% Triton-X-100/TBS in the dark, cell nuclei were stained with 5 µl/ml of a propidium iodide solution (red fluorescence, Fluka, Switzerland) diluited in 0.1% Triton-X-100/TBS. Coverslips were aspirated dry, sealed with glass slides in the presence of Gel Mount (Sigma, Italy), to avoid the bleaching of the probe and observed by a TCS-SP5 confocal microscopy (Leica Microsystems, Germany), using a 488 nm argon ion laser line for FITC excitation.

2. 8. Cell viability assays on H9c2 cells

2. 8. 1. MTT assay

To evaluate the cytotoxic effect of the inhibitors used during post-ischemic reperfusion, MTT assays were performed on H9c2 normoxic control cells[254]. The rational behind this approach is that MTT (3-(4, 5-Dimethylthiazol-2-yl)-2, 5-diphenyltetrazolium

bromide) is reduced by mitochondrial reductases to purple formazan (fig. 2.4), which absorbs between 500 and 600 nm depending on the buffer used. The reaction takes place only in living cells with functional mitochondria and active reductases, therefore the amount of formazan can be considered an indirect marker of cellular viability.

Experiments were performed into 96-well plates. After 24 h incubation at 37° C in 5% CO_2 humidified atmosphere in complete medium, cells were washed twice with PBS. Cells were exposed to fresh culture medium and incubated for 60 min at 37° C in 5% CO_2 humidified atmosphere in complete medium in the absence or in the presence of 10 μM DPI (Sigma, Italy), 100 μM apocynin (Sigma, Italy), 10 μM rotenone (Sigma, Italy), 100 μM oxypurinol (Sigma, Italy), 20 μM SP600125 (Sigma, Italy) and 10 mM tiron (Sigma, Germany).

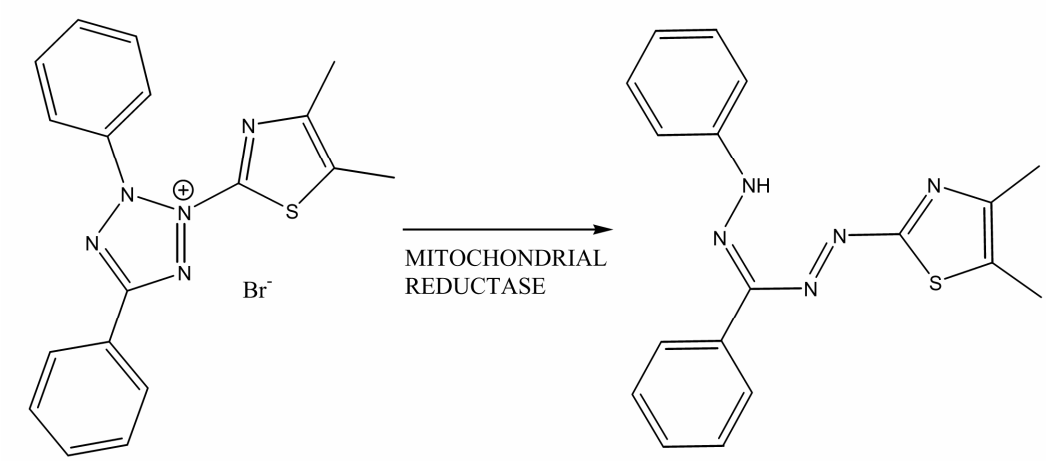

Figure 2.4. MTT reduction to formazan.

Since some of these compounds were dissolved in dimethyl sulphoxide (DMSO) the same amount of this solvent was used to treat cells and to evaluate its possible toxic effects. Cells were washed with PBS and incubated with 100 μl/well of a 0.5 mg/ml MTT solution dissolved in DMEM without red phenol for 120 min at 37° C in the dark. 100 μl of a lysis buffer containing 20% SDS and 50% N-N- dimethylformammide were added to each well. After incubation over night at 37° C, absorbance at 470 nm was measured on a Microplate Reader model 550 (Bio-RAD Laboratories, Italy)

spectrophotometer. MTT reduction in treated cells was expressed as percentage relative to control cells without either inhibitors or DMSO.

2. 8. 2. Lactate dehydrogenase release assay

Lactate dehydrogenase (LDH) release from cells with a damaged membrane is a well established marker of cell necrotic death. LDH release was determined through the CytoTox-ONE Homogeneous Membrane Integrity Assay (Promega, Italia s. r. l., Italy).

The assay is based on the reaction catalysed by diaphorase, which consists in the conversion of resazurin dye into fluorescent resorufin using NADH as electron donor (fig. 2.5). The source of NADH is represented by LDH, the enzyme which converts lactate into pyruvate using NAD^+ as an oxidizing agent.

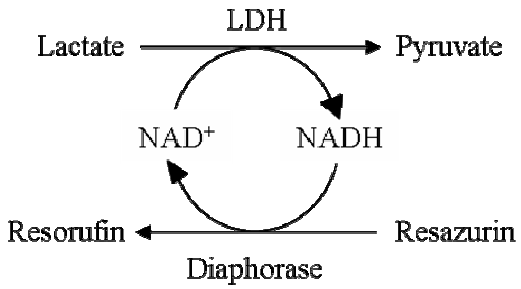

Figure 2.5. Scheme of the reactions used for LDH release assay.

Hence, the production of resorufin is proportional to the amount of LDH in the sample. Lactate, NAD^+, resazurin and diaphorase were provided with the kit. The coupled reactions are shown in fig. 2.5. Experiments were performed into a 96-well plate. After simulated ischemia and reperfusion, cells were equilibrated at 22° C for 5 min. The CytoTox-ONE reagent was added directly to the culture medium in a 1:1 proportion for each well and then cells were incubated at 22° C for 10 min in the dark. Fluorescence signal was measured with a Fluoroskan Ascent Fluorometer (Thermo Electron Corporation, Finland), using excitation and emission wavelengths equal to 544 nm 590 nm, respectively. For each experiment a buffer blank, and a positive control were prepared. The blank solution, constituted by 1:1 culture medium and assay reagent, was used to avoid interferences due to the LDH amount contained into FBS or

to pyruvate contained into DMEM. The positive control, constituted by cells lysed with 1% Triton-X-100 and assay reagent, was used to obtain the highest LDH release level of this specific cell line.

After subtraction of the buffer blank signal, LDH release in each sample was expressed as the percentage of LDH release and related to the total LDH content measured in the positive control.

2. 8. 3. Trypan blue dye exclusion assay

Cell viability was determined by Trypan blue (TB) dye exclusion assay. After simulated ischemia/reperfusion, cells were gently harvested with a 0.25% Trypsin-EDTA solution (Sigma, Italy) and the cellular suspension was mixed with a 0.4% TB solution (Sigma, Italy), in a 1:1 proportion. Cellular suspension was observed under a phase-contrast inverted microscope. The viable cells with intact plasma membranes, which were able to exclude the dye, and the necrotic cells with damaged plasma membranes, that were marked by the dye, were counted using a hemocytometer. Cell viability was expressed as percentage of viable cells over the total counted.

2. 9. Statistical analysis

All values are expressed as mean ± standard error mean (S.E.M.). Comparisons were performed using Analysis of Variance (ANOVA) followed by a Tukey-Kramer multiple comparison test. Correlation coefficient r was obtained using a linear (Pearson) correlation test. Probabilities of $p \leq 0.05$ were considered statistically significant.

2. 10. Experimental model PART II: human biopsies of end-stage failing hearts

All studies were performed on left and right ventricular biopsies of human non failing and end-stage failing hearts, in collaboration with the Departments of Experimental Medicine and Pathology, at “La Sapienza” University of Rome, and the Department of

Preclinical and Clinical Pharmacology, at the University of Florence. Experiments were conformed to the Declaration of Helsinki and institutional ethical regulations and they were carried out after informed consent of relatives (in the case of autopsy samples) or patients. Non failing (NF) donor hearts, which were unsuitable for transplantation for technical reasons, were used as controls. Explanted failing hearts were obtained from patients undergoing transplantation for end-stage heart failure secondary to ischemic heart disease or idiopathic dilated cardiomyophaties. In the case of maternally inherited cardiomyophaties, myocardial tissues were obtained after death (Family #1, Patient #1) or heart transplant (Family #2, Patient #2 and #3).

Immediately after explant, myocardial tissue samples were snap-frozen in liquid nitrogen-chilled isopentane for protein, RNA analysis, and biochemistry. All tissues were stored at -80° C. Sections stained with hematoxylin-eosin and Masson Trichrome stain, were obtained from each sample for morphological examination prior to each experiment. Histologic slides from both failing and non failing hearts were observed under light microscopy. Myocyte hypertrophy was a common finding in all failing hearts, associated with variable degrees of interstitial fibrosis, graded from mild (+ 1) to severe (+ 3) on a semi quantitative basis. According to the results of histologic examination, myocardial samples with minimal amounts of fibrosis and devoid of inflammatory infiltrates were selected for molecular and biochemical studies. In addition, atrial natriuretic factor (ANF), and myosin heavy chain (MHC)-α and -β isoforms mRNA expression, molecular markers of cardiac hypertrophy, were evaluated by quantitative RT-PCR on both NF and failing hearts using the Platinum SYBR Green qPCR Super Mix- UDG (Invitrogen). The clinical characteristic of the patient are reported below in the text (§ 2. 10. 1, § 2. 10. 2, § 2. 10. 3) and in the tables (2. 1, 2. 2 and 2. 3). These evaluations were accomplished at the Department of Experimental Medicine and Pathology, at “La Sapienza” University of Rome.

2. 10. 1. Human biopsies of end-stage failing hearts - 1st study -

Experiments on the role of NADPH oxidase in the biochemical pathways related to the progression of heart failure were carried out on biopsies of both left and right ventricles from non failing (n = 6; no cardiac medication) and failing hearts secondary to ischemic heart disease (n = 7) or idiopathic dilated cardiomyophaties (n = 7). All patients affected

by IHD and DCM had New York Heart Association class IV heart failure, with a mean LV ejection fraction of 21.5 ± 1.14 and a mean pulmonary artery pressure of 34.2 ± 3.8 (see Table 2. 1).

	NF	IHD	DCM
Total number	6	7	7
Sex (M/F)	4/2	6/1	4/3
Age (range)	44 (38-52)	52 (41-67)	45 (33-62)
LVEF (%)		26 ± 1.89	17 ± 0.38
CI (l/min/m^2)		2.37 ± 0.23	1.8 ± 0.07
PAP (mm Hg)		39.2 ± 4.87	29.2 ± 5.36
PCWP (mm Hg)		25.2 ± 2.92	21 ± 5.36
RAP (mm Hg)		17 ± 5.79	10.6 ± 4.78
NYHA		IV	IV
Diuretics	-	7	7
Digoxin	-	0	0
Antiarrhythmics	-	3	2
ACE-I	-	7	7
B-blockers	-	7	7
Nitrates	-	4	0
HMGCoA-Inh	-	-	-
ANF/rRNA 18S	1.04 ± 0.013	10.83 ± 1.06	11.93 ± 1.1
MHC-α/rRNA 18S	1.30 ± 0.04	0.057 ± 0.004	0.03 ± 0.007
MHC-β/rRNA 18S	1.36 ± 0.12	0.04 ± 0.007	0.46 ± 0.03

Table 2. 1. Clinical characteristics of the donor patients (1st study).

2. 10. 2. Human biopsies of end-stage failing hearts -2nd study –

Experiments on the role of NADPH oxidase-dependent antioxidant enzymes activation during the progression to heart failure, were carried out on biopsies of both left and right ventricles from non failing (n = 5; no cardiac medication) and failing hearts secondary to IHD (n = 7) or DCM (n = 5).

	NF	**IHD**	**DCM**
Total number	5	7	5
Sex (M/F)	4/1	6/1	4/1
Age (range)	44 ± 2.1	39 (30-60)	60 (53-69)
LVEF (%)		23 ± 4.8	20 ± 2.5
CI (l/min/m^2)		2.4 ± 0.2	1.8 ± 0.05
PAP (mm Hg)		38 ± 3.2	29 ± 5.4
PCWP (mm Hg)		24 ± 3	21 ± 5.4
RAP (mm Hg)		15 ± 4.2	10.5 ± 2.3
NYHA		III/IV	III/IV
Diuretics	-	7	5
Digoxin	-	0	1
Antiarrhythmics	-	2	1
ACE-I	-	7	5
B-blockers	-	7	5
Nitrates	-	4	0
HMGCoA-Inh	-	2	0
ANF/rRNA 18S	1.03 ± 0.001	12.4 ± 1.05	12.3 ± 0.98
MHC-α/rRNA 18S	1.30 ± 0.03	0.06 ± 0.01	0.04 ± 0.002
MHC-β/rRNA 18S	1.36 ± 0.2	0.06 ± 0.02	0.54 ± 0.05

Table 2. 2. Clinical characteristics of the donor patients (2nd study).

All patients had New York Heart Association class III/IV heart failure, with a mean LV ejection fraction of 21.5 ± 1.14 and a mean pulmonary artery pressure of 34.2 ± 3.8. Clinical characteristics of the three groups are shown in Table 2. 2.

2. 10. 3. Human biopsies of end-stage failing hearts - 3rd study -

Experiments on the role of NADPH oxidase redox signalling during the progression to heart failure in patients affected by maternally inherited cardiomyopaties were performed only on left ventricular tissues obtained from 2 families with MIC (n = 3)[15]. The number of clinical biopsies was restricted because of the difficulty to get tissues from such a rare type of pathology. In addition, samples from patients with end-stage heart failure secondary to ischemic heart disease (n = 9) or idiopathic dilated cardiomyopathy (n = 4) were used, in which metabolic disorders (including diabetes) were ruled out on the basis of clinical records. Non failing heart samples were obtained from donor hearts unsuitable for transplantation for technical reasons (n = 4) and, within 2 h from death, from pediatric patients who died for non cardiac causes in whom mitochondrial disease was excluded on the basis of histologic, histochemical, and respiratory chain enzyme studies. Clinical characteristics of the 3 groups are reported in Table 2. 3.

	NF	**MIC**	**IHD**	**DCM**
Total number	8	3	9	4
Sex (M/F)	4/4	3/0	6/3	4/0
Age (range)	21 (1 month-44)	18 (5-26)	59 (45-67)	45 (33-48)
LVEF (%)	NA	12 ± 4.04	26 ± 7.2	23 ± 4.6
ANF/rRNA 18S	1.06 ± 0.007	8.95 ± 1.92	10.83 ± 1.92	11.93 ± 4.45
MHC-α/rRNA 18S	1.20 ± 0.04	0.06 ± 0.01	0.06 ± 0.02	0.03 ± 0.01
MHC-β/rRNA 18S	1.20 ± 0.05	0.05 ± 0.01	0.46 ± 0.05	0.05 ± 0.01

Table 2. 3. Clinical characteristics of the donor patients (3rd study).

2. 11. Sample preparation

2. 11. 1. Tissue homogenation

Left and right ventricular samples from non failing and failing hearts were differently homogenized in ice-cold 20 mM Tris-HCl, pH 7.4, for lucigenin chemiluminescence assay and lipid peroxidation assay, or in ice-cold 20 mM Hepes pH 7.2 containing 1 mM EGTA, 210 mM mannitol, 70 mM sucrose, for Western blotting and enzymatic activity assays. Both homogenation buffers were supplemented with 10 mg/L leupeptin, 10 mg/L aprotinin, 0.2 mM PMSF and phosphatase inhibitor cocktail. After three times sonication on ice for an overall 15 sec time period, samples were centrifuged for 10 min at 20800 x g (4° C), for Western blotting and CAT activity assays, or for 10 min at 960 x g (4° C), for the other assays, on the Eppendorf Centrifuge 5804 R (Eppendorf, Italy). Heart homogenate aliquots were also separated into soluble (cytosolic) and membrane fractions by ultracentrifugation for 60 min at 100000 x g (4° C) on the L8-70M Ultracentrifuge (Beckman Coulter Inc., Fullerton; CA, USA) and used for immunoblotting to detect NOX2/gp91^{phox} protein expression and p47^{phox} membrane translocation.

2. 11. 2. Protein content evaluation

Protein concentration was measured by bicinchoninic acid (BCA) protein assay (Pierce, Italy), as previously described (§ 2. 2. 2.).

2. 12. Luminometric evaluation of superoxide production in tissue homogenates

Superoxide production was assessed by lucigenin-enhanced chemiluminescence, as previously described (§ 2. 4.). Experiments were performed on a luminometer (Lumat LB 9507 EG&G Berthold) in 20mM Tris-HCl, pH 7.2, with 100 μg of tissue homogenate and a non redox–cycling 5 μM lucigenin.

Superoxide generation was measured at room temperature in the absence or in the presence of substrates of the most important oxidase complexes: 300 μM NADPH (Sigma, Italy), 5 mM succinate (Sigma, Italy) or 1 mM xanthine (Sigma, Italy). Measurements were also taken after a 10 min pre-incubation with the oxidase inhibitors: 20 μM DPI, 50 μM rotenone, 100 μM oxypurinol, 100 μM Nω-nitro-L-arginine methyl ester hydrochloride (L-NAME, Sigma, Italy) or 20 mM tiron. The signal of a blank buffer (consisting of the reaction mixture without oxidases substrates) was subtracted from each reading. Superoxide production was expressed as mean arbitrary light units (MLU) per mg protein per sec over a 10 min period.

2. 13. Lipid peroxidation assay on tissue homogenates

MDA content was measured using a "Biooxytech LPO-586 Assay" kit (Oxis International Inc, Prodotti Gianni, Italy) as previously described (§ 2. 5.).

2. 14. Western blotting on tissue homogenates

Equal protein amounts of tissue homogenates or membrane and cytosolic fractions (35 μg) for every sample were separated on 12% SDS-PAGE and transferred to Immobilion-P transfer membranes (Millipore, MA, USA), as previously described (§ 2. 6.). After blocking with 5% (w/v) BSA in 0.1% (v/v) TBS-Tween, membranes were incubated overnight at 4° C with one the following antibodies:

1) goat polyclonal anti-gp91^{phox} (1:500, sc-20782), and anti-p47^{phox} (1:2000, sc-14015) antibodies (Santa Cruz Biotechnology, Santa Cruz, CA, USA), for NADPH oxidase subunities detection;
2) rabbit monoclonal antibodies that specifically recognize the phosphorylated active forms of MAP kinases (1:1000, #9938 Phospho-MAPK family kit, Cell Signaling Technology, MA, USA);
3) rabbit polyclonal anti-SOD2 (1:1000, sc-30080) and anti-GPx1/2 (1:1000, sc-30147) or goat polyclonal anti-CAT (1:1000, sc-34282) antibodies (Santa Cruz Biotechnology, Santa Cruz, CA, USA), for antioxidant enzymes detection.

To ensure equal protein loading, membranes were washed 3 times with 0.1% (v/v) TBS-Tween and then stripped with a Restore Western blotting Stripping buffer (Pierce, Italy) for 40 min at 37° C. After a blocking with 5% (w/v) BSA in 0.1% (v/v) TBS-Tween, membranes were incubated with one the following antibodies:

1) anti-β-tubulin antibody (1:1000, sc-5274, Santa Cruz Biotechnology, Santa Cruz, CA, USA), for NOX2 and for $p47^{phox}$;
2) rabbit polyclonal anti-JNK (1:1000, sc-571), anti-ERK (1:1000, sc-93) and anti-p-38 (1:1000, sc-535) antibodies (Santa Cruz Biotechnology, Santa Cruz, CA, USA), for phospho-MAP kinases;
3) rabbit polyclonal anti-GAPDH antibody (1:5000, sc-25778, Santa Cruz Biotechnology, Santa Cruz, CA, USA), for antioxidant enzymes.

The membranes examined for CAT were stripped with Stripping buffer and incubated with monoclonal anti-p-Tyr antibody (1:1000, sc-7020, Santa Cruz Biotechnology, Santa Cruz, CA, USA), which specifically recognizes phosphorylated tyrosines.

After washing in 0.1% (v/v) TBS-Tween, membranes were incubated for 60 min at room temperature with anti-goat (1: 3000, sc-2020) and anti-rabbit (1:10000, sc-2004) peroxidase-conjugated antibodies (Santa Cruz Biotechnology, Santa Cruz, CA, USA), diluted in 1% (w/v) BSA in 0.1% (v/v) TBS-Tween, were used. Immunoreactive bands were detected by chemiluminescence Immobilion Western ERP Substrate (Millipore, MA, USA) and quantified by densitometric analysis using a Gel Logic 2200 Imaging System and a Kodak Molecular Imaging Software (Kodak, CT, USA). MAP kinases activation was expressed relative to their total protein content. NOX2 and $p47^{phox}$ protein expression were expressed relative to α-actin and β-tubulin protein content, respectively. $p47^{phox}$ membrane translocation was expressed relative to its cytosolic content. SOD2, GPx and CAT protein expression was expressed relative to GAPDH protein content.

2. 15. Enzymatic activity assays on tissue homogenates

2. 15. 1. Catalase activity assay

Catalase (CAT) activity was evaluated with spectrophotometrical measurements of H_2O_2 dismutation. The reaction mixture contained 100 mM phosphate buffer, pH 6.8, and 70 µg of sample homogenates. After the addition of 10 mM H_2O_2, change in optical density of H_2O_2 at 240 nm was recorded for 30 sec at 25° C with the Ultrospec 2000 spectrophotometer (Pharmacia Biotech, NJ, USA). A quartz cuvette with a 0.5 cm optical path length was used. A molar extinction coefficient for H_2O_2 (ε_{240}) of 43.6 M^{-1} cm^{-1} was used. The ΔE associated to the kinetic of H_2O_2 dismutation was used to evaluate CAT activity through the Lambert-Beer equation. The average value of three measurements was calculated. Enzymatic activity was expressed as µmol/min/mg protein.

2. 15. 2. Glutathione peroxidase activity assay

Glutathione peroxidase (GPx) catalyses the oxidation of reduced glutathione (GSH) to GSSG, using an organic peroxide as electron acceptor. Its activity can be indirectly measured through a reaction coupled with glutathione reductase (GR), which reduces GSSG using NADPH as electron donor and producing $NADP^+$. The reaction is shown in fig. 2.6.

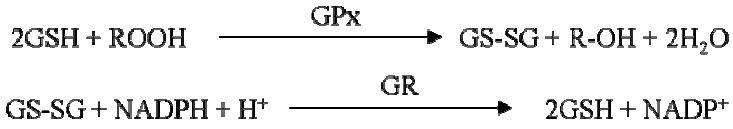

Figure 2.6. Coupled reactions of GPx and GR.

Hence, the decrease in NADPH concentration can be related to GPx activity. The reaction mixture contained 100 mM phosphate buffer, pH 7.4, 0.5 mM EDTA, pH 7.6, 1 mM NaN_3, 0.25 mM NADPH, 2.25 mM GSH, 1 U/ml GR and 70 µg of sample homogenates. After the addition of 0.24 mM tert-butil hydroperoxide (Sigma, Italy), the

organic peroxide which triggers the reaction, change in optical density of NADPH at 340 nm was recorded for 2 min at 25° C with the Ultrospec 2000 spectrophotometer (Pharmacia Biotech, NJ, USA). A quartz cuvette with a 0.5 cm optical path length was used. A molar extinction coefficient for NADPH (ε_{340}) of 6.22 x 10^3 M^{-1} cm^{-1} was used. The ΔE associated to the kinetic of NADPH concentration decrease was used to evaluate GPx activity through the Lambert-Beer equation. The average value of three measurements was calculated. Enzymatic activity was expressed as nmol/min/mg protein.

2. 15. 3. Superoxide dismutase activity assay

Total superoxide dismutase (SOD) activity was evaluated using the Chemical Superoxide Dismutase Assay kit (Cayman Chemical, Ann Arbor, Michigan). The assay uses a tetrazolium salt for the detection of superoxide anion generated by xanthine oxidase and hypoxanthine. In the presence of superoxide anion, the tetrazolium salt is oxidised with the formation of the formazan dye, whose amount increases as SOD concentration in the sample decreases. The reaction is shown in fig. 2.7.

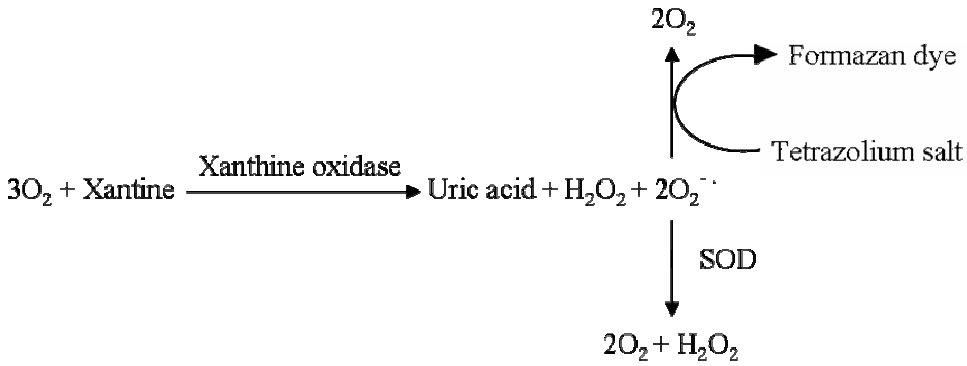

Figure 2.7. Reactions used for measurements of Mn-SOD activity.

One unit of SOD is defined as the amount of enzyme needed to obtain 50% dismutation of superoxide radical. The reaction was performed in a 96 well multiwell, according to the manufacturer protocol. The assay mixture comprised 50 mM Tris-HCl, pH 8, 10 μg of sample homogenates and a solution of tetrazolium salt (the radical detector). Specific Mn-SOD activity was obtained by the addition of 1 mM sodium

cyanide to the samples in order to inhibit the relative amount of cytosolic Cu/Zn-SOD. After incubation at 25° C for 30 min in the dark, xanthine oxidase was added to each well, as reported by the manufacturer protocol. The average value of three measurements was calculated after 15 min incubation with xanthine oxidase at 25° C in the dark. Sample absorbance was measured on a Microplate Reader model 550 (Bio-RAD Laboratories, Italy) using a 450 nm filter. SOD activity for each sample was extrapolated from a standard curve obtained with a standard SOD solution provided with the kit. The Mn-SOD activity was obtained by subtracting the Cu/Zn-SOD activity from the total SOD activity and it was expressed as μmol/min/mg protein.

2. 15. 4. Citrate syntase activity assay

Citrate synthase catalyses the production of citrate from oxaloacetate with the reduction of acetyl-CoA to CoA-SH. The subsequent reaction between CoA-SH and 5, 5'-dithiobis (2-nitro-benzoic acid) (DTNB, Sigma, Italy) leads to the production of 5-thio-2 nitrobenzoic acid (TNB). Therefore, the increase in TNB concentration can be considered an indicator of citrate synthase activity. The reaction is shown in fig. 2.8.

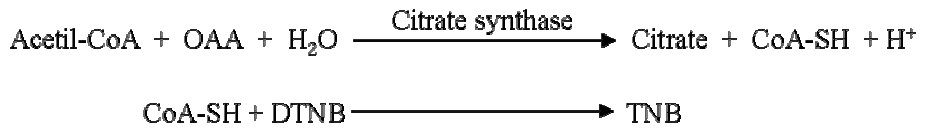

Figure 2.8. Reactions used for the evaluation of Citrate synthase activity.

The reaction mixture contained 100 mM Tris-HCl, pH 8, 100 μM DTNB, 50 μM acetyl-CoA, 250 μM potassium oxaloacetate and 10 μg of sample homogenates. Change in optical density of TNB at 412 nm was recorded for 2 min at 25° C with the Ultrospec 2000 spectrophotometer (Pharmacia Biotech, NJ, USA). A quartz cuvette with a 1 cm optical path length was used. A molar extinction coefficient for TNB (ε_{412}) of 13.6 x M^{-1} x cm^{-1} was used. The ΔE associated to the kinetic of TNB concentration increase was used to evaluate Citrate synthase activity through the Lambert-Beer equation. The average value of three measurements was calculated. Enzymatic activity was expressed as μmol/min/mg protein.

2. 16. Statistical analysis

All values are expressed as mean ± standard error mean (S.E.M.). Comparisons were performed using Analysis of Variance (ANOVA) followed by a Tukey-Kramer multiple comparison test, for three groups analysis, or unpaired test followed by two tails comparison test, for two groups analysis. Correlation coefficient r was obtained using a linear (Pearson) correlation test. Probabilities of $p \leq 0.05$ were considered statistically significant.

CHAPTER 3

RESULTS

3. 1. PART I: Role of NADPH oxidase in simulated ischemia and reperfusion injury

3. 1. 1. Evaluation of possible cytotoxic effects of the inhibitors

To avoid possible cytotoxic effects due to the inhibitors used during reperfusion, MTT assays were performed on normoxic control H9c2 cells not treated and treated for 60 min with all the drugs. Since some inhibitors were dissolved in DMSO, the possible cytotoxic effect of the solvent was also evaluated. The level of MTT reduction observed in treated cells, expressed as percentage relative to non treated cells, was similar to the one observed in non treated cells (data not shown). Hence, no significant cytotoxic effects were observed depending neither to the inhibitors used nor to DMSO.

3. 1. 2. Intracellular ROS increase

Cells subjected to simulated I/R showed a significant increase in intracellular ROS production, as revealed by H_2DCF-DA fluorescence intensity measurements compared to normoxic controls (fig. 3.1). To determine the source of ROS generation we examined the effects of DPI, a flavoprotein inhibitor, and apocynin, both commonly used as NADPH oxidase inhibitors[125], of rotenone, a mitochondrial oxidase complex I inhibitor, and of oxypurinol, a xanthine oxidase inhibitor. As shown in fig. 3.1, DPI and apocynin treatments induced a significant decrease in fluorescence, although the difference in DPI and apocynin concentration must be taken into account. Albeit not sufficient to completely restore the conditions of normoxic control cells, both

compounds reduced ROS production to a value similar to that obtained with the superoxide scavenger tiron. Rotenone and oxypurinol had no effect on I/R-induced ROS generation.

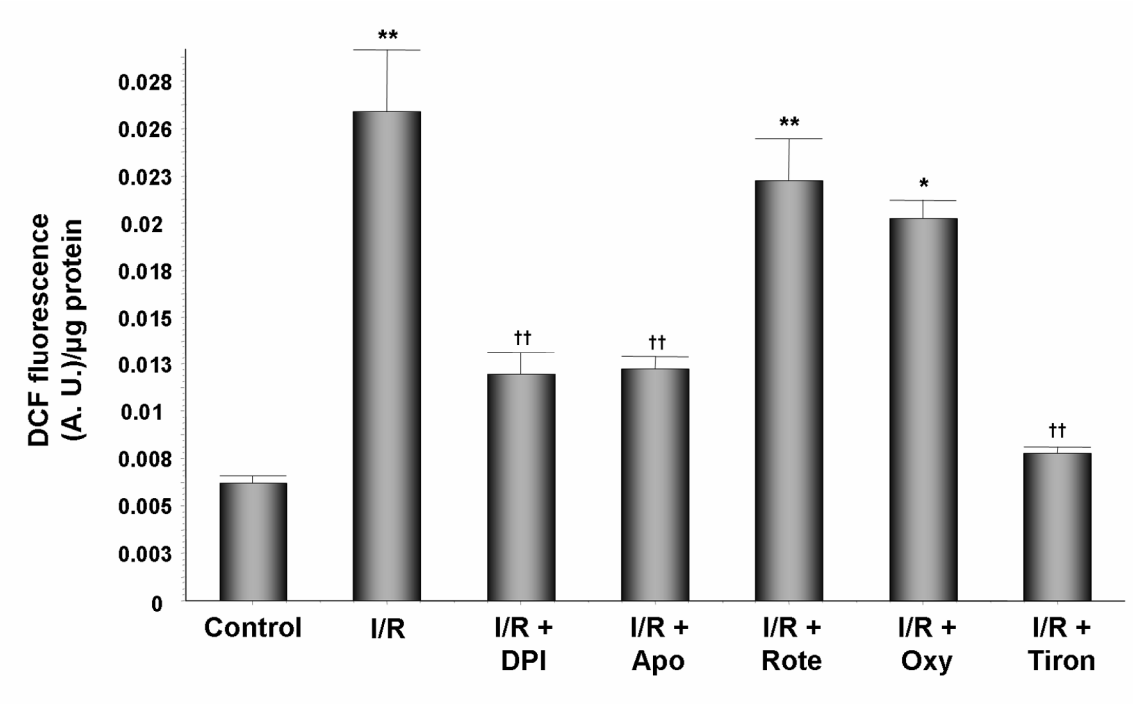

Figure 3.1. Effects of specific inhibitors of oxidase systems on intracellular ROS production in H9c2 cardiac muscle cells exposed to simulated ischemia and reperfusion. DCF fluorescence is expressed as arbitrary units (A. U.) normalized to cellular protein content. Values are means ± S.E.M.; DPI and apocynin (Apo), inhibitors of NADPH oxidase; rotenone (Rote), inhibitor of mitochondrial oxidase complex I; oxypurinol (Oxy), xanthine oxidase inhibitor; tiron, superoxide scavenger, used as a positive control. * $p < 0.05$, ** $p < 0.01$ *Vs* control (normoxic condition); †† $p < 0.01$ *Vs* I/R; n = 6.

3. 1. 3. NADPH oxidase activity

To confirm that simulated I/R-induced ROS production was mainly attributable to the activation of NADPH oxidase, superoxide production was measured by lucigenin chemiluminescence in the absence and in the presence of specific oxidase substrates. Neither succinate nor xanthine, substrates of mitochondrial oxidase complex I and of

xanthine oxidase, respectively, were able to induce any increase in $O_2^{\cdot -}$ production in I/R cells (fig. 3.2 A).

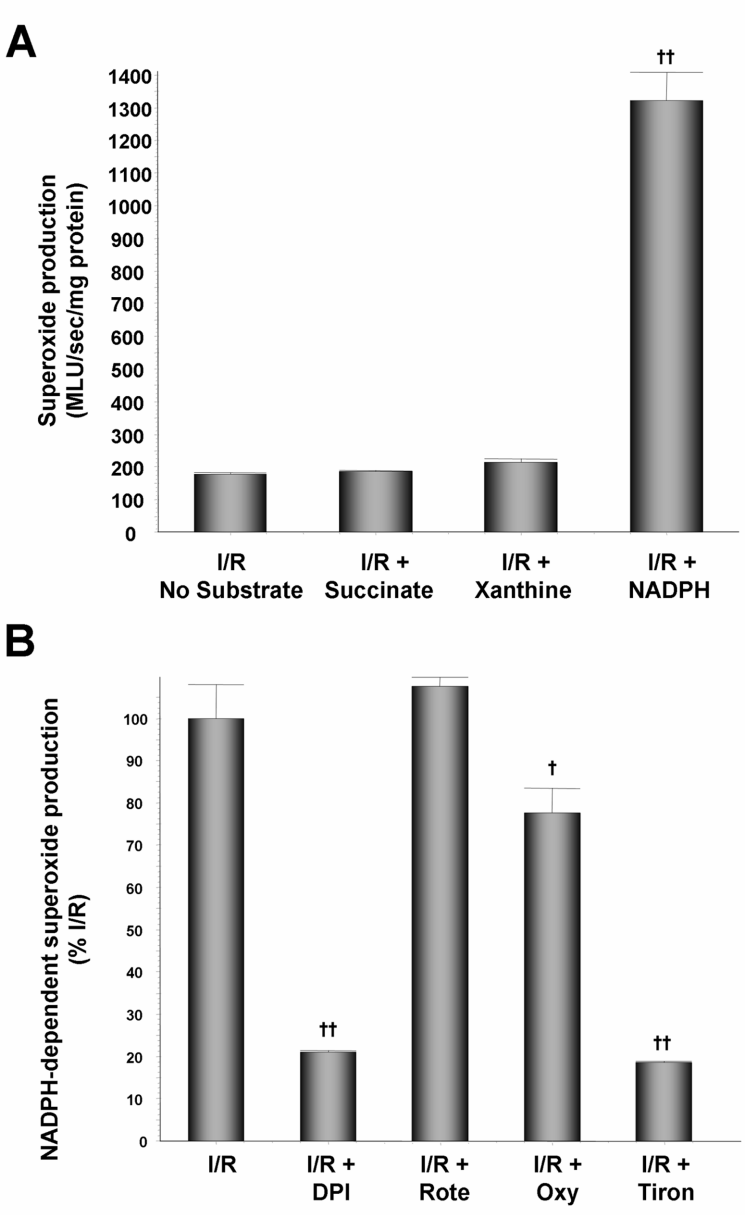

Figure 3.2. (A) Superoxide production in I/R H9c2 homogenate in response to several substrates and (B) NADPH-dependent superoxide production in I/R cells in the absence or presence of oxidase inhibitors detected by lucigenin chemiluminescence. Results are expressed as MLU/sec normalized to protein content. Values are means ± S.E.M.; NADPH, NADPH oxidase substrate; succinate, mitochondrial oxidase complex I substrate; xanthine, xanthine oxidase substrate. MLU, mean arbitrary light units. Rote, rotenone; Oxy, oxypurinol. $^{\dagger}p < 0.05$, $^{\dagger\dagger}p < 0.01$ and $^{\dagger\dagger\dagger}p < 0.001$ *Vs* I/R; n = 6.

By contrast, significantly higher $O_2^{\cdot -}$ generation was detected in I/R cells in the presence of NADPH compared to I/R cells without substrate (fig. 3.2 A). The increase of NADPH dependent superoxide production was significantly inhibited by DPI and tiron (fig. 3.2 B), but was unaffected by rotenone or oxypurinol, supporting the hypothesis of NADPH oxidase as a major source of $O_2^{\cdot -}$ in cells exposed to simulated I/R.

3. 1. 4. NADPH oxidase activation mechanism

To elucidate the mechanisms underlying NADPH oxidase activation in cells subjected to simulated I/R, we analyzed the expression of the catalytic subunit NOX2/gp91^{phox} by Western blot and immunofluorescence. As shown in fig. 3.3 A, immunoblotting of NOX2 membrane protein expression with a goat polyclonal antibody, widely used by other authors[255-257] gave two different bands that migrated at a position of approximately 55–65 kDa. These bands presumably represented unglycosylated NOX2[198], while the band at around 80 kDa, corresponding to glycosylated NOX2, was not detected. Notwithstanding the molecular properties of NOX2 detected by the antibody, it is evident that both bands are more intense in I/R samples relative to the control, thus suggesting an effective over-expression of NOX2 protein after I/R. DPI addition had no effect on NOX2 expression.

The increase in NOX2 expression was further confirmed by immunofluorescence (fig. 3.3 B). In control H9c2 cells confocal images showed NOX2 localized in the plasma membrane and in the cytosol, including the perinuclear region (fig. 3.3 B-a). After simulated I/R, NOX2 labelling appeared more intense and showed a vesicular or granular pattern in all these compartments, (fig. 3.3 B-b), which was not modified by DPI treatment (fig. 3.3 B-c).

To assess whether NADPH oxidase activation in cells exposed to simulated I/R was also attributable to a p47^{phox} over-expression and/or membrane translocation, which is likely to modulate oxidase activation[65,66,100,258], we undertook immunofluorescence staining. As shown in fig. 3.4 A, p47^{phox} expression was enhanced in I/R H9c2 compared to control cells; moreover, the cellular localization of the fluorescent probe appeared increased in the cytosol and especially in the plasma membrane.

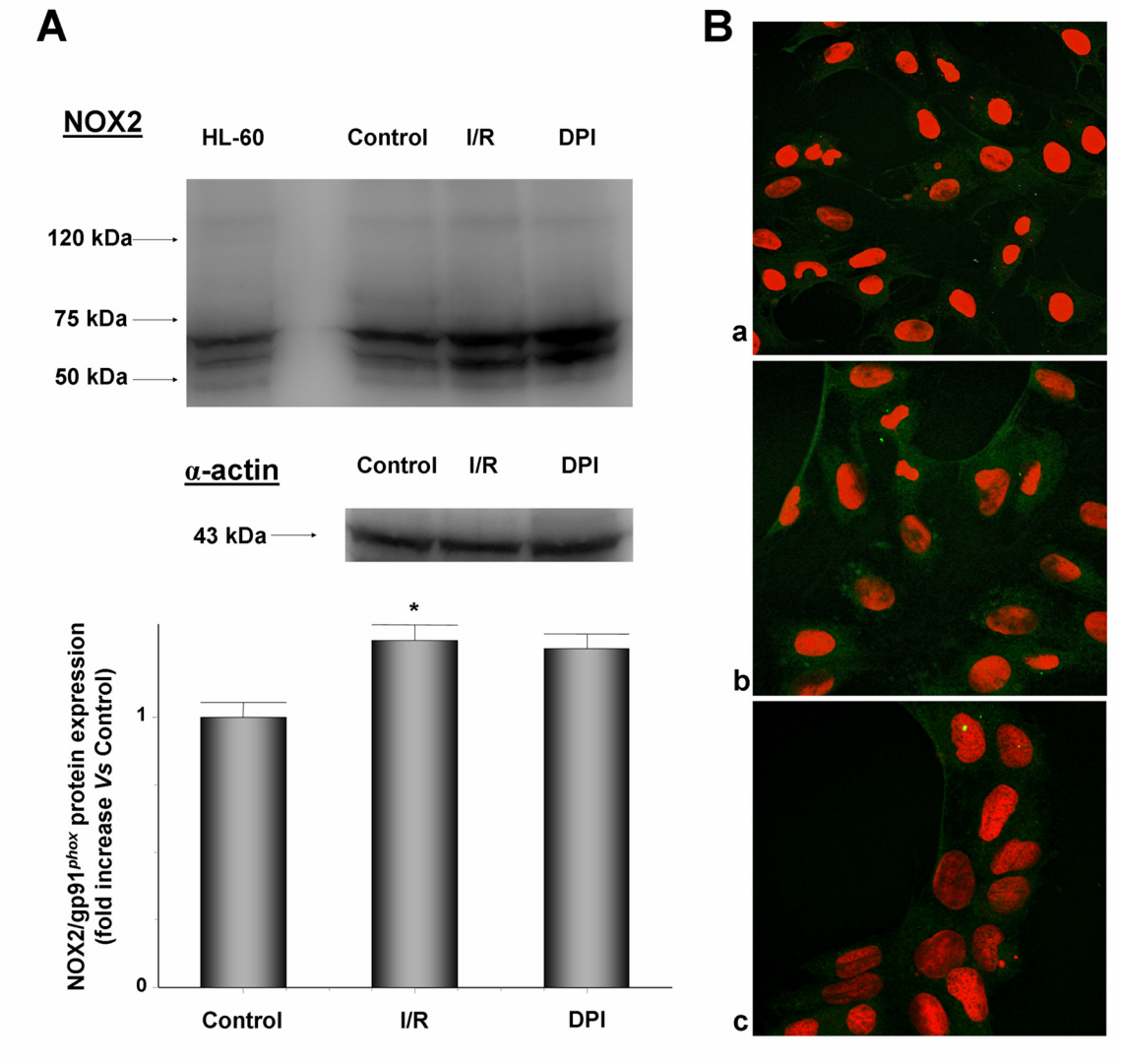

Figure 3.3. Changes in NOX2/gp91^{phox} protein expression in H9c2 cardiac muscle cells subjected to simulated ischemia and reperfusion in the absence and in the presence of DPI. (A) Representative immunoblot of NOX2/gp91^{phox} (top) and densitometric quantification of membrane protein expression relative to α-actin protein expression (bottom) expressed as fold increase relative to control. HL-60 cell lysate was used as a positive control for the detection of NOX2/gp91^{phox}. Values are means ± S.E.M.; * $p <$ 0.05 *Vs* control; n = 6. (B) Confocal images of (a) control, (b) ischemic-reperfused and (c) DPI treated H9c2 cells.

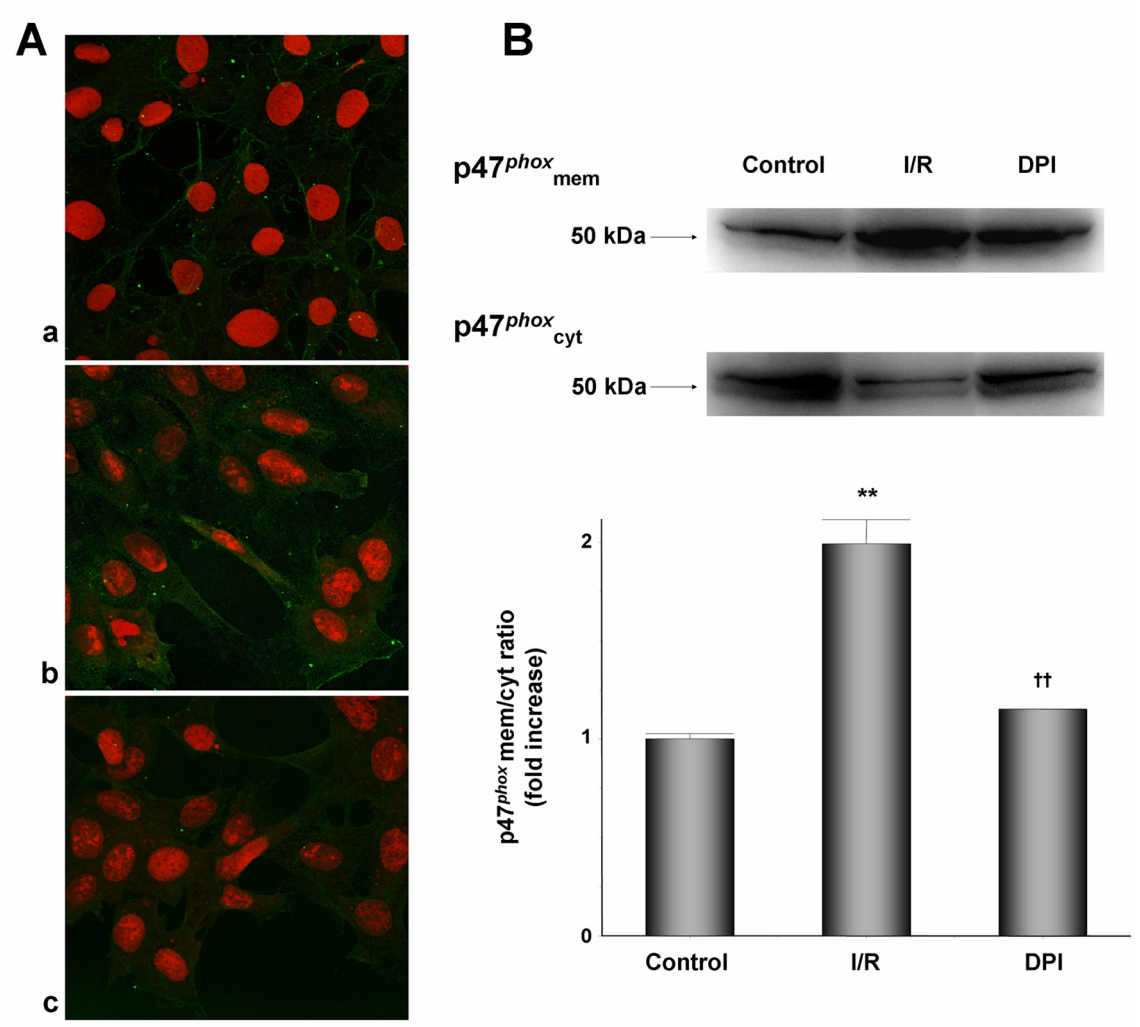

Figure 3.4. p47^{phox} membrane translocation in H9c2 cardiac muscle cells following simulated ischemia and reperfusion in the absence and in the presence of DPI. (A) Immunofluorescence of (a) control, (b) ischemic-reperfused and (c) DPI treated H9c2 cells. (B) Representative immunoblots of p47^{phox} protein expression of membrane and cytosolic fraction of H9c2 cardiac muscle cells (top). Densitometric quantification of the ratio of membrane to cytosolic protein expression of p47^{phox} (bottom). Values are means ± S.E.M. ** $p < 0.01$ *Vs* control; $^{\dagger\dagger}p < 0.01$ *Vs* I/R; n = 6.

Treatment with DPI resulted in a decreased p47^{phox} immunofluorescence staining, which was mainly evident in the sarcolemma, suggesting a change in p47^{phox} distribution and supporting the hypothesis of a p47^{phox} translocation from the cytosol to plasma membrane after simulated I/R. To confirm these data we analyzed p47^{phox}

content in the membrane and cytosolic fractions by Western blotting. The fig. 3.4 B shows a significantly higher membrane/cytosolic ratio of $p47^{phox}$ in I/R cells than in control. DPI treatment abolished this increase (fig. 3.4). These results point out that, in our experimental conditions, the increase in NADPH oxidase activity is due not only to NOX2 overexpression but also to the membrane translocation of the cytosolic subunit $p47^{phox}$.

3. 1. 5. NADPH oxidase-related redox signalling: lipid peroxidation

Lipid peroxidation resulting from oxidative stress has been implicated in cell death.

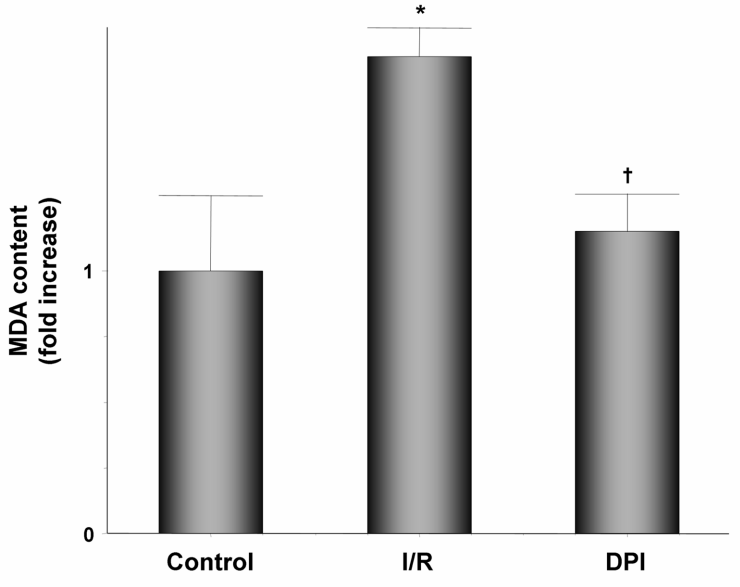

Figure 3.5. Lipid peroxidation, assessed by intracellular MDA content evaluation, in H9c2 cardiac muscle cells subjected to simulated ischemia followed by reperfusion in the absence and in the presence of DPI. Values are expressed as fold increase relative to control. * $p < 0.05$ *Vs* control; † $p < 0.05$ *Vs* I/R; n = 6.

To test whether simulated I/R-mediated NADPH oxidase activation was involved in lipoperoxidative cell damage we measured MDA cell content, as an indirect index of ROS activity[259]. Measurements were performed in the absence and in the presence of DPI. Accordingly to the differences observed in ROS production, MDA levels were

significantly increased in cells subjected to simulated I/R. In the presence of DPI, MDA content was significantly reduced, as we observed with tiron treatment (fig. 3.5), suggesting that NADPH oxidase-derived ROS are the main responsible for lipid peroxidation in I/R cells.

3. 1. 6. NADPH oxidase-related redox signalling: MAPKs activation

To elucidate the signal transduction pathway involved in simulated I/R injury, we evaluated the phosphorylation level of the three principal members of the MAPK family (p38, ERK and JNK) by Western blotting.

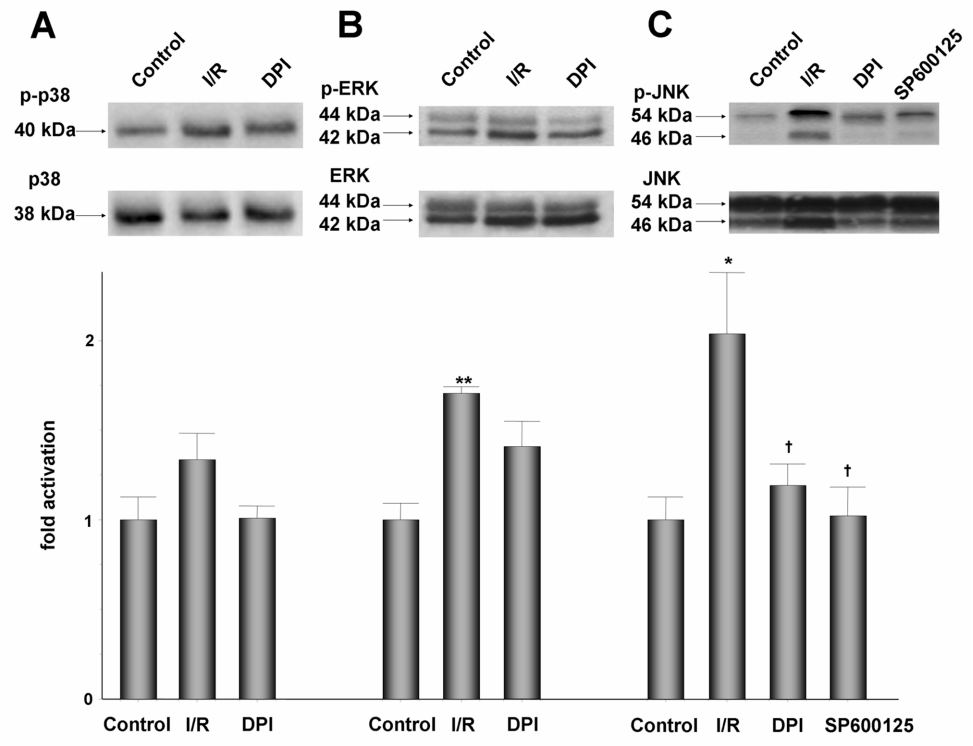

Figure 3.6. Effect of DPI (A, B, C) and of SP600125 (C) on MAPKs activation induced by simulated ischemia and reperfusion in H9c2 cardiac muscle cells. Representative immunoblots for p-p38 (A), p-ERK (B) and p-JNK (C) (top) and respective total protein in H9c2 homogenate (bottom). Densitometric quantification of the ratio of phosphorylated/total MAPKs protein content expressed as fold activation relative to control. SP600125, selective JNK inhibitor compound. * $p < 0.05$ and ** $p < 0.01$ *Vs* control; † $p < 0.05$ *Vs* I/R; n = 6.

Cells exposed to simulated I/R showed no significant changes in the p38 phosphorylation status (expressed as p-p38/p38 ratio) relative to control cells (fig. 3.6 A). By contrast, ERK (p-ERK/ERK ratio) and JNK (p-JNK/JNK ratio) phosphorylation was significantly increased (1.7-fold, $p < 0.01$; and 2-fold, $p < 0.05$; both *V*s control; fig. 3.6 B and C). In order to verify a possible link between these events and NADPH oxidase activation, we analyzed ERK and JNK phosphorylation in the presence of DPI. DPI treatment significantly decreased only the p-JNK/JNK ratio; a similar result was obtained with the selective JNK inhibitor, SP600125[260], which reduced the p-JNK/JNK ratio to control level (fig. 3.6).

In agreement with this effect, a positive correlation ($r = 0.74$, $p < 0.01$) was found between NADPH oxidase-derived superoxide production and JNK activation.

3. 1. 7. NADPH oxidase-related redox signalling: cell viability and LDH release

As determined with the Trypan blue dye exclusion assay (fig. 3.7 A), the viability of cells subjected to I/R was decreased by 26% relative to the control. Accordingly, the fraction of total LDH released in the culture medium (fig. 3.7 B) by I/R cardiomyoblasts was significantly increased (1.6-fold, $p < 0.05$ *Vs* control). All these effects were significantly reduced by the treatment with the two unrelated inhibitors DPI or SP600125; in fact, cell treatment with both inhibitors resulted in the same protective effect against simulated I/R induced cell death. Moreover, the percentage of both viable cells and LDH released showed a significant correlation with JNK phosphorylation ($r = -0.73$, $p < 0.01$ and $r = 0.75$, $p < 0.01$, respectively).

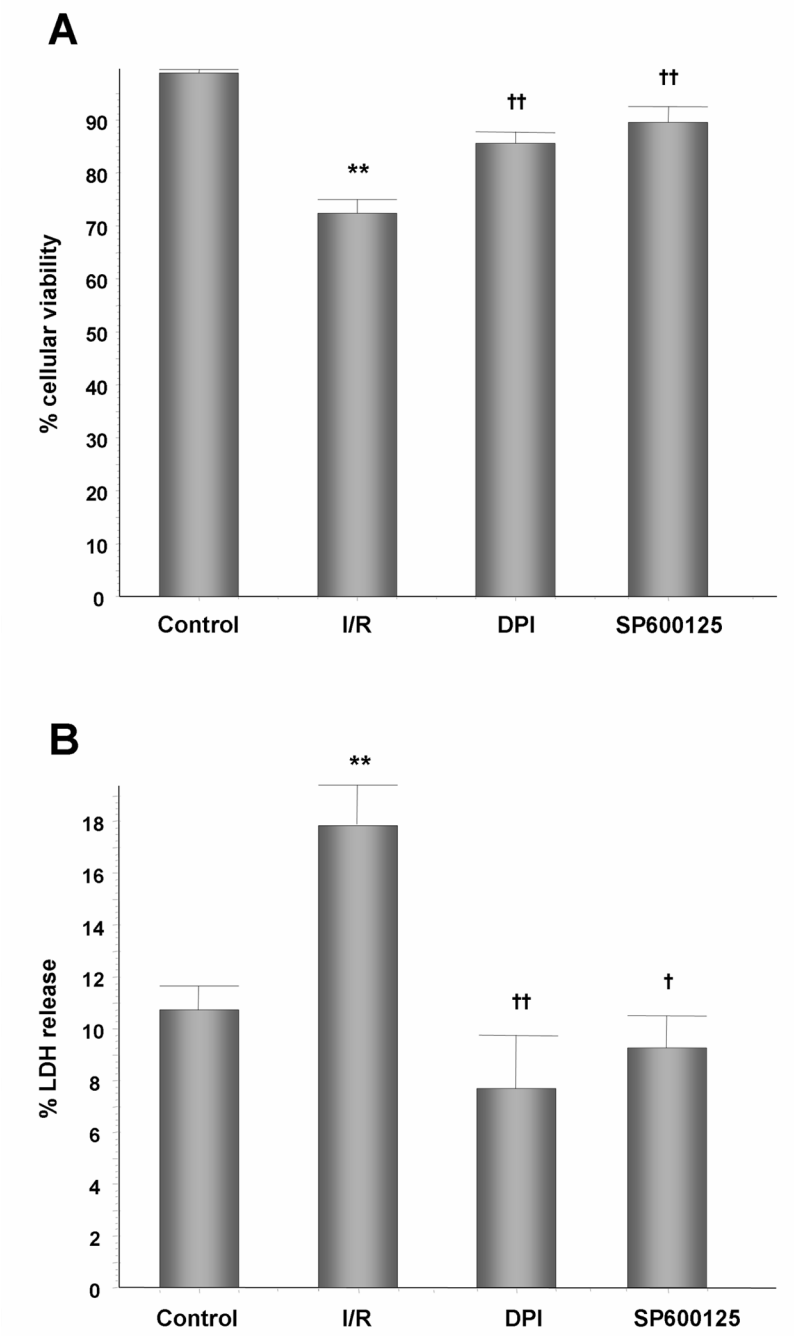

Figure 3.7. Effect of DPI and of SP600125 on cell death of H9c2 cardiac muscle cells exposed to simulated ischemia and reperfusion. Cell death was evaluated by Trypan blue dye exclusion assay (A) and by LDH released into the culture medium (B). For Trypan blue assay results are expressed as percentage of viable cells over the total cell counted. For LDH release, results are expressed as percentage of total LDH content. ** $p < 0.01$ *Vs* control; $^{\dagger}p < 0.05$ and $^{\dagger\dagger}p < 0.01$ *Vs* I/R; n = 6.

3. 2. PART II - 1st STUDY: NADPH oxidase-dependent redox signalling in end-stage human failing hearts secondary to IHD and DCM

3. 2. 1. NADPH oxidase activity

Superoxide production was measured by lucigenin chemiluminescence in the absence or presence of NADPH, succinate or xanthine. Both succinate and xanthine provided a minimal $O_2^{\cdot-}$ production in the RV and LV homogenate, which did not differ between non failing (NF) and failing hearts (data not shown). In the presence of NADPH, significantly higher $O_2^{\cdot-}$ generation was detected in non failing LV compared to non failing RV (240.14 ± 8.1 MLU/sec/mg protein *Vs* 160 ± 10.6 MLU/sec/mg protein, respectively). Diseased LV and RV specimens exhibited a marked increase in $O_2^{\cdot-}$ production compared to NF controls. In particular, the increase in superoxide generation was less marked, although statistically significant, in failing LVs (IHD 1.38-fold, $p < 0.001$ *Vs* NF; DCM 1.23-fold, $p < 0.05$ *Vs* NF), while a 2-fold and 1.65-fold increase in NADPH-dependent $O_2^{\cdot-}$ production was observed in the RVs from IHD and DCM hearts ($p < 0.001$ *Vs* NF) (fig. 3.8 A). Interestingly, in RV samples from failing hearts, $O_2^{\cdot-}$ production, attributable to NADPH oxidase activity, was positively related to the respective pulmonary arterial pressure (PAP; $r = 0.86$, $p = 0.0014$) (fig. 3.8 B). To investigate the sources of superoxide production, experiments were performed in the presence of potential ROS-generating systems inhibitors. NADPH-dependent $O_2^{\cdot-}$ production was virtually abolished by tiron, thus confirming $O_2^{\cdot-}$ as a major source of ROS detected in our experimental conditions. In both RV and LV samples from failing hearts, NADPH-dependent $O_2^{\cdot-}$ generation was significantly decreased by DPI, but was unaltered by L-NAME, the nitric oxide syntase inhibitor, rotenone, or oxypurinol, supporting the idea that a phagocyte-type NADPH oxidase is likely to be a major source of $O_2^{\cdot-}$ in the human failing heart (fig. 3.8 C, D).

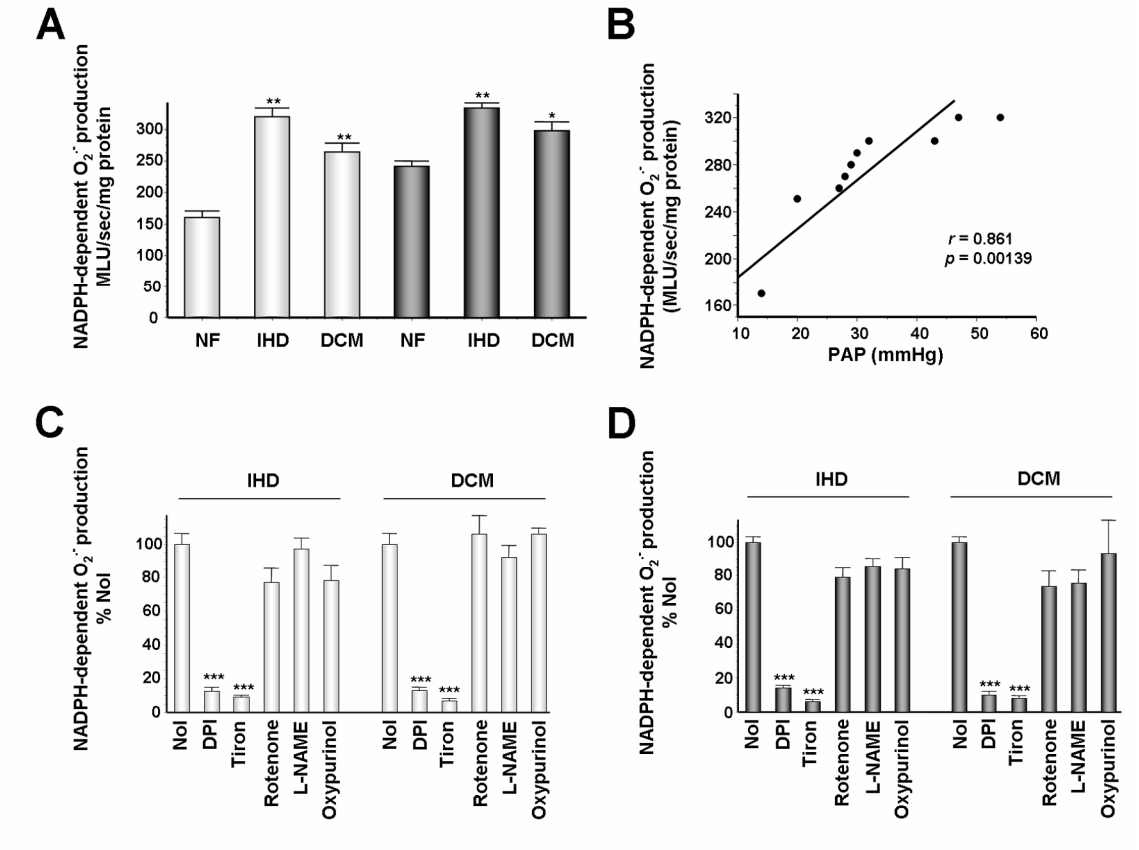

Figure 3.8. (A) NADPH-dependent $O_2^{\cdot-}$ production in human non failing (NF) and failing RV (open bars) and LV (solid bars) hearts detected by lucigenin chemiluminescence. MLU, mean arbitrary light units; * $p< 0.05$ *Vs* NF; ** $p<0.01$ *Vs* NF. n = 6 NF and n = 7 failing ventricles from hearts with IHD or DCM. (B) Correlation between pulmonary artery pressure (PAP) and right ventricle NADPH-dependent superoxide production of IHD and DCM; n = 5 for each group. (C and D) Effect of specific inhibitors of oxidase systems on NADPH-dependent $O_2^{\cdot-}$ production in human failing RV (C) and LV (D). Data are presented as mean ± S.E.M. and expressed as percentage of the value measured in the absence of inhibitors (NoI). *** $p < 0.001$ *Vs* NoI.

3. 2. 2. NADPH oxidase activation mechanism: the role of p47^{phox}

To elucidate the mechanisms underlying the increased NADPH oxidase activity in the failing myocardium, experiments were designed to investigate NOX2/gp91^{phox} and its regulatory subunit p47^{phox}. NOX2 protein expression, assessed by Western blotting in

the same RV and LV homogenates used for measurements of NADPH-dependent superoxide production, did not differ between NF and failing hearts (data not shown).

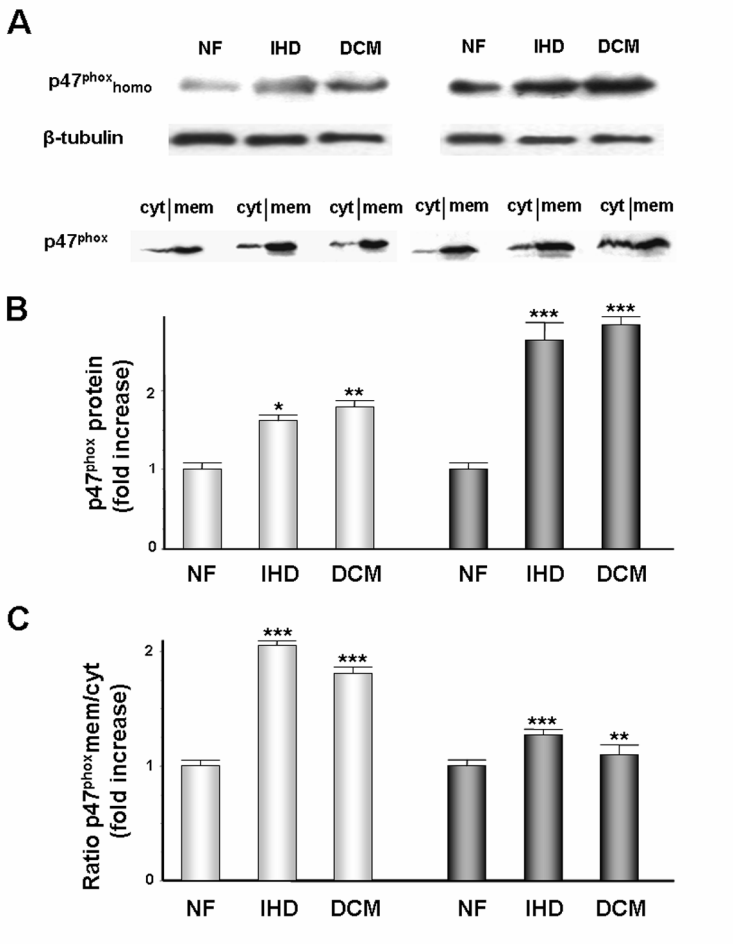

Figure 3.9. p47^{phox} protein expression and membrane translocation in human RV and LV. (A) Representative immunoblotting of p47^{phox} protein expression in the homogenates and in the membrane and cytosolic fractions of non failing (NF) and failing RV and LV. (B) Densitometric quantification of p47^{phox} homogenate protein expression relative to β-tubulin protein expression. (C) Densitometric quantification of the membrane/cytosolic ratio of p47^{phox} protein expression. Data are calculated as mean ± S.E.M. and expressed as fold increase of failing *Vs* non failing hearts. RV, open bars; LV, solid bars; homo, homogenate; mem, membrane; cyt, cytosolic; n=6 non failing, NF and n=7 failing ventricles from hearts with IHD or DCM; * $p < 0.05$, ** $p < 0.01$, and *** $p < 0.001$ *Vs* NF.

By contrast, p47^{phox} was significantly over-expressed in RV and, more markedly, in LV homogenates from failing hearts compared to NF, regardless of the aetiology of the disease (IHD or DCM) (fig. 3.9 A, B). p47^{phox} membrane content was higher in non failing LV than in non failing RV (1.29 ± 0.12 *Vs* 0.82 ± 0.10, respectively, $p < 0.001$). On the other hand, the increment in membrane/cytosolic ratio of p47^{phox} was significantly higher in the failing RV membrane fraction (IHD 1.99-fold, $p < 0.001$ *Vs* NF; DCM 1.64- fold, $p < 0.001$, *Vs* NF) compared to the failing LV (IHD 1.32-fold, $p < 0.001$ *Vs* NF; DCM 1.22-fold, $p < 0.05$, *Vs* NF) (fig. 3.9 A and C). The prominent role of p47^{phox} membrane translocation as a mechanism for NADPH oxidase activation was further supported by the positive correlation between NADPH oxidase activity and sarcolemmal fraction of p47^{phox}, both in RV ($r = 0.76$, $p = 0.001$) and in LV specimens ($r = 0.79$, $p = 0.001$).

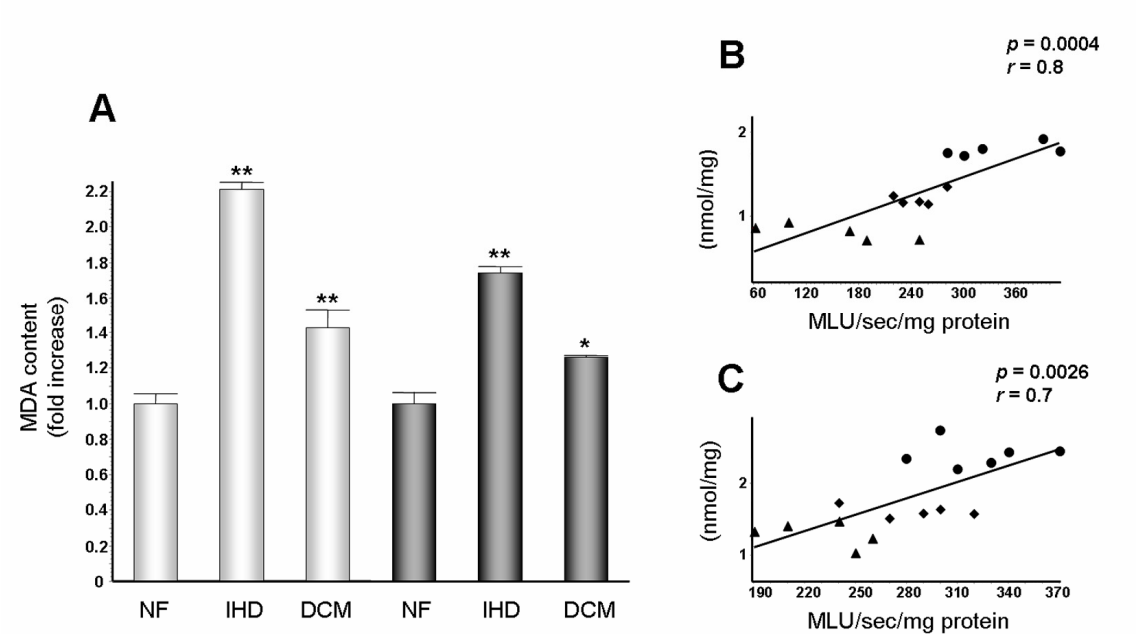

Figure 3.10. (A) MDA content in human RV (open bars) and LV (solid bars). n=6 non failing, NF, and n=7 failing ventricles from hearts with IHD or DCM. * $p < 0.05$; ** $p < 0.01$ *Vs* NF. (B and C) Correlations between NADPH-dependent superoxide production and MDA content in human RV (B) and LV (C). NF (▲), DCM (●), IHD (♦); n=5 for each group.

3. 2. 3. NADPH oxidase-related redox signalling: lipid peroxidation

Accordingly to the differences observed in ROS production, MDA levels were significantly increased in RV and LV samples from failing hearts (fig. 3.10 A, previous page). In addition, MDA content was positively correlated to NADPH-dependent superoxide generation in both ventricles (fig. 3.10 B and C, previous page) (RV: $r = 0.8$, $p = 0.0004$; LV: $r = 0.7$, $p = 0.0026$).

3. 2. 4. NADPH oxidase-related redox signalling: MAPKs activation

To investigate the possible activation of redox-sensitive MAPKs, we evaluated the phosphorylation level of JNK, ERK and p38. JNK phosphorylation status did not change in failing ventricles compared to the respective NF controls (fig. 3.11 A).

Conversely, fig. 3.11 B shows a significant increase in ERK1/2 phosphorylation level in RV from IHD (2.96-fold, $p < 0.001$ *Vs* NF) and, to a lesser extent, from DCM (1.80-fold, $p < 0.01$ *Vs* NF); in LV specimens, a significant increase (1.58-fold, $p < 0.01$ *Vs* NF) was observed only in IHD. Furthermore, ERK activation positively correlated with NADPH oxidase activity in both ventricles (RV: $r = 0.83$, $p = 0.0001$; LV: $r = 0.62$, $p = 0.014$). p38 as well showed a significant enhancement in the phosphorylation status both in RV and LV specimens from failing myocardium compared to respective controls (fig. 3.11 C). The increase in p38 phosphorylation was comparable in the RV and LV, obtained from either IHD (RV 3.90-fold, $p < 0.001$ *Vs* NF; LV 3.92-fold, $p < 0.001$ *Vs* NF) or DCM hearts (RV 2.21-fold, $p < 0.05$ *Vs* NF; LV 2.85-fold, $p < 0.001$ *Vs* NF). Interestingly, MDA content in failing hearts showed a significant correlation with p38 phosphorylation status in both RV ($r = 0.95$; $p = 0.0001$) and LV specimens ($r = 0.86$; $p = 0.0001$). Overall, these findings suggest that ERK phosphorylation is associated with increased NADPH oxidase activity, and support a role for elevated MDA levels in p38 activation, in agreement with previous reports in cellular models[259].

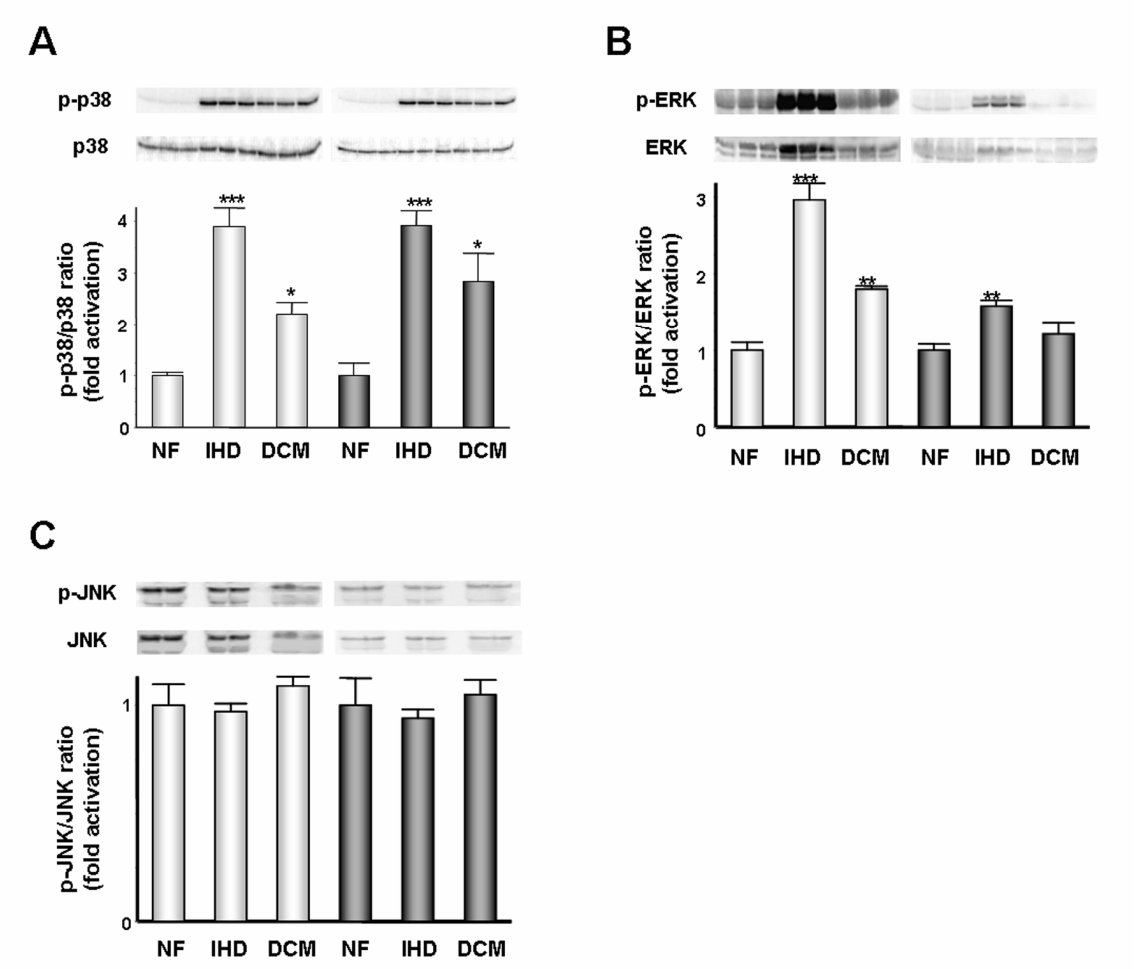

Figure 3.11. Activation of p-38 (A), ERK1/2 (B) and JNK (C) in human RV and LV. Every panel shows representative immunoblotting for p-p38, p-ERK1/2 and p-JNK and relative total protein in non failing and failing ventricle homogenates (top). The densitometric quantification of the phosphorylated/total MAPKs protein content ratio (bottom) is also reported; RV, open bars; LV, solid bars. n=6, non failing, NF and n=7 failing ventricles from IHD or DCM. * $p < 0.05$; ** $p < 0.01$; *** $p < 0.001$ *Vs* NF.

3. 2. 5. Relationship between left and right ventricles

The results shown so far suggest the occurrence of a similar sequence of biochemical events in both ventricles from failing hearts. Furthermore, a significant correlation was found between the values measured in LV and RV of the same hearts for all relevant steps of the oxidative stress pathway (fig. 3.12), in particular NADPH-dependent $O_2^{\cdot -}$ production (A), MDA content (B), p38 (C) and ERK1/2 activation (D).

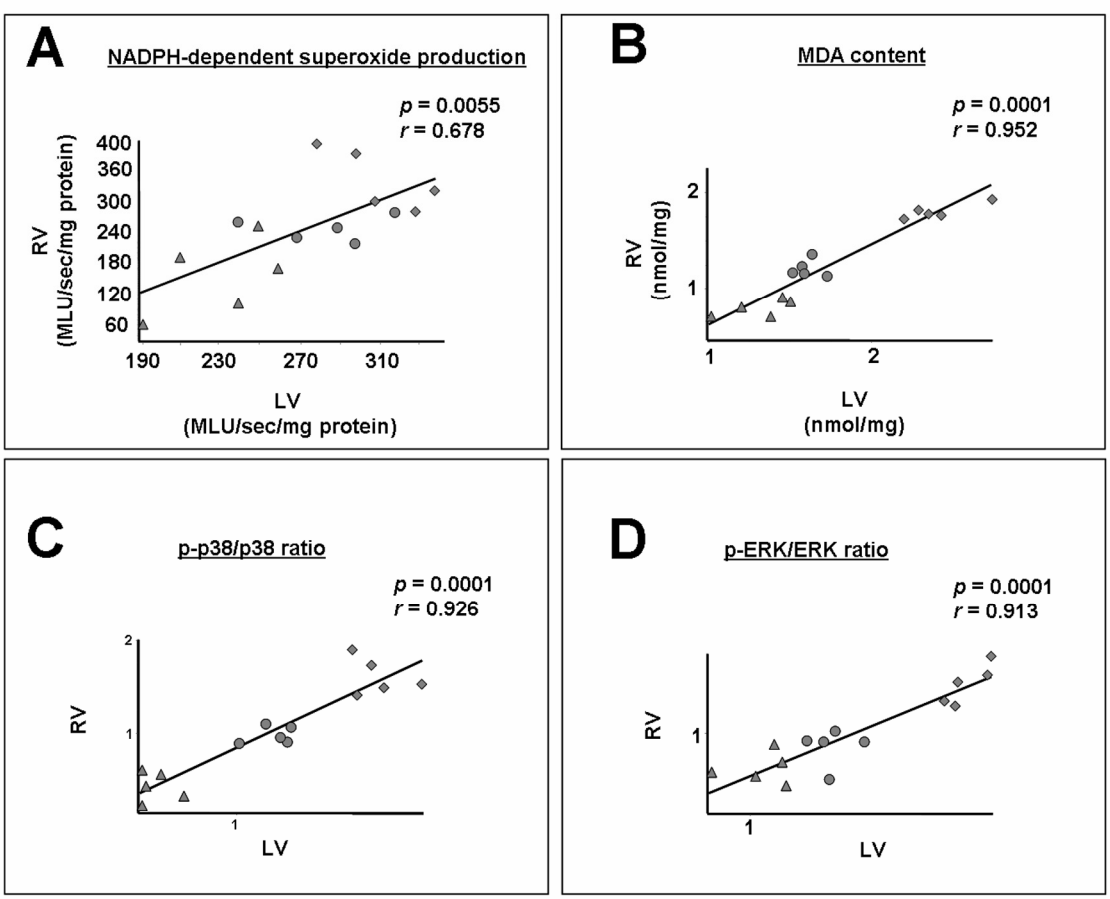

Figure 3.12. Oxidative stress pathway. Correlations between: RV and LV NADPH-dependent $O_2^{\cdot-}$generation (A), RV and LV MDA content (B), RV and LV p-38 activation (C) and RV and LV ERK 1/2 activation (D). NF (▲), DCM (●) and IHD (◆) ventricles. n=5 for each group.

3. 3. PART II – 2nd STUDY: NADPH oxidase-dependent antioxidant enzymes activation in end-stage human failing hearts secondary to IHD and DCM

3. 3. 1. NADPH oxidase activity

Our previous results demonstrated an involvement of NADPH oxidase in human failing hearts regardless of the aetiology of the disease (IHD or DCM)[53]. For this reason, in this study we did not distinguish samples from ischemic and non ischemic cardiomyopathy.

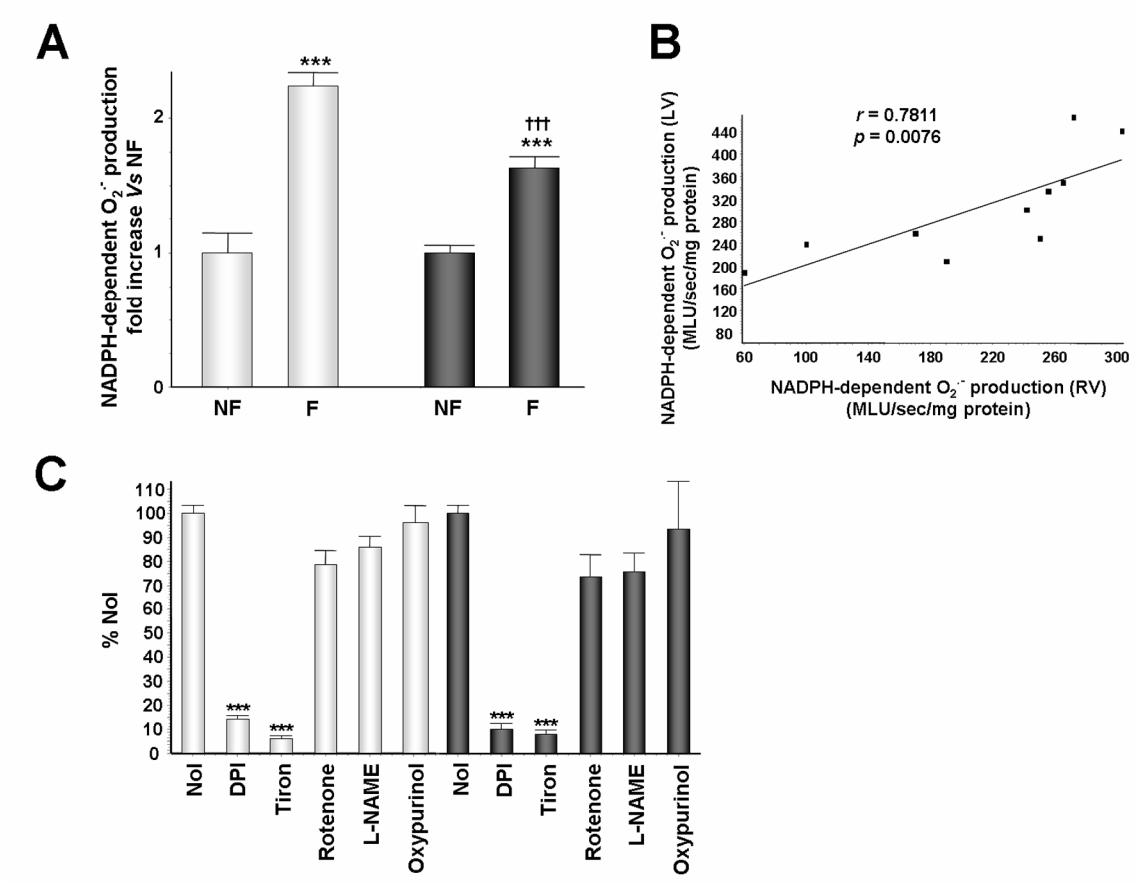

Fig. 3.13: (A) NADPH-dependent superoxide production in human RV (open bars) and LV (solid bars) from non failing (NF) and failing hearts (F) detected by lucigenin chemiluminescence. *** $p < 0.001$ *Vs* NF; ††† $p < 0.001$ *Vs* RV failing hearts. n = 5 NF and n = 12 failing ventricles from hearts with IHD or DCM. Data are presented as mean ± S.E.M. and expressed as fold increase relative to NF. (B) Correlation between left and

right ventricle NADPH-dependent superoxide production of the same failing and non failing hearts; n =5 for each group. MLU, mean arbitrary light units. (C) Effect of specific oxidases inhibitors on NADPH-dependent superoxide production in RV and LV from human failing hearts. Data are presented as mean ± S.E.M. and expressed as percentage of the value measured in the absence of inhibitors (NoI). *** $p < 0.001$ *Vs* NoI.

We confirmed a higher and significant NADPH-dependent $O_2^{\cdot-}$ production in new samples of diseased LV and RV from human failing heart compared to new samples of NF controls. In particular, a 2.23-fold increase ($p<0.001$ *Vs* NF) was observed in the RV from failing hearts, while in failing LV the increase (1.64-fold) was less marked, although statistically significant (fig. 3.13 A). In addition, a significant correlation was found between the values observed in LV and RV of the same failing heart (fig. 3.13 B) ($r=0.7811$; $p=0.0076$). NADPH dependent superoxide production was greatly inhibited in both failing RV and LV samples only by the NADPH oxidase inhibitor DPI (85%; $p<0.001$) and by the $O_2^{\cdot-}$ scavenger tiron (90%; $p<0.001$) (fig. 3.13 C), whereas it was unaffected by the xanthine oxidase inhibitor, oxypurinol, and reduced non significantly by NOS inhibitor (L-NAME) and by the inhibitor of the mitochondrial electron transport chain, rotenone.

3. 3. 2. Antioxidant enzymes defences: catalase

We performed a systematic analysis of antioxidant enzymes by measuring protein levels as well as activities of CAT, GPx and Mn-SOD, in failing and non failing ventricular specimens. As shown in fig. 3.14, protein levels (fig. 3.14 A) of CAT showed a trend for a decrease in their expressions that did not reach statistical significance between NF and failing RV and LV. By contrast, the enzymatic activity was significantly enhanced in both ventricles from failing hearts and, in particular, diseased LV exhibited a marked increase compared to NF control (fig. 3.14 B) (RV 1.76-fold, $p<0.05$; LV 3.04-fold, $p<0.001$; F *Vs* NF). Interestingly, the level of CAT activity in failing LV was also significantly higher than that observed in failing RV (RV:17.13 ± 1.29 μmol/min/mg protein; LV: 23.88 ± 1.50 μmol/min/mg protein $p<0.005$).

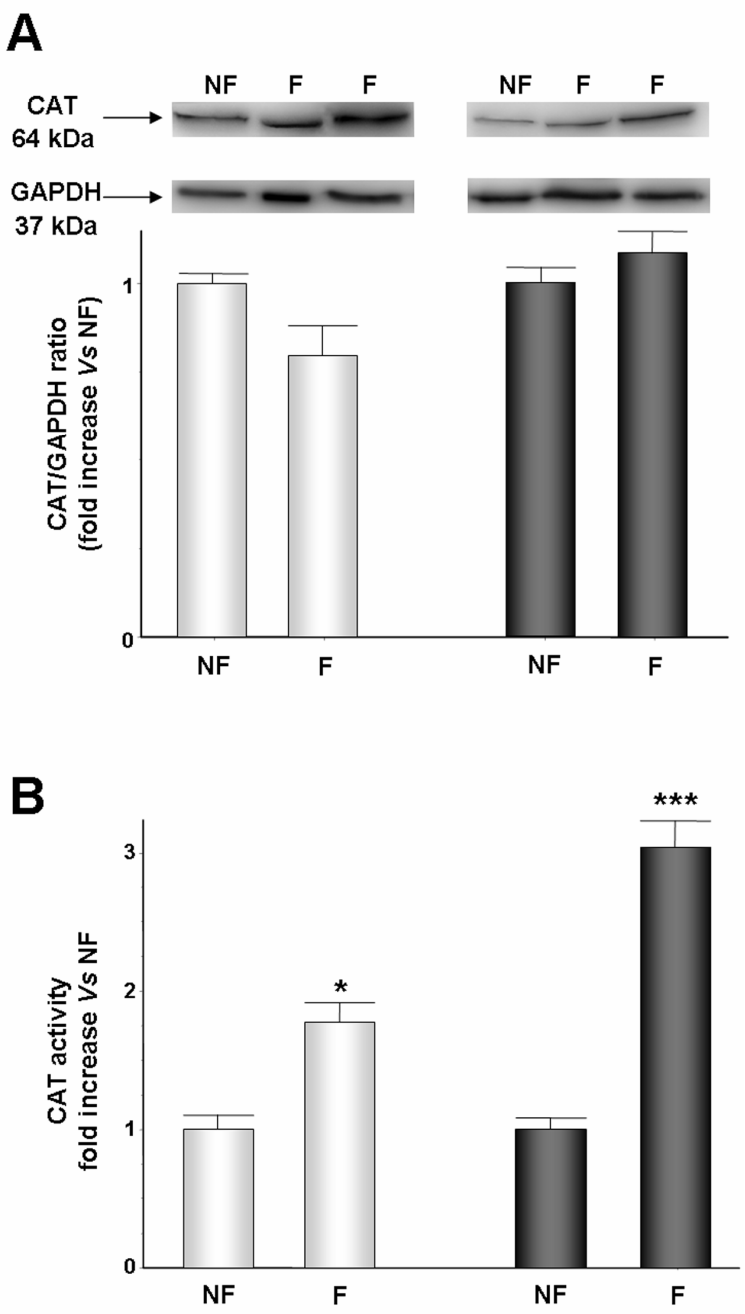

Fig. 3.14: Catalase (CAT) protein expression and catalytic activity in human RV (open bars) and LV (solid bars) from non failing and failing hearts. (A) Representative immunoblot (top) and densitometric quantification (bottom) of CAT protein expression relative to GAPDH expression. (B) Enzymatic activity of CAT detected by a spectrophotometric method. Data are presented as mean ± S.E.M. and expressed as fold increase relative to NF. * $p < 0.05$ *Vs* NF; *** $p < 0.001$ *Vs* NF. n = 5 NF and n = 12 failing ventricles from hearts with IHD or DCM.

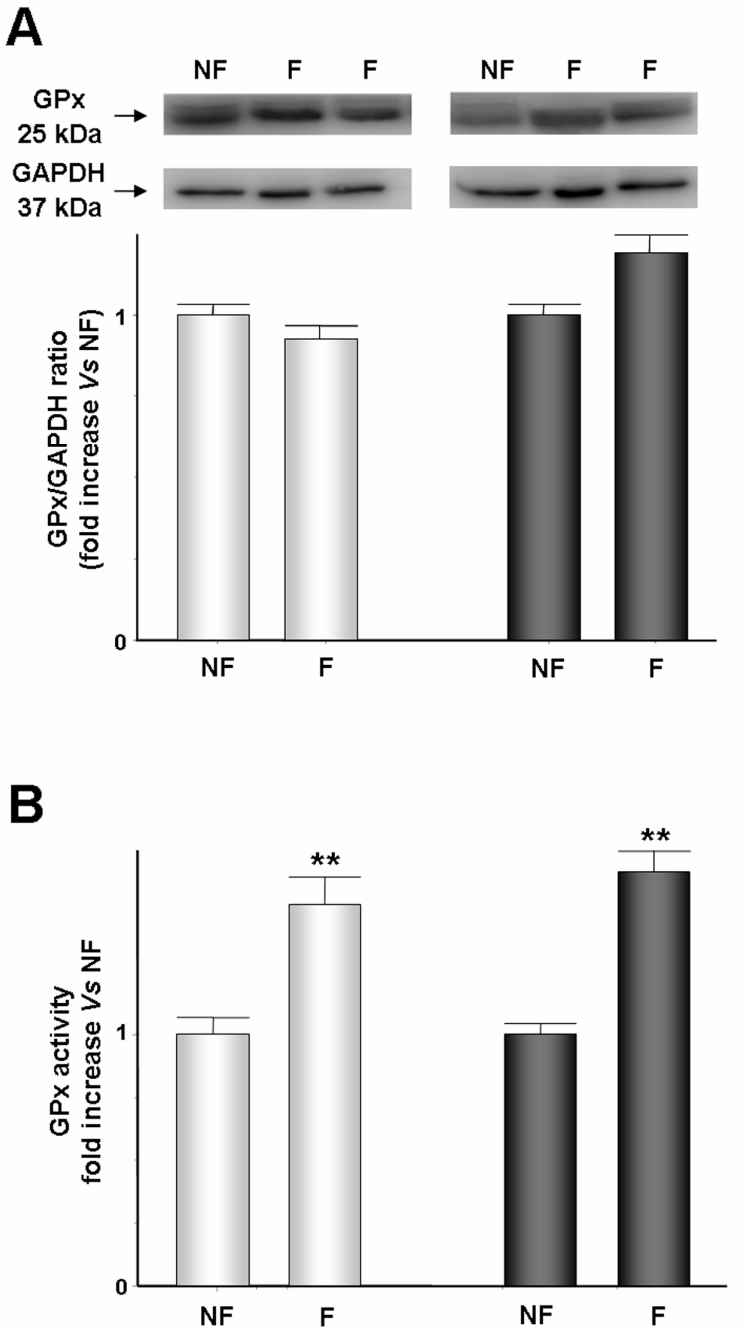

Fig. 3.15: Glutathione peroxidase (GPx) protein expression and catalytic activity in human RV (open bars) and LV (solid bars) from non failing and failing hearts. (A) Representative immunoblot (top) and densitometric quantification (bottom) of GPx protein expression relative to GAPDH expression. (B) Enzymatic activity of GPx detected by a spectrophotometric method. Data are presented as mean ± S.E.M. and expressed as fold increase relative to NF. ** $p < 0.01$ *Vs* NF. n = 5 NF and n = 12 failing ventricles from hearts with IHD or DCM.

3. 3. 3. Antioxidant enzymes defences: glutathione peroxidase

Immunoblotting of GPx protein expression, detected with a commercially available rabbit polyclonal antibody, gave two different bands that, in unboiled and boiled samples, migrated, respectively, to a position of approximately 92 kDa and, of 22 kDa, representing GPx homotetramer and monomer. The intensity of both bands from failing RV and LV appeared unchanged relative to the control (fig. 3.15 A, previous page). Densitometric analysis of 22 kDa band confirmed that no differences in protein expression exists between failing and NF RV and LV. Instead, GPx activity was significantly increased in failing RV and LV (fig. 3.15 B, previous page) with a similar increment in their activities relative to NF hearts (RV 1.52-fold, $p<0.01$; LV 1.65-fold, $p<0.01$; F *Vs* NF).

3. 3. 4. Antioxidant enzymes defences: mitochondrial superoxide dismutase

Mn-SOD is the mitochondrial isoenzyme that accounts for 90% of total SOD activity in heart . Mn-SOD protein expression was unaffected in both failing ventricles, compared with NF ones (fig.3.16 A). Mn-SOD enzymatic activity, normalized to citrate synthase activity as a marker of mitochondrial mass, appeared significantly decreased in failing RV and LV (fig.3.16 B).

These findings suggest that a similar adaptive response occurs in human failing LV and RV and that the increase or the decrease in antioxidant enzymes activities is largely attributable to post-translational modifications induced by oxidative stress.

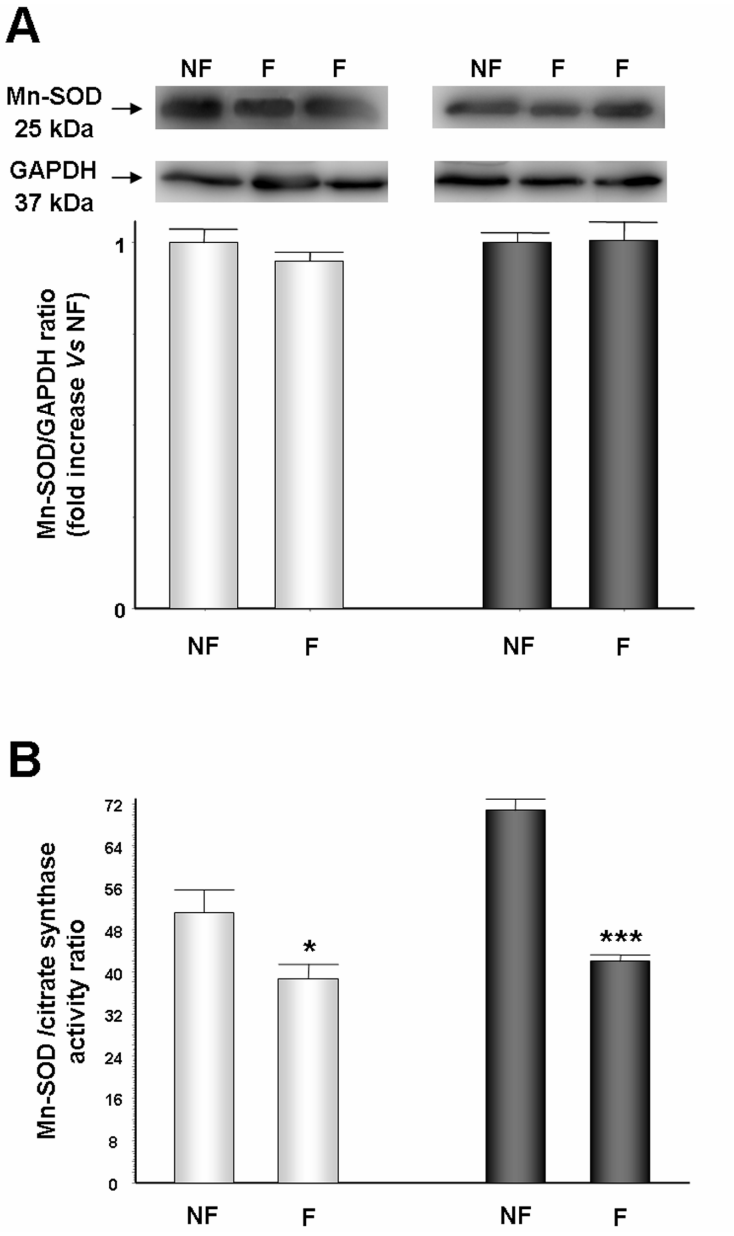

Fig. 3.16: Mn-Superoxide Dismutase (Mn-SOD) protein expression and catalytic activity in human RV (open bars) and LV (solid bars) from non failing and failing hearts. (A) Representative immunoblot (top) and densitometric quantification (bottom) of Mn-SOD protein expression relative to GAPDH expression. (B) Enzymatic activity of Mn-SOD detected by a spectrophotometric method and related to Cytrate synthase activity, a marker of mitochondrial mass. Data are presented as mean ± S.E.M. and expressed as fold increase relative to NF.* $p < 0.05$ *Vs* NF; *** $p < 0.001$ *Vs* NF. n = 5 NF and n = 12 failing ventricles from hearts with IHD or DCM.

3. 3. 5. Tyrosine-phosphorylation in failing hearts

Recent studies from Cao and co-workers reported that in response to increased oxidative stress the Abl family of mammalian non-receptor tyrosine kinases, including c-Abl and Arg, were activated. This activation was associated with a phosphorylation of CAT and GPx with a subsequent stimulation of their activity[214,222].

To determine if catalase activity was regulated by (Tyr) phosphorylation, the same membrane used to analyze CAT protein expression was reblotted with the anti-Tyr(P) antibody. Interestingly, as shown in fig. 3.17, the bands corresponding to failing RV and LV samples appeared markedly phosphorylated while no signal was found in NF samples.

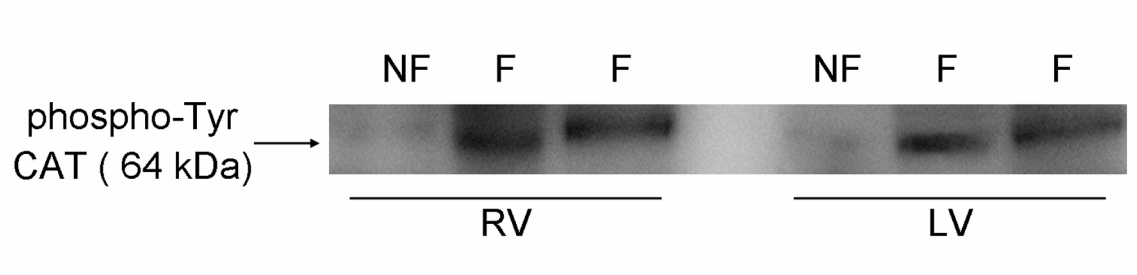

Fig. 3.17: Representative immunoblot of tyrosine phosphorylation of catalase (CAT) in human RV and LV from non failing (NF) and failing (F) hearts with IHD or DCM. The bands were detected with a specific antibody for phospho-tyrosine, as described in Chapter 2.

3. 3. 6. Correlation between NADPH oxidase and antioxidant enzymes activities

In order to verify the link between oxidative stress and the activation of antioxidant enzymes, we investigated possible correlations between the activity of NADPH oxidase and the activity of CAT and GPx in the RV and LV. As shown in fig. 3.18, a significant and positive correlation was found between the values of NADPH oxidase-dependent superoxide production and both CAT (fig. 3.18 A) (RV: $r = 0.8142$, $p < 0.0007$; LV: $r =$

0.7784, $p < 0.0001$) and GPx (fig. 3.18 B) (RV: $r = 0.6897$, $p = 0.0091$; LV: $r = 0.8744$, $p = 0.0001$) activities in LV and RV.

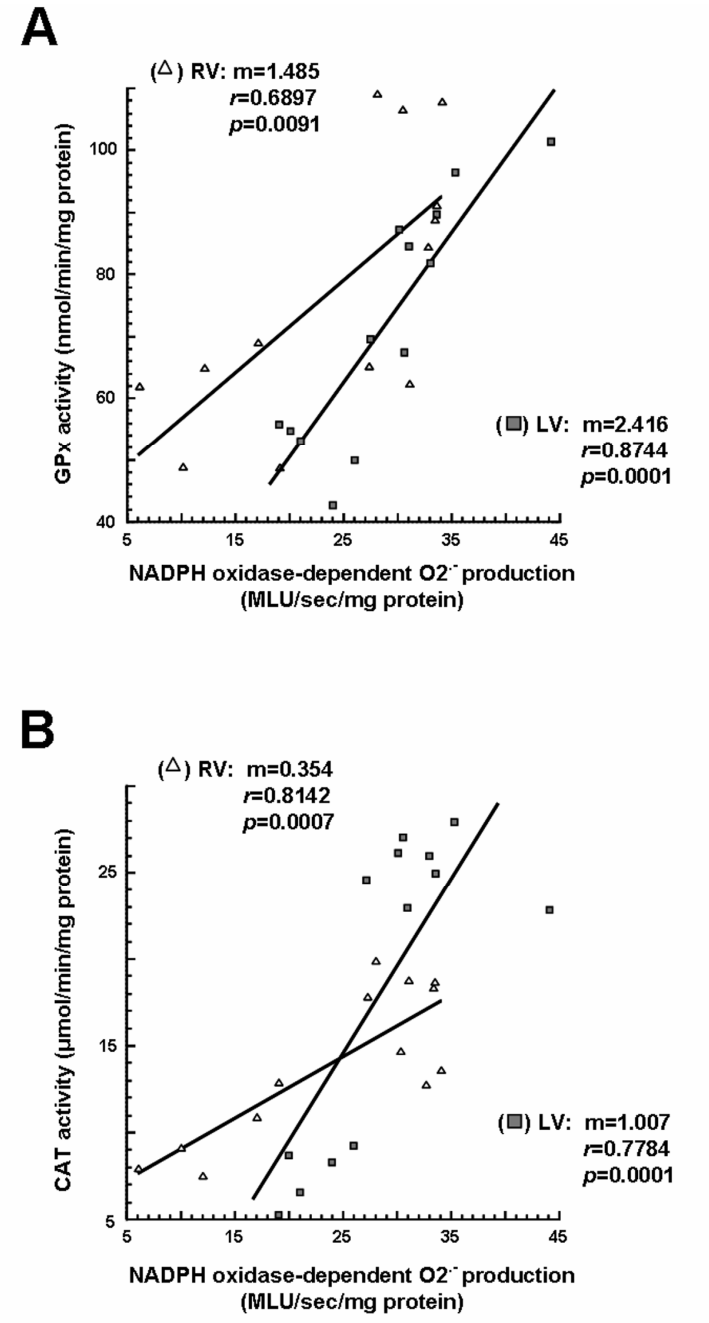

Fig. 3.18: Correlations between NADPH-dependent superoxide production and GPx (A) or CAT (B) enzymatic activity of the same failing and non failing hearts; n = 5 NF and n = 8 failing ventricles from hearts with IHD and DCM. MLU, mean arbitrary light units. ▲, RV; ■, LV.

Of interest, the slope of linear correlation appeared to be steeper in LV than in RV for both CAT (LV: m = 1.007; RV: m = 0.354) and GPx (LV: m = 2.416; RV: m = 1.485), suggesting that antioxidant defences react more intensively to oxidative stress damage in LV than in RV.

3. 3. 7. Lipid peroxidation

Consistently with the differences observed in antioxidant enzymes activities, MDA levels measured as an indirect marker of ROS activity, were significantly elevated in both ventricles from failing hearts (fig. 3.19). However, diseased RV exhibited a particularly marked increase in lipoperoxidative damage compared to NF control (RV from failing hearts: 1.80 fold increase *Vs* RV from non failing hearts; LV from failing hearts: 1.51 fold increase *Vs* LV from non failing hearts).

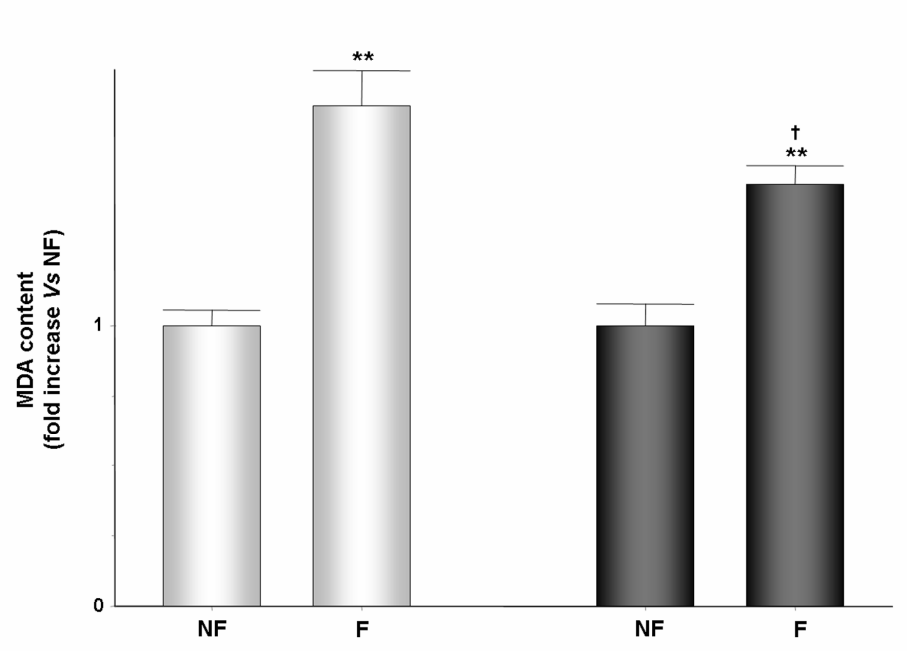

Fig. 3.19: MDA content in human RV (open bars) and LV (solid bars) from non failing and failing hearts. Data are presented as mean ± S.E.M. and expressed as fold increase relative to NF. ** $p < 0.01$ *Vs* NF; † $p < 0.05$ *Vs* RV failing hearts. n = 5 NF and n = 12 failing ventricles from hearts with IHD or DCM.

3. 4. PART II – 3rd STUDY: NADPH oxidase-dependent redox signalling in end-stage human failing hearts secondary to MIC

3. 4. 1. NADPH-dependent superoxide production

As observed for the precedent two studies, superoxide production was minimal in myocardial homogenate from LV failing and non failing hearts both in the absence of substrates and in the presence of succinate (data not shown). After the addition of NADPH, $O_2^{\cdot -}$ production raised significantly in all FH compared with control samples. However, this phenomenon was more intense in MIC, with a 2-fold increase in $O_2^{\cdot -}$ production compared with DCM and IHD (fig. 3.20 A). Detection of superoxide was virtually abolished by tiron. To investigate the sources of superoxide production, experiments were repeated in the presence of specific inhibitors of potential ROS-generating systems. In all failing hearts samples, $O_2^{\cdot -}$ generation was significantly decreased by DPI, confirming the phagocyte-type NADPH oxidase as a major source of $O_2^{\cdot -}$. In addition, MIC hearts showed a significant decrease in $O_2^{\cdot -}$ production in the presence of rotenone and oxypurinol (fig. 3.20 B), whereas the presence of L-NAME ester hydrochloride had no effect (data not shown).

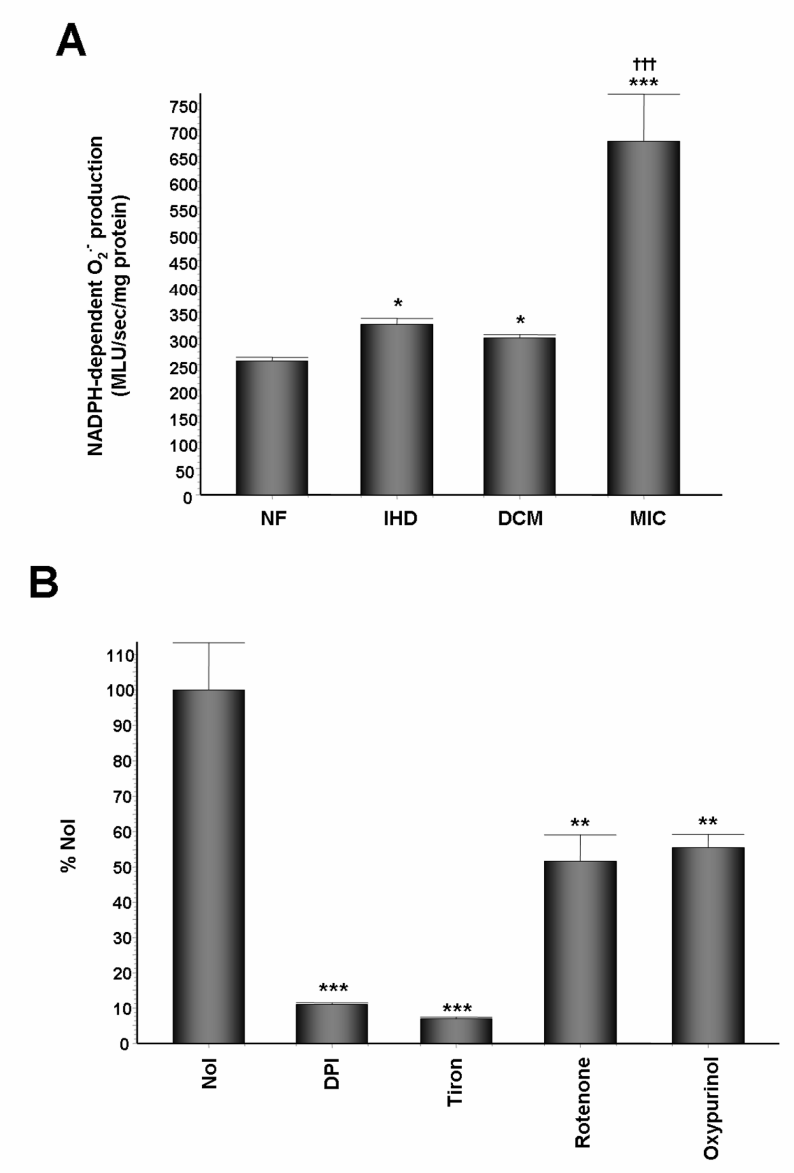

Fig. 3.20: (A) NADPH-dependent superoxide production in human LV from non failing (NF) and failing hearts secondary to IHD, DCM and MIC detected by lucigenin chemiluminescence. MLU, mean arbitrary light units. * $p < 0.05$ and *** $p < 0.001$ *Vs* NF; ††† $p < 0.001$ *Vs* IHD and DCM. n = 8 NF and n = 9, n = 4, n = 3 failing ventricles from hearts with IHD, DCM and MIC, respectively. Data are presented as mean ± S.E.M. (B) Effect of specific oxidases inhibitors on NADPH-dependent superoxide production in LV from human failing hearts secondary to MIC in the absence (NoI) or presence of the specific inhibitors DPI, tiron, rotenone or oxypurinol. Data are presented as mean ± S.E.M and expressed as percentage *Vs* NoI sample. *** $p < 0.001$ and ** $p < 0.01$ *Vs* NoI.

3. 4. 2. Antioxidant enzymes defences: glutathione peroxidase

GPx enzymatic activity did not show any significant change in LV MIC hearts, despite a clear trend toward an increase (fig. 3.21). The lack of statistically significant change in GPX activity may be due to variability within the control groups. The same variability should be also the main cause of both the apparent or the statistically significant decrease of GPx activity in LV DCM or IHD, respectively. Such a decrease appears in contrast with the results showed in § 3. 3. 3.

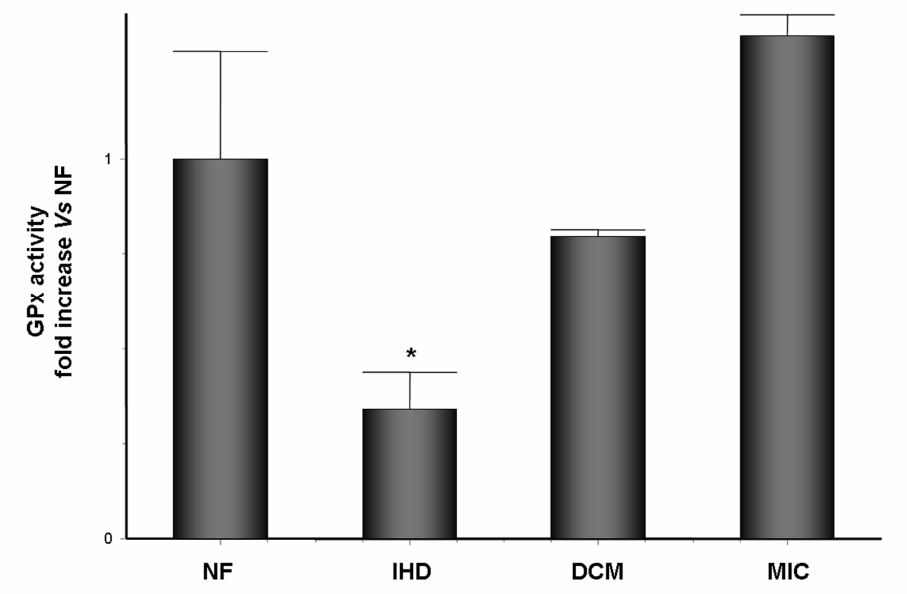

Fig. 3.21: Enzymatic activity of GPx in human LV from non failing (NF) and failing hearts secondary to IHD, DCM and MIC detected by a spectrophotometric method. * $p < 0.05$ *Vs* NF. n = 8 NF and n = 9, n = 4, n = 3 failing ventricles from hearts with IHD, DCM and MIC, respectively. Data are presented as mean ± S.E.M and expressed as fold increase *Vs* NF hearts.

3. 4. 3. Antioxidant enzymes defences: mitochondrial superoxide dismutase

Mn-SOD enzymatic activity appeared unchanged in LV failing hearts from MIC, IHD and DCM biopsies, relative to LV non failing hearts (fig. 3.22).

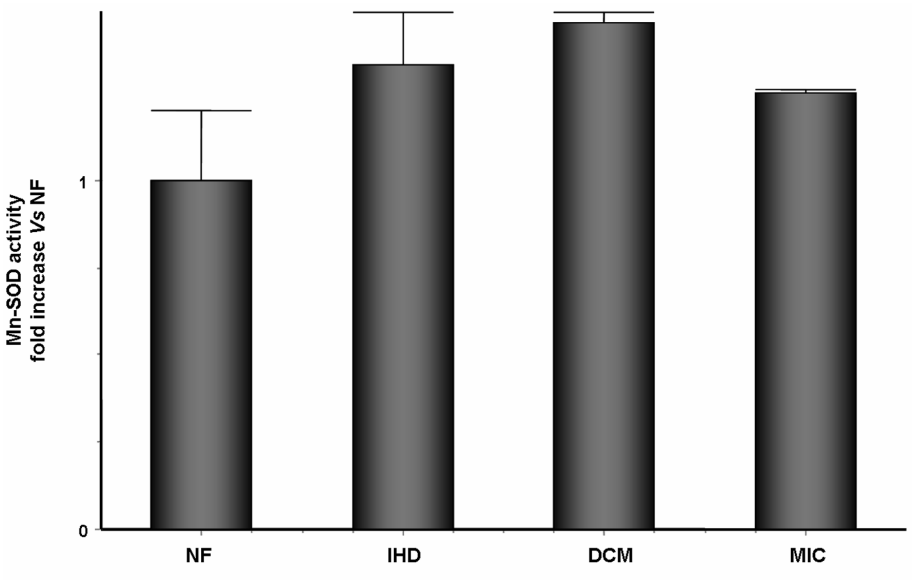

Fig. 3.22: Enzymatic activity of Mn-SOD in human LV from non failing (NF) and failing hearts secondary to IHD, DCM and MIC detected by a spectrophotometric method. n = 8 NF and n = 9, n = 4, n = 3 failing ventricles from hearts with IHD, DCM and MIC, respectively. Data are presented as mean ± S.E.M and expressed as fold increase *Vs* NF hearts.

CHAPTER 4

DISCUSSION

4. 1. Role of NADPH oxidase-dependent superoxide production in H9c2 cells subjected to simulated ischemia/reperfusion

The most novel finding of this study is that the production of ROS derived from NADPH oxidase was enhanced in cardiac myoblasts subjected to a prolonged simulated ischemia followed by 1 h reperfusion. The increased ROS intracellular content was associated to an enhanced lipid peroxidation, to the activation of specific redox-sensitive kinases and to cell death. The use of NADPH oxidase activity inhibitor DPI during reperfusion largely prevented simulated I/R induced ROS production; the latter matched a reduction in MDA content, a significant decrease in p-JNK/JNK ratio and an evident protection against cell death.

The main aim of our study was to describe the role of NADPH oxidase in cardiac muscle cells exposed to simulated I/R. In fact, albeit several recent studies have examined the influence of myocardial I/R on NADPH oxidase, there are only few and conflicting data about the contribution of this oxidase complex to I/R-cell damage and its regulation. The present investigation follows our previous demonstration that, in the myocardium from end-stage ischemic and non ischemic cardiomyopathies, an increased NADPH oxidase activity was significantly correlated with enhanced lipid peroxidation and activation of redox sensitive kinases, particularly ERK and p38. The limitation on finding a clear evidence for a cause-effect relationship in end-stage hearts[53] is the reason for using H9c2 cardiomyoblasts line in the present study. This cell line, sharing features of adult cardiomyocytes[261], is considered a valuable model for mechanicistic studies aimed to investigate the pathways implicated in cardiac cell death following oxidative

stress[262]. Previous works in this area include studies of oxidative cell damage caused by doxorubicin[262], hydrogen peroxide[263] and ischemia/reperfusion[264]. As described in the chapter of "Experimental procedures", H9c2 cells were subjected to an *in vitro* simulated 24 h ischemia followed by 1 h of simulated "reperfusion". Several reports have documented the need for long term hypoxia (24–72 h) for the appearance of evident damages in primary cultures of neonatal rat cardiac myocytes[264] and this is the reason why such a prolonged ischemia was used. Unpublished data from our laboratory confirmed a similar behaviour also for H9c2 cardiomyoblasts, indicating 24 h of simulated ischemia followed by 1 h of reperfusion as the optimal experimental condition to obtain significant alterations in this cell line.

Potential sources of oxidative stress during I/R include mitochondria, NADPH oxidase, and xanthine oxidase. However, a comprehensive understanding of the relative contributions of these systems during I/R has not yet emerged. In the present study cardiomyoblasts exposed to simulated I/R conditions showed an increased intracellular ROS production that, as indicated by DCF fluorescence, was remarkably suppressed by the superoxide scavenger Tiron. A similar significant reduction was obtained with apocynin, widely considered as a specific NADPH oxidase inhibitor, and DPI, a potent flavoprotein inhibitor non specific for NADPH oxidase but commonly used as a NOX inhibitor. On the other hand, rotenone, a specific mitochondrial oxidase inhibitor and oxypurinol, a xanthine oxidase inhibitor, appeared to fail in reducing ROS production. These findings suggest that, under our simulated I/R conditions, superoxide was the main ROS produced and NADPH oxidase was its major source, although other contribution in ROS generation can not be ruled out. The prominent role of NADPH oxidase in superoxide generation was confirmed by lucigenin chemiluminescent measurements showing that NADPH, but not other added substrates, increased the capacity of cardiomyoblasts exposed to simulated I/R to produce this particular radical specie.

Previous investigations in cell and animal models highlighted that NADPH oxidase activation occurs through either increased expression or post-translational modifications and translocation of the oxidase subunits[66,100,265]. Recent studies have reported in H9c2 cell line the presence of the NOX2/gp91^{phox} isoform previously identified in human cardiomyocytes[266]. In the present study we have confirmed this

observation and we have additionally found that the same cells subjected to simulated I/R showed an increased expression of NOX2/gp91^{phox}; this effect, observed through Western blotting, was furthermore confirmed by immunocytochemical analysis. The increase in NOX2/gp91^{phox} after simulated I/R was not abolished by DPI treatment but this is a not surprising finding since DPI is an oxidase activity inhibitor and no data report its effects on protein expression.

A parallel translocation of p47^{phox} from the cytosol to the membrane was also observed, as shown by a significant increase of the p47^{phox} membrane/cytosol ratio. Serine phosphorylation of p47^{phox} by protein kinase C appears to be the prerequisite for p47^{phox} translocation and its stable interaction with membrane-bound cytochrome b_{558}, which results in oxidase activation[100]. It is well known that many stimuli, such as angiotensin II or TNF-α, can increase NADPH oxidase activity by PKC phosphorylation[100]. PKCs are also important for stress responses in various tissues and PKCε is the primary PKC isoform that is affected by hypoxia or ischemia in heart muscle[267]. Recently, some authors have shown that the addition of chelerythrine, a broad spectrum PKC inhibitor, or apocynin, a NADPH oxidase inhibitor, before reoxygenation of anoxic endothelial cells, decreased $O_2^{-\cdot}$ production to comparable levels, indicating a PKC-dependent NADPH oxidase activation[268]. It seems reasonable that also in our experimental model the activation of PKC induces p47^{phox} phosphorylation, its subsequent translocation to the membrane and its interaction with membrane-bound cytochrome b_{558}, followed by the increased production of superoxide radical.

Recent studies reported that ischemia resulted in NOX2/gp91^{phox} upregulation in H9c2 cells and that DPI had no effect on NOX2/gp91^{phox} expression[266]. In line with this finding, we found that DPI treatment did not decrease NOX2/gp91^{phox} expression in our cells exposed to simulated I/R, rather it reduced $O_2^{-\cdot}$ generation and p47^{phox} translocation. While it is generally accepted that DPI decreases NADPH oxidase-derived ROS production, a reduced p47^{phox} translocation did not appear so obvious. To our knowledge, whereas it is recognized that the interaction of apocynin with the oxidase may form a structure that impedes the binding between p47^{phox} subunit and cytochrome b_{558}, no data exists about the mechanism by which DPI might interfere with the formation of the oxidase complex. This aspect surely needs further investigation, but

the above reported findings suggest that under our experimental conditions both the increase in NOX2/gp91^{phox} expression and p47^{phox} translocation to the membrane contribute to the observed NADPH oxidase activation.

The ROS-mediated membrane lipid peroxidation has been proposed as a main chemical modification resulting in cell death[269]. In our experimental conditions, cardiomyoblasts subjected to simulated I/R displayed significant increases in lipid peroxidation, as shown by their MDA levels, and in cell death. Both these events were prevented by DPI treatment, which indicates, in agreement with previous findings[270], NADPH oxidase-generated ROS as one of the most important contributors to the I/R-induced lipid peroxidation and the related effects, including cell death.

In this connection, although the downstream pathways through which NADPH oxidase activation could lead to cardiac cell death remain to be fully elucidated, it has recently been demonstrated that myocardial I/R activates MAPK subfamilies, including the stress responsive JNK and p38, both involved in cell death, and ERK, implicated in cell survival signalling. However, p38 does not appear to be activated in all I/R models and some authors reported that during ischemia the increase of p38 activity is initially rapid but subsequently declines rapidly[271]. In agreement with these observations, we did not find any modification of the p-p38/p38 ratio under our experimental conditions. Instead, we observed a significant activation of ERK and, to a higher extent, of JNK, whose phosphorylation was positively and significantly correlated with the cell death indexes. DPI treatment of I/R cardiac myoblasts did not affect p-ERK/ERK ratio, whereas it significantly decreased JNK phosphorylation, suggesting a different mechanism of I/R-induced activation for these two MAPKs. The DPI effect on JNK activation was similar to that observed with SP600125, a specific inhibitor of JNK. Interestingly, these two unrelated inhibitors displayed a similar protective effect also in preventing I/R cell death. Taken together, these findings suggest that the NADPH oxidase-derived superoxide production plays a relevant role in JNK activation, as demonstrated by the positive and significant correlation between the two events. In turn, JNK activation appears to be determinant to induce cell death after simulated I/R.

The simultaneous activation of this kinase and ERK is not surprising and many *in vivo* and *in vitro* studies reported a concomitant activation of these two kinases after hypoxia/ischemia and reoxygenation. Moreover, when stimuli concomitantly activate

multiple MAPKs the physiological response to stimulus will depend on the time course and strength of the signal. The balance between MAPK activation levels may influence cellular fate and turn towards cell death or life. In our experimental model, the concomitant activation of ERK and JNK might explain the moderate increase (about 26%) in cell death observed in post-ischemic reperfused cells. Moreover, the partial reduction of ERK phosphorylation following DPI treatment suggests that this process, at least in our experimental conditions, was activated by other factors in addition to oxidative stress.

I/R-triggered cardiomyocyte death can occur by either apoptosis or necrosis. However, it should be considered that the mode of cell death resulting from I/R injury depends, to some extent, on the experimental conditions, and that necrosis and apoptosis represent only the extremes of a continuum of various modes of cell death. At any rate, we did not assess the relative incidence of these two forms of cell death, since this issue was beyond the scope of the study.

In conclusion, in this study we have pointed out the NADPH oxidase as a critical enzyme for the increase in I/R-induced oxidant generation in cardiac cells. At the same time, we provided evidence for the mechanism of NADPH oxidase activation. Furthermore, the inhibition of the NADPH oxidase by the flavoenzyme inhibitor DPI largely prevents I/R induced lipoperoxidative damage and the activation of JNK pathway, associated to cell death, without affecting the ERK related survival response. We are conscious that this study was performed using both a non-contractile cell line, that poorly took account of the load factor, and an *in vitro* model of simulated ischemia/reperfusion, that is devoid of any exogenous neuro-humoral influence. In spite of these limitations, the marked improvement of cell survival, as a result of NOX2/gp91^{phox} inhibition in our experimental conditions, stress the importance to perform further investigation, including *in vivo* studies to outline cardioprotective strategies against I/R injury, a condition of great importance in the clinical setting.

4. 2. Role of NADPH oxidase-dependent superoxide production in end-stage human failing hearts secondary to ischemic and non ischemic cardiomyopathies

4. 2. 1. First study

This study demonstrates for the first time that in human heart failure, increased ROS generation by NADPH oxidase is significantly related with enhanced lipid peroxidation and activation of redox-sensitive kinases. Our results extend the previous and scant findings obtained in the diseased human heart, mostly focused on single aspects of the complex oxidative stress pathway[66,272], and those inferred from studies in cellular and animal models[65,100,273]. Our data give an insight into the chain of biochemical mechanisms arising from increased NADPH oxidase activity, and originally demonstrate that these events are present in the right and left ventricle, with a significant correlation between the two chambers.

NADPH oxidase has been addressed as a major source of $O_2^{-\cdot}$ in human vascular cells and cardiomyocytes[66,188]. Studies in cellular and animal models of hypertrophy highlighted that NADPH oxidase activation occurs in response to hypertrophic stimuli, including angiotensin II, noradrenaline and mechanical overload. In this study, we provide evidence of a coordinated increase of NADPH oxidase activity in the right and left ventricle of individual failing hearts. We focused our attention on the NOX2/gp91^{phox} NADPH oxidase subunit and on p47^{phox}. In agreement with a recent study performed in animal model of pacing-induced heart failure[274], we did not find an increased NOX2/gp91^{phox} protein expression in LV or RV homogenates from terminally failing hearts (data not shown). These data appeared in contrast with previous observation in human acutely infarcted heart[198]. This may not be contradictory, since in the infarcted heart, a localized increase in NOX2/gp91^{phox} is likely the expression of an inflammatory phase of tissue repair[198]. Conversely, in the present molecular and biochemical study, myocardial samples with minimal amounts of fibrosis and devoid of inflammatory infiltrate were selected. Another piece of the complex picture of NADPH oxidase-mediated signalling comes from recent studies in knockout mice, challenged with different hypertrophic stimuli. NOX2/gp91^{phox} contributed to interstitial fibrosis

and contractile dysfunction caused by pressure overload, but was not essential to NADPH-dependent superoxide generation and for cardiac hypertrophy. In contrast, NOX2/gp91^{phox} seems to play a crucial role in the hypertrophic response to angiotensin II. Taken together, the present and previous data suggest that increased NOX2/gp91^{phox} expression is not a prerequisite for increased NADPH-dependent ROS production.

On the other hand, we found both overexpression and membrane translocation of the regulatory subunit p47^{phox}. Consistently with our findings, an increased expression of p47^{phox} mRNA consequent to aortic constriction occurs in NOX2$^{-/-}$ mice, where it supports enhanced NADPH oxidase activity[191]. Interestingly, the relative contribution of the two regulatory mechanisms to NADPH oxidase activation appeared different in the two ventricles. Despite a lower homogenate p47^{phox} subunit expression, the ratio of p47^{phox} membrane bound to its cytosolic protein expression was higher in RV than in LV. Likely, this may depend on the fact that even a relatively low number of overexpressed p47^{phox} subunits translocated from cytosol to membrane are sufficient to produce a sharp increase in p47^{phox} membrane/cytosol ratio and, accordingly, in NADPH oxidase activity. Indeed, p47^{phox} translocation well correlated with NADPH oxidase activity in both ventricles, thus reinforcing the hypothesis that - in the human diseased heart - this mechanism is a requirement for enzyme activation. These results agree with previous findings showing that angiotensin II-induced ROS production is critically dependent on the p47^{phox} subunit and that pressure overload-induced myocardial hypertrophy in gp91^{phox} deficient mice is associated with increased mRNA p47^{phox}[191]. An original feature of the present study consists in trying to establish a precise correlation between NADPH oxidase-dependent superoxide generation and specific redox-regulated signalling pathways in human heart failure. In fact, the increased NADPH oxidase activity was associated with a parallel development of oxidative stress, as judged by the levels of MDA, the classical marker of lipid peroxidation. The latter mechanism is known to contribute to loss of membrane integrity and alteration of cellular functions. Moreover, experimental evidence exists of a relationship between MDA levels and the activation of redox-sensitive kinases, in particular p38[259]. In turn, p38 activation elicits a negative inotropic effect on cardiac myocytes and is possibly implicated in the progression of heart failure. In agreement with these observations, we found a significant positive correlation between relative

MDA content and p38 activation in human failing hearts. However, signalling pathways linking oxidative stress to pathophysiological response appear to be complex and differently regulated. In fact, first of all, we observed that, besides the aforementioned p38, ERK but not JNK was correlated to NADPH-dependent ROS production in end-stage failing hearts. The explanation of this finding is not obvious, since JNK is also known to be a stress-activated protein kinase. In experimental models, the activation of JNK is an early event in the onset of LV hypertrophy and declines during the development of heart failure, despite persistently increased NADPH oxidase activity[65]. On the contrary, activation of p38 and ERK occurs at the transition toward heart failure[65], and all our diseased samples were obtained from terminally failing hearts. Second, we found a higher degree of ERK activation in failing RV than LV. A merely speculative hypothesis is that ERK activation in response to oxidative stress depends on the increment rather than the absolute value of ROS levels.

Another novel finding of this study is the demonstration of a coordinated increase in NADPH oxidase activity, ROS generation and activation of specific redox-sensitive signalling pathways in the two ventricles. These data elicit questions about the mechanisms operating in this setting. Myocytes stretching, as a result of increased hemodynamic load, appears different in the two ventricles, although pressure overload due to secondary pulmonary hypertension occurs in end-stage heart failure. Interestingly, we observed a significant correlation between NADPH oxidase activity assessed in RV and the pulmonary artery pressure measured in the same patient. This finding suggests that mechanical overstretch of the right ventricle causes an increase in NADPH oxidase-dependent ROS generation. On the other hand, systemic and local alterations of the neurohormonal environment are likely operative in both ventricles, and may equally activate NADPH oxidase.

The findings of our study should be interpreted in the contest of their limitations. A mechanistic interpretation of the events downstream to NADPH oxidase activation is prevented in human end-stage hearts and therefore our results cannot provide a clear evidence for a cause–effect relationship. However, the highly significant correlations among ROS production, $p47^{phox}$ translocation and phosphorylation of specific MAP kinases are suggestive of a close association among these factors. Another insight provided by the present investigation is the correlation between the left and right

ventricle from the same patient, a report of scientific and prospectively clinical relevance. A rigorous statistical interpretation of such a correlation is difficult, since control, IHD or DCM values tend to cluster. This might indicate that, in our conditions, the etiology rather than the severity of the disease is crucial for the tested parameters; however, all diseased samples came from patients with end-stage heart failure. Studies in animal models with different degree of cardiac disease will hopefully allow a deeper understanding of the mutual relationship between left and right ventricular remodelling and causal mechanisms. Notwithstanding these limitations, as recently pointed out[275], advancing knowledge about molecular and functional characteristics of the right ventricle might lead to progress in the treatment of cardiomyopathies. In conclusion, notwithstanding the relative contribution of systemic and hemodynamic factors operative in human heart failure, that could differently activate distinct ROS sources and related redox signalling, our data strongly suggest that oxidative stress may contribute to harmful RV (besides LV) remodelling. Taking into account the role of RV function as a predictor of survival in heart failure patients, this observation provides new insights into the pathophysiological processes involved in the progression to end-stage heart failure and supports the therapeutic targeting of ROS-dependent processes.

4. 2. 2. Second study

The main finding of the present study is that, in human heart failure, activation of antioxidant enzymes is related to an increase in oxidative stress. This adaptive response mainly occurs through a post-translation modification of antioxidant enzymes coordinated in the right and left ventricle, without any changes in their relative protein expression. Moreover, human failing LV appears more protected than RV against oxidative stress damage.

The present results extend our previous findings aimed to assess the cascade of events triggered by increased NADPH oxidase activation in human failing right and left ventricles (§ 4. 2. 1). Besides confirming a high and significant $O_2^{-\cdot}$ production by a NADPH oxidase system in human failing hearts, this study sheds light on the molecular mechanisms underlying the increase of this activity. Through collaboration with the Department of Preclinical and Clinical Pharmacology at the University of Florence, mRNA expression of the two cardiac isoforms of the catalytic subunit of NADPH

oxidase, NOX2 and NOX4, were examined. These subunits are known to be differently modulated by hypertrophic stimuli . We did not observe any increase in their expressions, being mRNA levels for NOX4 unchanged and those for NOX2 significantly decreased in both RV and LV compared to non failing ventricles. This latter finding raises the possibility of a cross-regulation of NADPH oxidase subunits, such that loss of NOX2/gp91^{phox} leads to increased expression of other subunits involved in NADPH oxidase activation . Indeed, such an hypothesis is in good agreement with our previous observation of an overexpression and membrane translocation of p47^{phox} in human failing hearts and supports the prominent role of p47^{phox} for NADPH oxidase activation .

A major contribution of our results consists in the characterization of the mutual relationship between oxidant and antioxidant activity in RV and LV from human failing hearts. Experiments on the level of antioxidant enzymes mRNA were performed at the Department of Experimental Medicine at “La Sapienza” University of Rome.

Previous studies on antioxidant enzymes in human heart failure showed inconsistent results. In line with some authors we did not find changes in mRNA expression and protein levels of CAT and GPx in human failing hearts. On the contrary, CAT and GPx enzyme activities were markedly increased in failing RV and LV compared with NF ventricles. These data suggest that dissociation might occur between mRNA/protein expression of these enzymes and their activities. Therefore, the adaptive response to increased oxidative stress does not lead to increase transcription of these antioxidant enzymes but may reflect a post-translational modification.

Although the molecular mechanism underlying CAT (or GPx) activation could not be thoroughly instigated in this setting, both recent evidence in literature and our present results indicate a role of protein (Tyr)-phosphorylation. As a matter of fact, Cao and co-worker reported that in response to *in vitro* exposure to hydrogen peroxide the Abl family of mammalian non-receptor tyrosine kinases, including c-Abl and Arg, were activated. This activation was associated with the phosphorylation of CAT and GPx in specific tyrosine residues and with subsequent stimulation of their activity. Our evidence of an increased CAT (Tyr)-phosphorylation in both ventricles of failing hearts strongly suggests that this mechanism is operative also in human failing hearts. So, it is reasonable to hypothesize that the activation of c-Abl and Arg kinases and subsequent

stimulation of the catalytic activities of CAT and GPx provide a mechanism, albeit insufficient, to normalize the level of oxidative stress. To our knowledge, this is the first evidence supporting this intriguing hypothesis in human heart.

Differently from CAT and GPx, Mn-SOD activity was decreased in failing human ventricles, despite its gene expression was unchanged or even increased in RV. Therefore, similarly to CAT and GPx, the decrease in Mn-SOD activity might be attributed to post-translational modification. Indeed, experimental evidence *in vivo* indicates that MnSOD is nitrated and inactivated under pathological conditions, including cardiovascular disease . Thus, the possibility that inactivation of Mn-SOD by nitration in human heart failure remains a potential explanation that warrants deeper studies.

Notwithstanding the molecular mechanism underlying the modulation of antioxidant enzymatic defences, another original feature of the present study is the establishment of a correlation between NADPH-dependent ROS production and antioxidant enzyme activity in failing right and left ventricles. For both CAT and GPx activities, the slope of linear correlation appeared steeper in LV than in RV, suggesting a greater protection of the LV against oxidative stress damage. Consistently, failing LV exhibited higher CAT activity and lower MDA content compared to those measured in the failing RV. This finding underlines the involvement and the contribution of RV on the pathophysiological process leading to end-stage heart failure, and, as recently pointed out , support for its further investigation.

The present results suggest a correlation between oxidative stress and activation of antioxidant enzymes both in the left and the right ventricle from failing hearts. Despite the difficulties related to the clarification of a molecular mechanism interpretation in human end-stage hearts, our findings support the hypothesis that this activation may be due to post-translation modifications, in particular through phoshorylation of Tyr residues. Although qualitatively similar changes occur in both chambers, RV seems to be less protected than LV against oxidative stress damage. In the paucity of basic knowledge on RV alterations, this finding provides new hints to the involvement of the RV in the pathophysiology of heart disease. In this perspective, our study is in keeping with the expectation that gathering information on RV maladaptation may translate into a better treatment and prevention of heart failure.

4. 3. Role of oxidative stress in end-stage human failing hearts secondary to mitochondrial cardiomyopathies

To better clarify the molecular mechanisms linking mtDNA mutations to cardiac hypertrophy and failure, we performed a study on failing hearts from 3 patients with $tRNA^{Ile}$ mutation-related MIC. We evaluated myocardial oxidative stress by assessing myocardial superoxide production, and activity of the antioxidant enzymes mitochondrial MnSOD and GPx. In collaboration with the Department of Experimental Medicine at "La Sapienza" University of Rome gene expression profiles of antioxidant enzymes were evaluated. Moreover, key regulators of mitochondrial biogenesis and cardiac energy metabolism to failing human hearts due to other causes and to non failing hearts were compared.

Emerging evidence points to energy derangement as a major culprit for development of cardiac hypertrophy and progression to heart failure, both in acquired and in inherited disease. In recent years, numerous studies using experimental models of pressure overload and in human FH have consistently demonstrated a myocardial shift from fatty acid oxidation toward glucose oxidation for energy production[276]. This metabolic switch is associated with the down-regulation of genes involved in mitochondrial biogenesis and fatty acid metabolism and is mediated by deactivation of the transcriptional regulator PPAR-α and its coactivator PGC-1α[277,278]. The increased reliance of hypertrophic myocytes on glycolytic pathways is likely finalized to reduce oxygen consumption; however, it may contribute to the progression of cardiac disease, possibly creating a relative energy-deficient state. In the study, we revealed that there was a specific metabolic gene expression profile in a cardiomyopathy caused by a significant derangement of the mitochondrial energy production pathway. As a matter of fact, a marked up-regulation of PPAR-α and its coactivator PGC-1α, along with a slight increase in the expression of PGC-1β, were observed. Accordingly, the induction of genes involved in fatty acid metabolism, glucose transport, and mitochondrial biogenesis was detected. This last change is consistent with a dramatic increase in mtDNA content per cell, as well as with histologic and ultrastructural features of marked mitochondrial proliferation. In contrast, down-regulation of the PPAR- α /PGC-1 α complex and their targets, as well as reduced expression of glucose transporters, was

observed in DCM and IHD from failing hearts, confirming previous observations[278]. Interestingly, the expression level of PGC-1 β showed opposite behaviour in DCM and IHD. These data suggest that the 2 homologues are regulated by different mechanisms in cardiac myocytes, as reported for brown adipose tissue[279]. The coordinated induction in bioenergetic gene expression observed in MIC is likely to represent a compensatory response to energy deficiency. A global defect of oxidative phosphorylation (OXPHOS) in MIC hearts, with very low activities of respiratory chain complexes I and IV (both containing mtDNA-encoded subunits), was previously observed[15]. Increase of mitochondrial biogenesis (i.e., an increase in mitochondrial mass and induction of OXPHOS gene as well as enzymes of intermediary metabolism) is a well known phenomenon in mitochondrial disorders. In skeletal muscle, mitochondrial proliferation has been shown to partly compensate for the respiratory dysfunction by maintaining overall ATP production[280]; the histopathologic hallmark of this phenomenon is the presence of an increased number of mitochondria, mostly in the subsarcolemmal region. However, in cardiac muscle, induction of mitochondrial biogenesis has been proposed as a maladaptive response. In fact, cardiac-specific induction of PGC-1α in mice results in cardiac dysfunction with morphologic features of myocyte mitochondrial proliferation and myofibrillar disorganization and loss. Intriguingly, both mitochondrial proliferation and cardiomyopathy are reversible upon cessation of transgene expression. The present findings parallel the features reported in that experimental model, suggesting that mitochondrial proliferation is linked to progressive cardiac dysfunction also in the human heart.

Histological analysis performed at the Department of Experimental Medicine, at Rome, showed an altered sarcomere alignment, suggesting that mitochondrial proliferation per se may possibly interfere with contractile function; this phenomenon is limited to cardiomyocytes: In fact, in skeletal muscle from patients, lack of morphologic evidence of mitochondrial proliferation correlates with normal muscle function[15]. This observation opens new perspectives on the complex issue of tissue specificity of homoplasmic mitochondrial mutations.

An interesting result of our present study is the observation of a more pronounced increase in myocardial ROS production in MIC compared with DCM and IHD. In our experimental conditions, NADPH oxidase was a major source of ROS in all failing

hearts, as previously reported[66]. However, the present results implicate both the mitochondrial respiratory chain and xanthine oxidase as a source of excessive superoxide. Thus, mitochondrial dysfunction may contribute to the increased oxidative stress both by mitochondrial-derived $O_2^{-\cdot}$ and by a reduction of ATP/adenosine monophosphate ratio, which in turn activates the xanthine oxidase pathways. A somewhat paradoxic observation in the present study relates to the observation of high levels of ROS in the presence of increased expression of UCP2 and UCP3 in MIC. In fact, UCPs are expected to dissipate the proton electrochemical gradient formed during mitochondrial respiration and generate heat instead of ATP, thus reducing mitochondrial superoxide production. On the other hand, this mechanism may also lead to an increase in mitochondrial oxygen consumption, thus amplifying the energy dysfunction observed in MIC. We may speculate that the increase in UCP expression in MIC is insufficient to decrease ROS production through the mechanism of uncoupling respiration, and, therefore, high levels of ROS are maintained. Alternatively, recent studies on adipose tissue and skeletal muscle suggest that UCPs are regulated at post-translational level[281]. Increased ROS production in MIC was not reflected by a parallel induction of antioxidant enzyme activity, despite a marked up-regulation of MnSOD and GPx genes. Similar results have been previously reported in human FH[210] and in a mouse model of MIC[16] and support the hypothesis that end-stage heart muscle is unable to respond to oxidative stress by adequately increasing antioxidant countermeasures. The increase in ROS production observed in MIC is of great interest because growing evidence has implicated ROS signalling in cardiac maladaptive remodelling. However, additional work is required to fully address this issue. A metabolic gene expression profile similar to MIC has been reported in the cardiomyopathy that develops in the context of diabetes. In that condition, increase of circulating free fatty acids may lead to activation of PPAR-α/PGC-1α complex, which in turn causes induction of mitochondrial biogenesis and fatty acid oxidation.

The present results suggest that mitochondrial biogenesis is a maladaptive response in MIC and, possibly, in other metabolic cardiomyopathies. Besides energy deficiency, mechanical interference with sarcomere alignment and contraction, increased oxidative stress, and uncoupled respiration are possible detrimental factors to myocyte function.

ACKNOWLEDGEMENTS

I want to especially thank my supervisors, Prof. Paolo Antonio Nassi and Prof. Chiara Nediani for their support and their helpful suggestions.

Special thanks to my co-workers, Riccardo Favilli and Valentina Bargelli, for their technical assistance.

I gratefully acknowledge Prof. Elisabetta Cerbai, from the Department of Preclinical and Clinical Pharmacology, University of Florence, and Prof. Giulia d'Amati and Dr. Carla Giordano, from the Department of Experimental Medicine and Pathology, "La Sapienza" University of Rome, for their experimental help.

SPECIAL THANKS

Desidero qui ringraziare tutte le persone che hanno contribuito in qualsiasi modo al raggiungimento di un così importante traguardo.

In primo luogo ringrazio la mia famiglia per avermi sostenuta in tutti i modi possibili, ma soprattutto emotivamente, durante gli anni del Dottorato. Posso tranquillamente dire che senza l'aiuto dei miei genitori questa tesi non sarebbe mai stata scritta, pertanto spero che anche loro possano dirsi soddisfatti del mio lavoro.

Ringrazio mille volte Francesco, per il suo sostegno morale, per il suo aiuto, la sua disponibilità, la sua dedizione, il suo affetto e per altri cento motivi che non elencherò qui, ma che di certo lui conosce bene.

Un pensiero speciale va sia a Dana che a Lucy, le mie due gatte, ma in particolar modo proprio a Dana, semplicemente per essere stata con me per dodici anni… e per tutte le sue fusa antistress.

Ringrazio Chiara che non ha soltanto svolto il ruolo di attento supervisore, ma si è dimostrata anche una cara amica capace di comprendermi, sostenermi nei momenti di bisogno e, soprattutto, sopportare i miei frequenti sbalzi d'umore.

Ringrazio il Prof. Paolo Nassi per la sua continua disponibilità, per gli utili consigli e per la pazienza dimostrata durante tutto il mio periodo di ricerca.

Poi, naturalmente, ci sono Giusy, Assia, Riccardo e Valentina, i miei preziosi compagni di laboratorio, amici e colleghi, che hanno condiviso con me una marea di

prove al bancone, gli orari più assurdi, i momenti di crisi e di gioia… e qualcuno di loro anche la laurea!

E, infine, ringrazio tutte le mie "Bighe" (Laura, Gemma, Valentina, Francesca, Silvia e Luisa), per i pranzi insieme e le risate in Dipartimento, per i discorsi "pesissimi" durante le pause caffè, per le imitazioni di Alberto e per il sostegno che ci siamo date nelle lunghe giornate di esperimenti!

Grazie, di cuore, a tutti quanti!

REFERENCES

1. McMurray JJ, Pfeffer MA. Heart failure. *Lancet*. 2005;365:1877-89.
2. Criteria Committee NYHA. Diseases of the heart and blood vessels. Nomenclature and criteria for diagnosis. *6th ed. Boston: Little, Brown and co*. 1964;114.
3. Hunt SA, Abraham WT, Chin MH, Feldman AM, Francis GS, Ganiats TG, Jessup M, Konstam MA, Mancini DM, Michl K, Oates JA, Rahko PS, Silver MA, Stevenson LW, Yancy CW, Antman EM, Smith SCJ, Adams CD, Anderson JL, Faxon DP, Fuster V, Halperin JL, Hiratzka LF, Jacobs AK, Nishimura R, Ornato JP, Page RL, Riegel B, American College of Cardiology, American Heart Association Task Force on Practice Guidelines, American College of Chest Physicians, International Society for Heart and Lung Transplantation, Heart Rhythm Society. ACC/AHA 2005 Guideline Update for the Diagnosis and Management of Chronic Heart Failure in the Adult: a report of the American College of Cardiology/American Heart Association Task Force on Practice Guidelines (Writing Committee to Update the 2001 Guidelines for the Evaluation and Management of Heart Failure): developed in collaboration with the American College of Chest Physicians and the International Society for Heart and Lung Transplantation: endorsed by the Heart Rhythm Society. *Circulation*. 2005;112:e154-235.
4. Martino T, Liu P, Sole M. Viral infection and the pathogenesis of dilated cardiomyopathy. *Circ Res*. 1994;74:182-8.
5. Ross J. Dilated cardiomyopathy: concepts derived from gene deficient and transgenicanimal models. *Circ J*. 2002;66:219-24.
6. Chinnery PF, Turnbull DM. Mitochondrial DNA and disease. *Lancet*. 1999;354 Suppl 1:SI17–21.

7. DiMauro S, Schon EA. Mitochondrial DNA mutations in human disease. *Am J Med Genet*. 2001;106:18-26.
8. Schon EA, Bonilla E, DiMauro S. Mitochondrial DNA mutations and pathogenesis. *J Bioenerg Biomembr*. 1997;29:131-49.
9. Wallace DC, Singh G, Lott MT, Hodge JA, Schurr TG, Lezza AM, Elsas LJ, Nikoskelainen EK. Mitochondrial DNA mutation associated with Leber's hereditary optic neuropathy. *Science*. 1988;242:1427-30.
10. Jun AS, Brown MD, Wallace DC. A mitochondrial DNA mutation at nucleotide pair 14459 of the NADH dehydrogenase subunit 6 gene associated with maternally inherited Leber hereditary optic neuropathy and dystonia. *Proc Natl Acad Sci USA*. 1994;91:6206-10.
11. Prezant TR, Agapian JV, Bohlman MC, Bu X, Oztas S, Qiu WQ, Arnos KS, Cortopassi GA, Jaber L, Rotter JI, et al. Mitochondrial ribosomal RNA mutation associated with both antibiotic-induced and non-syndromic deafness. *Nat Genet*. 1993;4:289-94.
12. Reid FM, Vernham GA, Jacobs HT. A novel mitochondrial point mutation in a maternal pedigree with sensorineural deafness. *Hum Mutat*. 1994;3:243-7.
13. Santorelli FM, Tessa A, D'Amati G, Casali C. The emerging concept of mitochondrial cardiomyopathies. *Am Heart J*. 2001;141:E1.
14. Hirano M, Davidson M, DiMauro S. Mitochondria and the heart. *Curr Opin Cardiol*. 2001;16:201-10.
15. Taylor RW, Giordano C, Davidson MD, d'Amati G, Bain H, Hayes CM, Leonard H, Barron MJ, Casali C, Santorelli FM, Hirano M, Lightowlers RN, DiMauro S, Turnbull DM. A homoplasmic mitochondrial tRNA mutation as a cause of maternally-inherited hypertrophic cardiomyopathy. *J Am Coll Cardiol*. 2003;41:1786-96.
16. Esposito LA, Melov S, Panov A, Cottrell BA, Wallace DC. Mitochondrial disease in mouse results in increased oxidative stress. *Proc Natl Acad Sci U S A*. 1999;96:4820-5.
17. Hansson A, Hance N, Dufour E, Rantanen A, Hultenby K, Clayton DA, Wibom R, Larsson NG. A switch in metabolism precedes increased mitochondrial

biogenesis in respiratory chaindeficient mouse hearts. *Proc Natl Acad Sci U S A*. 2004;101:3136-41.

18. Russell LK, Mansfield CM, Lehman JJ, Kovacs A, Courtois M, Saffitz JE, Medeiros DM, Valencik ML, McDonald JA, Kelly DP. Cardiac-specific induction of the transcriptional coactivator peroxisome proliferator-activated receptor gamma coactivator-1alpha promotes mitochondrial biogenesis and reversible cardiomyopathy in a developmental stage-dependent manner. *Circ Res*. 2004;94:525-33.
19. Sugden PH, Clerk A. Cellular mechanisms of cardiac hypertrophy. *J Mol Med*. 1998;76:725-46.
20. Sugden PH. Ras, Akt, and mechanotransduction in the cardiac myocyte. *Circ Res*. 2003;93:1179-92.
21. Clerk A, Aggeli IK, Stathopoulou K, Sugden PH. Peptide growth factors signal differentially through protein kinase C to extracellular signal-regulated kinases in neonatal cardiomyocytes. *Cell Signal*. 2006;18:225-35.
22. Clerk A, Cole SM, Cullingford TE, Harrison JG, Jormakka M, Valks DM. Regulation of cardiac myocyte cell death. *Pharmacol Ther*. 2003;97:223-61.
23. Kwon SH, Pimentel DR, Remondino A, Sawyer DB, Colucci WS. H_2O_2 regulates cardiac myocyte phenotype via concentration-dependent activation of distinct kinase pathways. *J Mol Cell Cardiol*. 2003;35:615-621.
24. Nelson DP, Setser E, Hall DG, Schwartz SM, Hewitt T, Klevitsky R, Osinska H, Bellgrau D, Duke RC, Robbins J. Proinflammatory consequences of transgenic Fas ligand expression in the heart. *J Clin Invest*. 2000;105:1199-1208.
25. Jeremias I, Kupatt C, Martin-Villalba A, Habazettl H, Schenkel J, Boekstegers P, Debatin KM. Involvement of CD95/Apo1/Fas in cell death after myocardial ischemia. *Circulation*. 2000;102:915-20.
26. Pretorius L, Owen KL, Jennings GL, McMullen JR. Promoting physiological hypertrophy in the failing heart. *Clin Exp Pharmacol Physiol*. 2004;35:438-41.
27. De Windt LJ, Lim HW, Taigen T, Wencker D, Condorelli G, Dorn GWI, Kitsis RN, Molkentin JD. Calcineurin-mediated hypertrophy protects cardiomyocytes from apoptosis in vitro and in vivo: an apoptosis-independent model of dilated heart failure. *Circ Res*. 2000;86:255-63.

28. Valks DM, Cook SA, Pham FH, Morrison PR, Clerk A, Sugden PH. Phenylephrine promotes phosphorylation of Bad in cardiac myocytes through the extracellular signal-regulated kinases 1/2 and protein kinase A. *J Mol Cell Cardiol*. 2002;34:749-63.

29. Hausenloy DJ, Yellon DM. New directions for protecting the heart against ischaemia-reperfusion injury: targeting the reperfusion Injury Salvage Kinase (RISK)-pathway. *Cardiovasc Res*. 2004;61:448-60.

30. Heineke J, Molkentin JD. Regulation of cardiac hypertrophy by intracellular signalling pathways. *Nat Rev Mol Cell Biol*. 2006;7:589-600.

31. Hausenloy DJ, Yellon DM. Survival kinases in ischemic preconditioning and postconditioning. *Cardiovasc Res*. 2006;70:240-53.

32. Wilkins BJ, Molkentin JD. Calcineurin and cardiac hypertrophy: where have we been? Where are we going? *J Physiol Rev*. 2002;541:1-8.

33. Matsui T, Rosenzweig A. Convergent signal transduction pathways controlling cardiomyocyte survival and function: the role of PI 3-kinase and Akt. *J Mol Cell Cardiol*. 2005;38:63-71.

34. Clerk A, Fuller SJ, Michael A, Sugden PH. Stimulation of "stress-regulated" mitogen-activated protein kinases (stress-activated protein kinases/c-Jun N-terminal kinases and p38-mitogen-activated protein kinases) in perfused rat hearts by oxidative and other stresses. *J Biol Chem*. 1998;273:7228-34.

35. Bogoyevitch MA, Ketterman AJ, Sugden PH. Cellular stresses differentially activate c-Jun N-terminal protein kinases and extracellular signal-regulated protein kinases in cultured ventricular myocytes. *J Biol Chem*. 1995;270:29710-7.

36. Bogoyevitch MA, Gillespie-Brown J, Ketterman AJ, Fuller SJ, Ben-Levy R, Ashworth A, Marshall CJ, Sugden PH. Stimulation of the stress-activated mitogen-activated protein kinases subfamilies in perfused heart. p38/RK mitogen-activated kinases and c-Jun N-terminal kinases are activated by ischemia-reperfusion. *Circ Res*. 1996;79:162-73.

37. Clerk A, Harrison JG, Long CS, Sugden PH. Pro-inflammatory cytokines stimulate mitogen-activated protein kinases, increase phosphorylation of c-Jun

and ATF2 and upregulate c-Jun protein in neonatal rat ventricular myocytes. *J Mol Cell Cardiol*. 1999;31:2087-99.

38. Stanton LW, Garrard LJ, Damm D, Garrick BL, Lam A, Kapoun AM, Zheng Q, Protter AA, Schreiner GF, White RT. Altered patterns of gene expression in response to myocardial infarction. *Circ Res*. 2000;86:939-45.
39. Kukielka GL, Youker KA, Michael LH, Kumar AG, Ballantyne CM, Smith CW, Entman ML. Role of early reperfusion in the induction of adhesion molecules and cytokines in previously ischemic myocardium. *Moll Cell Biochem*. 1995;147:5-12.
40. Roy S, Khanna S, Kuhn DE, Rink C, Williams WT, Zweier JL, Sen CK. Transcriptome analysis of the ischemia-reperfused remodeling myocardium: temporal changes in inflammation and extracellular matrix. *Physiol Genomics*. 2006;25:367-74.
41. Tiret L, Godefroy T, Lubos E, Nicaud V, Tregouet DA, Barbaux S, Schnabel R, Bickel C, Espinola-Klein C, Poirier O, Perret C, Münzel T, Rupprecht HJ, Lackner K, Cambien F, Blankenberg S. Genetic analysis of the interleukin-18 system highlights the role of the interleukin-18 gene in cardiovascular disease. *Circulation*. 2005;112:643-50.
42. Zidar N, Dolenc-Strazar Z, Jeruc J, Strajer D. Immunohistochemical expression of activated caspase-3 in human myocardial infarction. *Virchows Arch*. 2005:1-5.
43. Kruidering M, Evan GI. Caspase-8 in apoptosis: the beginning of "the end"? *IUBMB Life*. 2000;50:85-90.
44. Omura T, Yoshiyama M, Takeuchi K, Hanatani A, Kim S, Yoshida K, Izumi Y, Iwao H, Yoshikawa J. Differences in time course of myocardial mRNA expression in non-infarcted myocardium after myocardial infarction. *Basic Res Cardiol*. 2000;95:316-23.
45. Hunter JJ, Chien KR. Signaling pathways for cardiac hypertrophy and failure. *N Engl J Med*. 1999;341:1276-83.
46. Giordano FJ. Oxygen, oxidative stress, hypoxia, and heart failure. *J Clin Invest*. 2005;115:500-8.

47. McMurray J, Chopra M, Abdullah I, Smith WE, Dargie HJ. Evidence of oxidative stress in chronic heart failure in humans. *Eur Heart J*. 1993;14:1493-8.

48. Valgimigli M, Merli E, Malagutti P, Soukhomovskaia O, Cicchitelli G, Antelli A, Canistro D, Francolini G, Macrì G, Mastrorilli F, Paolini M, Ferrari R. Hydroxyl radical generation, levels of tumor necrosis factor-alpha, and progression to heart failure after acute myocardial infarction. *J Am Coll Cardiol*. 2004;43:2000-8.

49. Dhalla AK, Hill MF, Singal PK. Role of oxidative stress in transition of hypertrophy to heart failure. *J Am Coll Cardiol*. 1996;28:506-14.

50. Date MO, Morita T, Yamashita N, Nishida K, Yamaguchi O, Higuchi Y, Hirotani S, Matsumura Y, Hori M, Tada M, Otsu K. The antioxidant N-2-mercaptopropionyl glycine attenuates left ventricular hypertrophy in in vivo murine pressure-overload model. *J Am Coll Cardiol*. 2002;39:907-12.

51. Kinugawa S, Tsutsui H, Hayashidani S, Ide T, Suematsu N, Satoh S, Utsumi H, Takeshita A. Treatment with dimethylthiourea prevents left ventricular remodeling and failure after experimental myocardial infarction in mice: role of oxidative stress. *Circ Res*. 2000;87:392-8.

52. Sia YT, Lapointe N, Parker TG, Tsoporis JN, Deschepper CF, Calderone A, Pourdjabbar A, Jasmin JF, Sarrazin JF, Liu P, Adam A, Butany J, Rouleau JL. Beneficial effects of long-term use of the antioxidant probucol in heart failure in the rat. *Circulation*. 2002;105:2549-55.

53. Nediani C, Borchi E, Giordano C, Baruzzo S, Ponziani V, Sebastiani M, Nassi P, Mugelli A, d'Amati G, Cerbai E. NADPH oxidase-dependent redox signaling in human heart failure: relationship between the left and right ventricle. *J Mol Cell Cardiol*. 2007;42:826-34.

54. Sebastiani M, Giordano C, Nediani C, Travaglini C, Borchi E, Zani M, Feccia M, Mancini M, Petrozza V, Cossarizza A, Gallo P, Taylor RW, d'Amati G. Induction of mitochondrial biogenesis is a maladaptive mechanism in mitochondrial cardiomyopathies. *J Am Coll Cardiol*. 2007;50:1362-9.

55. Finkel T. Signal transduction by reactive oxygen species in non-phagocytic cells. *J Leukoc Biol*. 1999;65:337-40.

56. Li JM, Shah AM. Endothelial cell superoxide generation: regulation and relevance for cardiovascular pathophysiology. *Am J Physiol*. 2004;287:R1014-30.

57. Gao WD, Liu Y, Marban E. Selective effects of oxygen free radicals on excitationcontraction coupling in ventricular muscle: implications for the mechanism of stunned myocardium. *Circulation*. 1996;94:2597-604.

58. Seddon M, Looi YH, Shah AM. Oxidative stress and redox signalling in cardiac hypertrophy and heart failure. *Heart*. 2007;93:903-7.

59. Ide T, Tsutsui H, Hayashidani S, Kang D, Suematsu N, Nakamura K, Utsumi H, Hamasaki N, Takeshita A. Mitochondrial DNA damage and dysfunction associated with oxidative stress in failing hearts after myocardial infarction. *Circ Res*. 2001;88:529-35.

60. Berry CE, Hare JM. Xanthine oxidoreductase and cardiovascular disease: molecular mechanisms and pathophysiological implications. *J Physiol Rev*. 2004;555:589-606.

61. Verhaar MC, Westerweel PE, van Zonneveld AJ, Rabelink TJ. Free radical production by dysfunctional eNOS. *Heart*. 2004;90:494-5.

62. Dixon LJ, Morgan DR, Hughes SM, McGrath LT, El-Sherbeeny NA, Plumb RD, Devine A, Leahey W, Johnston GD, McVeigh GE. Functional consequences of endothelial nitric oxide synthase uncoupling in congestive cardiac failure. *Circulation*. 2003;107:1725-8.

63. Lambeth JD. NOX enzymes and the biology of reactive oxygen. *Nat Rev Immunol*. 2004;4:181-9.

64. Cave AC, Grieve DJ, Johar S, Zhang M, Shah AM. NADPH oxidase-derived reactive oxygen species in cardiac pathophysiology. *Philos Trans R Soc Lond B Biol Sci*. 2005;360:2327-34.

65. Li JM, Gall NP, Grieve DJ, Chen M, Shah AM. Activation of NADPH oxidase during progression of cardiac hypertrophy to failure. *Hypertension*. 2002;40:477-84.

66. Heymes C, Bendall JK, Ratajczak P, Cave AC, Samuel JL, Hasenfuss G, Shah AM. Increased myocardial NADPH oxidase activity in human heart failure. *J Am Coll Cardiol*. 2003;41:2164-71.

67. Maack C, Kartes T, Kilter H, Schafers HJ, Nickenig G, Bohm M, Laufs U. Oxygen free radical release in human failing myocardium is associated with increased activity of rac1-GTPase and represents a target for statin treatment. *Circulation*. 2003;108:1567-74.

68. Borchi E, Parri M, Papucci L, Becatti M, Nassi N, Nassi P, Nediani C. Role of NADPH oxidase in H9c2 cardiac muscle cells exposed to simulated ischemia-reperfusion. *J Cell Mol Med*. 2008;[Epub ahead of print].

69. Herrera E, Barbas C. Vitamin E: action, metebolism and perspectives. *J Physiol Biochem*. 2001;57:43-56.

70. Grieve DJ, Byrne JA, Siva A, Layland J, Johar S, Cave AC, Shah AM. Involvement of the NADPH oxidase isoform NOX2 in cardiac contractile dysfunction occurring in response to pressure-overload. *J Am Coll Cardiol*. 2006;47:817-26.

71. Johar S, Cave AC, Narayanapanicker A, Grieve DJ, Shah AM. Aldosterone mediates angiotensin II-induced interstitial cardiac fibrosis via a Nox2-containing NADPH oxidase. *FASEB J*. 2006;20:1546-8.

72. Bendall JK, Cave AC, Heymes C, Gall N, Shah AM. Pivotal role of a gp91 phox -containing NADPH oxidase in angiotensin II-induced cardiac hypertrophy in mice. *Circulation*. 2002;105:293-6.

73. Fukui T, Yoshiyama M, Hanatani A, Omura T, Yoshikawa J, Abe Y. Expression of p22-phox and gp91-phox, essential components of NADPH oxidase, increases after myocardial infarction. *Biochem Biophys Res Commun*. 2001;281:1200-6.

74. Engberding N, Spiekermann S, Schaefer A, Heineke A, Wiencke A, Müller M, Fuchs M, Hilfiker-Kleiner D, Hornig B, Drexler H, Landmesser U. Allopurinol attenuates left ventricular remodeling and dysfunction after experimental myocardial infarction: a new action for an old drug? *Circulation*. 2004;110:2175-9.

75. Batot G, Martel C, Capdeville N, Wientjes F, Morel F. Characterization of neutrophil NADPH oxidase activity reconstituted in a cell-free assay using specific monoclonal antibodies raised against cytochrome b_{558}. *Eur J Biochem*. 1995;234:208-15.

76. Segal A, Garcia R, Goldstone A, Cross A, Jones O. Cytochrome b-245 of neutrophilsis also present in human monocytes, macrophages and eosinophils. *Biochem J*. 1981;196:363-7.
77. Fridovich I. Superoxide dismutases. *Annu Rev Biochem*. 1975;44:147-59.
78. Baldridge CW, Gerard RW. The extra respiration of phagocytosis. *Am J Physiol Cell Physiol*. 1933;103:235-6.
79. MacLeod J. The role of oxygen in the metabolism and motility of human spermatozoa. *Am J Physiol Cell Physiol*. 1943;138:512-8.
80. Iyer GYN, Islam DMF, Quastel JH. Biochemical aspects of phagocytosis. *Nature*. 1961;192:535-42.
81. Rossi F, Zatti M. Biochemical aspects of phagocytosis in polymorphonuclear leucocytes. NADH and NADPH oxidation by the granules of resting and phagocytizing cells. *Experientia*. 1964;20:21-3.
82. Babior BM, Kipnes RS, Curnutte JT. Biological defense mechanisms. The production by leukocytes of superoxide, a potential bactericidal agent. *J Clin Invest*. 1973;52:741-4.
83. Babior BM, Curnutte JT, Kipnes BS. Pyridine nucleotide-dependent superoxide production by a cell-free system from human granulocytes. *J Clin Invest*. 1975;56:1035-42.
84. Berendes H, Bridges RA, Good RA. A fatal granulomatosus of childhood: the clinical study of a new syndrome. *Minn Med*. 1957;40:309-12.
85. Babior B. NADPH oxidase: an update. *Blood*. 1999;93:1464-76.
86. Roos D, de Boer M, Kuribayashi F, Meischl C, Weening R, Segal A, Ahlin A, Nemet K, Hossle J, Bernatowska-Matuszkiewicz E, Middleton-Price H. Mutations in the X-linked and autosomal recessive forms of chronic granulomatous disease. *Blood*. 1996;87:1663-81.
87. Babior B, Woodman R. Chronic granulomatous disease. *Semin Hematol*. 1990;27:247-59.
88. Segal AW, Jones OT. Novel cytochrome b system in phagocytic vacuoles of human granulocytes. *Nature*. 1978;276:515-7.

89. Segal AW, Jones OT, Webster D, Allison AC. Absence of a newly described cytochrome b from neutrophils of patients with chronic granulomatous disease. *Lancet*. 1978;2:446-9.

90. Royer-Pokora B, Kunkel LM, Monaco AP, Goff SC, Newburger PE, Baehner RL, Cole FS, Curnutte JT, Orkin SH. Cloning the gene for an inherited human disorder– chronic granulomatous disease–on the basis of its chromosomal location. *Nature*. 1986;322:32-8.

91. Teahan C, Rowe P, Parker P, Totty N, Segal AW. The X-linked chronic granulomatous disease gene codes for the beta-chain of cytochrome b-245. *Nature*. 1987;327:720-1.

92. Geizt M, Leto T. The Nox Family of the NAD(P)H oxidases: host defence and bejond. *J Biol Chem*. 2004;279:51715-18.

93. Suh YA, Arnold RS, Lassegue B, Shi J, Xu X, Sorescu D, Chung AB, Griendling KK, Lambeth JD. Cell transformation by the superoxide-generating oxidase Mox1. *Nature*. 1999;401:79-82.

94. Banfi B, Molnar G, Maturana A, Steger K, Hegedus B, Demaurex N, Krause KH. A Ca2+-activated NADPH oxidase in testis, spleen, and lymph nodes. *J Biol Chem*. 2001;276:37594–601.

95. Cheng G, Cao Z, Xu X, van Meir EG, Lambeth JD. Homologs of gp91phox: cloning and tissue expression of Nox3, Nox4, and Nox5. *Gene*. 2001;269:131-40.

96. Geiszt M, Kopp JB, Varnai P, Leto TL. Identification of renox, an NAD(P)H oxidase in kidney. *Proc Natl Acad Sci*. 2000;97:8010-4.

97. Kikuchi H, Hikage M, Miyashita H, Fukumoto M. NADPH oxidase subunit, gp91phox homologue, preferentially expressed in human colon epithelial cells. *Gene*. 2000;254: 237-43.

98. Shiose A, Kuroda J, Tsuruya K, Hirai M, Hirakata H, Naito S, Hattori M, Sakaki Y, Sumimoto H. A novel superoxide-producing NAD(P)H oxidase in kidney. *J Biol Chem*. 2001;276:1417-23.

99. Yang S, Madyastha P, Bingel S, Ries W, Key L. A new superoxide-generating oxidase in murine osteoclasts. *J Biol Chem*. 2001;276:5452-8.

100. Li JM, Shah AM. Mechanism of endothelial cell NADPH oxidase activation by angiotensin II. Role of the p47phox subunit. *J Biol Chem*. 2003;278:12094-100.

101. Frey RS, Rahman A, Kefer JC, Minshall RD, Malik AB. PKCzeta regulates TNF-alpha-induced activation of NADPH oxidase in endothelial cells. *Circ Res*. 2002;90:1012-9.

102. Gorlach A, Brandes RP, Nguyen K, Amidi M, Dehghani F, Busse R. A $gp91^{phox}$ containing NADPH oxidase selectively expressed in endothelial cells is a major source of oxygen radical generation in the arterial wall. *Circ Res*. 2000;87:26–32.

103. Bayraktutan U, Blayney L, Shah AM. Molecular characterization and localization of the NAD(P)H oxidase components gp91-phox and p22-phox in endothelial cells. *Arterioscler Thromb Vasc Biol*. 2000;20:1903-11.

104. Xiao L, Pimentel DR, Wang J, Singh K, Colucci WS, Sawyer DB. Role of reactive oxygen species and NAD(P)H oxidase in alpha 1 -adrenoceptor signaling in adult rat cardiac myocytes. *Am J Physiol Cell Physiol*. 2002;282:C926-34.

105. Pagano P, Clark JK, Cifuentes-Pagano ME, Clark SM, Callis GM, Quinn MT. Localization of a constitutively active, phagocyte-like NADPH oxidase in rabbit aortic adventitia: enhancement by angiotensin II. *Proc Natl Acad Sci*. 1997;94:14483-8.

106. Lassègue B, Sorescu D, Szocs K, Yin Q, Akers M, Zhang Y, Grant SL, Lambeth JD, Griendling KK. Novel gp91 phox homologues in vascular smooth muscle cells: Nox1 mediates angiotensin II-induced superoxide formation and redox-sensitive signaling pathways. *Circ Res*. 2001;88:888-94.

107. Ago T, Kitazono T, Ooboshi H, Iyama T, Han YH, Takada J, Wakisaka M, Ibayashi S, Utsumi H, Iida M. Nox4 as the major catalytic component of an endothelial NAD(P)H oxidase. *Circulation*. 2004;109:227-33.

108. Byrne JA, Grieve DJ, Bendall JK, Li JM, Gove C, Lambeth JD, Cave AC, Shah AM. Contrasting roles of NADPH oxidase isoforms in pressure-overload versus angiotensin II-induced cardiac hypertrophy. *Circ Res*. 2003;93:802-5.

109. Li J, Stouffs M, Serrander L, Banfi B, Bettiol E, Charnay Y, Steger K, Krause KH, Jaconi ME. The NADPH oxidase NOX4 drives cardiac differentiation: role

in regulating cardiac transcription factors and MAP kinase activation. *Mol Biol Cell*. 2006;17:3978-88.

110. Clempus RE, Sorescu D, Dikalova AE, Pounkova L, Jo P, Sorescu GP, Schmidt HH, Lassègue B, Griendling KK. Nox4 is required for maintenance of the differentiated vascular smooth muscle cell phenotype. *Arterioscler Thromb Vasc Biol*. 2007;27:42-8.

111. Cucoranu I, Clempus RE, Dikalova AE, Phelan PJ, Ariyan S, Dikalov S, D S. NAD(P)H oxidase 4 mediates transforming growth factor-beta 1 -induced differentiation of cardiac fibroblasts into myofibroblasts. *Circ Res*. 2005;97:900-7.

112. De Deken X, Wang D, Many MC, Costagliola S, Libert F, Vassart G, Dumont JE, Miot F. Cloning of two human thyroid cDNAs encoding new members of the NADPH oxidase family. *J Biol Chem*. 2000;275:23227-33.

113. Dupuy C, Ohayon R, Valent A, Noel-Hudson MS, Deme D, Virion A. Purification of a novel flavoprotein involved in the thyroid NADPH oxidase. Cloning of the porcine and human cDNAs. *J Biol Chem*. 1999;274:37265-9.

114. Edens WA, Sharling L, Cheng G, Shapira R, Kinkade JM, Lee T, Edens HA, Tang X, Sullards C, Flaherty DB, Benian GM, Lambeth JD. Tyrosine crosslinking of extracellular matrix is catalyzed by Duox, a multidomain oxidase/peroxidase with homology to the phagocyte oxidase subunit gp91phox. *J Cell Biol*. 2001;154:879-91.

115. Kawahara T, Quinn MT, Lambeth JD. Molecular evolution of the reactive oxygen-generating NADPH oxidase (Nox/Duox) family of enzymes. *BMC Evolutionary Biology*. 2007;7.

116. Banfi B, Clark RA, Steger K, Krause KH. Two novel proteins activate superoxide generation by the NADPH oxidase NOX1. *J Biol Chem*. 2003;278:3510-13.

117. Banfi B, Maturana A, Jaconi S, Arnaudeau S, Laforge T, Sinha B, Ligeti E, Demaurex N, Krause KH. A mammalian H^+ channel generated through alternative splicing of the NADPH oxidase homolog NOH-1. *Science*. 2000;287:138-42.

118. Suh YA, Arnold RS, Lassegue B, Shi J, Xu X, Sorescu D, Chung A, Griendling KK, Lambeth JD. Cell transformation by the superoxide-generating oxidase Mox1. *Nature*. 1999;401:79-82.

119. Ambasta RK, Kumar P, Griendling KK, Schmidt HH, Busse R, Brandes RP. Direct interaction of the novel Nox proteins with p22phox is required for the formation of a functionally active NADPH oxidase. *J Biol Chem*. 2004;279:45935-41.

120. Cui XL, Brockman D, Campos B, Myatt L. Expression of NADPH oxidase isoform 1 (Nox1) in human placenta: involvement in preeclampsia. *Placenta*. 2006;27:422-31.

121. Janiszewski M, Lopes LR, Carmo AO, Pedro MA, Brandes RP, Santos CX, Laurindo FR. Regulation of NAD(P)H oxidase by associated protein disulfide isomerase in vascular smooth muscle cells. *J Biol Chem*. 2005;280:40813-9.

122. Ago T, Kitazono T, Kuroda J, Kumai Y, Kamouchi M, Ooboshi H, Wakisaka M, Kawahara T, Rokutan K, Ibayashi S, Iida M. NAD(P)H oxidases in rat basilar arterial endothelial cells. *Stroke*. 2005;36:1040-6.

123. Lee NK, Choi YG, Baik JY, Han SY, Jeong DW, Bae YS, Kim N, Lee SY. A crucial role for reactive oxygen species in RANKLinduced osteoclast differentiation. *Blood*. 2005;106:852-9.

124. Manea A, Raicu M, Simionescu M. Expression of functionally phagocyte-type NAD(P)H oxidase in pericytes: effect of angiotensin II and high glucose. *Biol Cell*. 2005;97:723-34.

125. Bedard K, Krause KH. The NOX family of ROS-generating NADPH oxidases: physiology and pathophysiology. *Physiol Rev*. 2007;87:245-313.

126. Chamulitrat W, Schmidt R, Tomakidi P, Stremmel W, Chunglok W, Kawahara T, Rokutan K. Association of gp91phox homolog Nox1 with anchorage-independent growth and MAP kinaseactivation of transformed human keratinocytes. *Oncogene*. 2003;22:6045-53.

127. Takeya R, Ueno N, Kami K, Taura M, Kohjima M, Izaki T, Nunoi H, Sumimoto H. Novel human homologues of p47phox and p67phox participate in activation of superoxide-producing NADPH oxidases. *J Biol Chem*. 2003;278:25234-46.

128. Takeya R, Sumimoto H. Molecular mechanismfor activation of superoxide-producing NADPH oxidase. *Mol. Cells*. 2003;16:271-7.

129. Geiszt M, Lekstrom K, Witta J, Leto TL. Proteins homologous to p47phox and p67phox support superoxide production by NAD(P)H oxidase 1 in colon epithelial cells. *J Biol Chem*. 2003;278:20006-12.

130. Kuribayashi F, Nunoi H, Wakamatsu K, Tsunawaki S, Sato K, Ito T, Sumimoto H. The adaptor protein p40phox as a positive regulator of the superoxide-producing phagocyte oxidase. *EMBO J*. 2002;21:6312-20.

131. Mizuki K, Kadomatsu K, Hata K, Ito T, Fan QW, Kage Y, Fukumaki Y, Sakaki Y, Takeshige K, Sumimoto H. Functional modules and expression of mouse p40phox and p67phox, SH3-domain-containing proteins involved in the phagocyte NADPH oxidase complex. *Eur J Biochem*. 1998;251:573-82.

132. Sumimoto H, Miyano K, Takeya R. Molecular composition and regulation of the Nox family NAD(P)H oxidases. *Biochem Biophys Res Commun*. 2005;338:677-86.

133. Ueyama T, Geiszt M, Leto TL. Involvement of rac1 in activation of multicomponent nox1- and nox3-based NADPH oxidases. *Mol Cell Biol*. 2006;26:2160-74.

134. Burritt JB, Foubert TR, Baniulis D, Lord CI, Taylor RM, Mills JS, Baughan TD, Roos D, Parkos CA, Jesaitis AJ. Functional epitope on human neutrophil flavocytochrome b558. *J Immunol*. 2003;170:6082-9.

135. Harper AM, Chaplin MF, Segal AW. Cytochrome b-245 from human neutrophils is a glycoprotein. *Biochem J*. 1985;227:783-8.

136. Finegold AA, Shatwell KP, Segal AW, Klausner RD, Dancis A. Intramembrane bis-heme motif for transmembrane electron transport conserved in a yeast iron reductase and the human NADPH oxidase. *J Biol Chem*. 1996;271:31021-4.

137. Clark RA, Leidal KG, Pearson DW, Nauseef WM. NADPH oxidase of human neutrophils. Subcellular localization and characterization of an arachidonate-activatable superoxide-generating system. *J Biol Chem*. 1987;262:4065-74.

138. Cross AR, Segal AW. The NADPH oxidase of professional phagocytes-prototype of the NOX electron transport chain systems. *Biochim Biophys Acta*. 2004;1657:1–22.

139. Borregaard N, Heiple JM, Simons ER, Clark RA. Subcellular localization of the b-cytochrome component of the human neutrophil microbicidal oxidase: translocation during activation. *J Cell Biol Cell*. 1983;97:52–61.

140. Kjeldsen L, Sengelov H, Lollike K, Nielsen MH, Borregaard N. Isolation and characterization of gelatinase granules from human neutrophils. *Blood*. 1994;83:1640-9.

141. Li JM, Shah AM. Intracellular localization and preassembly of the NADPH oxidase complex in cultured endothelial cells. *J Biol Chem*. 2002;277:19952-60.

142. Touyz RM, Chen X, Tabet F, Yao G, He G, Quinn MT, Pagano P, Schiffrin EL. Expression of a functionally active gp91phoxcontaining neutrophil-type NAD(P)H oxidase in smooth muscle cells from human resistance arteries: regulation by angiotensin II. *Circ Res*. 2002;90:1205-13.

143. Banfi B, Malgrange B, Knisz J, Steger K, Dubois-Dauphin M, Krause KH. NOX3: a superoxide-generating NADPH oxidase of the inner ear. *J Biol Chem*. 2004;279:46065-72.

144. Ueno N, Takeya R, Miyano K, Kikuchi H, Sumimoto H. The NADPH oxidase Nox3 constitutively produces superoxide in a p22phox-dependent manner: its regulation by oxidase organizers and activators. *J Biol Chem*. 2005;280:23328-39.

145. Kawahara T, Ritsick D, Cheng G, Lambeth JD. Point mutations in the proline-rich region of p22phox are dominant inhibitors of Nox1- and Nox2-dependent reactive oxygen generation. *J Biol Chem*. 2005;280:31859-69.

146. Cheng G, Ritsick D, Lambeth JD. Nox3 regulation by NOXO1, p47phox, p67phox. *J Biol Chem*. 2004;279:34250-5.

147. Kiss PJ, Knisz J, Zhang Y, Baltrusaitis J, Sigmund CD, Thalmann R, Smith RJ, Verpy E, Banfi B. Inactivation of NADPH oxidase organizer 1 results in severe imbalance. *Curr Biol*. 2006;16:208-13.

148. Hilenski LL, Clempus RE, Quinn MT, Lambeth JD, Griendling KK. Distinct subcellular localizations of Nox1 and Nox4 in vascular smooth muscle cells. *Arterioscler Thromb Vasc Biol*. 2004;24:677-83.

149. Byrne JA, Grieve DJ, Bendall JK, Li JM, Gove C, Lambeth JD, Cave AC, Shah AM. Contrasting roles of NADPH oxidase isoforms in pressure-overload versus angiotensin II-induced cardiac hypertrophy. *Circ Res*. 2003;93:802-5.

150. Colston JT, de la Rosa SD, Strader JR, Anderson MA, Freeman GL. H2O2 activates Nox4 through PLA2-dependent arachidonic acid production in adult cardiac fibroblasts. *FEBS Lett*. 2005;579:2533-40.

151. Cucoranu I, Clempus R, Dikalova A, Phelan PJ, Ariyan S, Dikalov S, Sorescu D. NAD(P)H oxidase 4 mediates transforming growth factor-beta1-induced differentiation of cardiac fibroblasts into myofibroblasts. *Circ Res*. 2005;97:900-7.

152. Yamagishi S, Nakamura K, Ueda S, Kato S, Imaizumi T. Pigment epithelium-derived factor (PEDF) blocks angiotensin II signaling in endothelial cells via suppression of NADPH oxidase: a novel anti-oxidative mechanism of PEDF. *Cell Tissue Res*. 2005;320:437-45.

153. Hwang J, Kleinhenz DJ, Lassegue B, Griendling KK, Dikalov S, Hart CM. Peroxisome proliferator-activated receptor-gamma ligands regulate endothelial membrane superoxide production. *Am J Physiol Cell Physiol*. 2005;288:C899-905.

154. Martyn KD, Frederick LM, von Loehneysen K, Dinauer MC, Knaus UG. Functional analysis of Nox4 reveals unique characteristics compared to other NADPH oxidases. *Cell Signal*. 2005;28:28.

155. Gorin Y, Ricono JM, Kim NH, Bhandari B, Choudhury GG, Abboud HE. Nox4 mediates angiotensin II-induced activation of Akt/protein kinase B in mesangial cells. *Am J Physiol Renal Physiol Genomics*. 2003;285:F219-29.

156. Park HS, Jung HY, Park EY, Kim J, Lee WJ, Bae YS. Cutting edge: direct interaction of TLR4 with NAD(P)H oxidase 4 isozyme is essential for lipopolysaccharide-induced production of reactive oxygen species and activation of NF-kappa B. *J Immunol*. 2004;173:3589-93.

157. Banfi B, Tirone F, Durussel I, Knisz J, Moskwa P, Molnar GZ, Krause KH, Cox JA. Mechanism of Ca^{2+} activation of the NADPH oxidase 5 (NOX5). *J Biol Chem*. 2004;279:18583-91.

158. Bjorkman U, Ekholm R. Generation of H2O2 in isolated porcine thyroid follicles. *Endocrinology*. 1984;115:392-8.

159. De Deken X, Wang D, Dumont JE, Miot F. Characterization of ThOX proteins as components of the thyroid H(2)O(2)-generating system. *Exp Cell Res*. 2002;273:187-96.

160. Morand S, Chaaraoui M, Kaniewski J, Deme D, Ohayon R, Noel-Hudson MS, Virion A, Dupuy C. Effect of iodide on nicotinamide adenine dinucleotide phosphate oxidase activity and Duox2 protein expression in isolated porcine thyroid follicles. *Endocrinology*. 2003;144:1241-8.

161. Park SM, Chatterjee VK. Genetics of congenital hypothyroidism. *J Med Genet*. 2005;42:379-89.

162. Vigone MC, Fugazzola L, Zamproni I, Passoni A, Di Candia S, Chiumello G, Persani L, Weber G. Persistent mild hypothyroidism associated with novel sequence variants of the DUOX2 gene in two siblings. *Hum Mutat*. 2005;26:395.

163. Ameziane-El-Hassani R, Morand S, Boucher JL, Frapart YM, Apostolou D, Agnandji D, Gnidehou S, Ohayon R, Noel-Hudson MS, Francon J, Lalaoui K, Virion A, Dupuy C. Dual oxidase-2 has an intrinsic Ca^{2+}-dependent H_2O_2-generating activity. *J Biol Chem*. 2005;280:30046-54.

164. Grasberger H, Refetoff S. Identification of the maturation factor for dual oxidase: evolution of an eukaryotic operon equivalent. *J Biol Chem*. 2006;281:18269-72.

165. Bokoch GM, Diebold BA. Current molecular models for NADPH oxidase regulation by Rac GTPase. *Blood*. 2002;100:2692-6.

166. Dusi S, Donini M, Rossi F. Mechanisms of NADPH oxidase activation: translocation of $p40^{phox}$, Rac1 and Rac2 from the cytosol to the membranes in human neutrophils lacking $p47^{phox}$ or $p67^{phox}$. *Biochem J*. 1996;314:409-12.

167. Heyworth PG, Curnutte JT, Nauseef WM, Volpp BD, Pearson DW, Rosen H, Clark RA. Neutrophil nicotinamide adenine dinucleotide phosphate oxidase assembly. Translocation of p47phox and p67phox requires interaction between $p47^{phox}$ and cytochrome b_{558}. *J Clin Invest*. 1991;87:352-6.

168. Kami K, Takeya R, Sumimoto H, Kohda D. Diverse recognition of non-PxxP peptide ligands by the SH3 domains from p67^{phox}, Grb2 and Pex13p. *EMBO J*. 2002;21:4268-76.

169. Leto TL, Adams AG, de Mendez I. Assembly of the phagocyte NADPH oxidase: binding of Src homology 3 domains to proline-rich targets. *Proc Natl Acad Sci*. 1994;91:10650-4.

170. Ago T, Nunoi H, Ito T, Sumimoto H. Mechanism for phosphorylation-induced activation of the phagocyte NADPH oxidase protein p47^{phox}. Triple replacement of serines 303, 304, and 328 with aspartates disrupts the SH3 domain-mediated intramolecular interaction in p47^{phox}, thereby activating the oxidase. *J Biol Chem*. 1999;274:33644-53.

171. El Benna J, Faust LP, Babior BM. The phosphorylation of the respiratory burst oxidase component p47^{phox} during neutrophil activation. Phosphorylation of sites recognized by protein kinase C and by proline-directed kinases. *J Biol Chem*. 1994;269:23431-6.

172. Rotrosen D, Leto TL. Phosphorylation of neutrophil 47-kDa cytosolic oxidase factor. Translocation to membrane is associated with distinct phosphorylation events. *J Biol Chem*. 1990;265:19910-5.

173. Karathanassis D, Stahelin RV, Bravo J, Perisic O, Pacold CM, Cho W, Williams RL. Binding of the PX domain of p47(phox) to phosphatidylinositol 3,4-bisphosphate and phosphatidic acid is masked by an intramolecular interaction. *EMBO J*. 2002;21:5057-68.

174. Heyworth PG, Bohl BP, Bokoch GM, Curnutte JT. Rac translocates independently of the neutrophil NADPH oxidase components p47phox and p67phox. Evidence for its interaction with flavocytochrome b558. *J Biol Chem*. 1994;269:30749-52.

175. Dang PMC, Babior BM, Smith RM. NADPH dehydrogenase activity of p67^{phox}, a cytosolic subunit of the leukocyte NADPH oxidase. *Biochemistry*. 1999;271:22578-82.

176. Noda Y, Kohjima M, Izaki T, Ota K, Yoshinaga S, Inagaki F, Ito T, Sumimoto H. Molecular Recognition in Dimerization between PB1 Domains. *J Biol Chem*. 2003;278:43516-24.

177. Sathyamoorthy M, de Mendez I, Adams AG, Leto TL. $p40^{phox}$ down-regulates NADPH oxidase activity through interactions with its SH3 domains. *J Biol Chem*. 1997;272:9141-6.

178. Duerrschmidt N, Wippich N, Goettsch W, Broemme HJ, Morawietz H. Endothelin-1 induces NAD(P)H oxidase in human endothelial cells. *Biochem Biophys Res Commun*. 2000;269:713-7.

179. Ushio-Fukai M, Tang Y, Fukai T, Dikalov SI, Ma Y, Fujimoto M, Quinn MT, Pagano PJ, Johnson C, W AR. Novel role of gp91(phox)-containing NAD(P)H oxidase in vascular endothelial growth factor-induced signaling and angiogenesis. *Circ Res*. 2002;91:1160-7.

180. Bae YS, Sung JY, Kim OS, Kim YJ, Hur KC, Kazlauskas A, Rhee SG. Plateled-derived growth factor-induced H2O2 production requires the activation of phosphatidylinositol 3-kinase. *J Biol Chem*. 2000;275:10527-31.

181. Park HS, Lee SH, Park D, Lee SL, Ryu SH, Lee WJ, Rhee SG, Bae YS. Sequential activation of PI3K, beta-Pix, Rac1, and Nox1 in growth factor-induced production of H_2O_2. *Mol Cell Biol*. 2004;24:4384-94.

182. Kashiwagi A, Shinozaki K, Nishio Y, Maegawa H, Maeno Y, Kanazawa A, Kojima H, Haneda M, Hidaka H, Yasuda H, Kikkawa R. Endothelium-specific activation of NAD(P)H oxidase in aortas of exogenously hyperinsulinemic rats. *Am J Physiol*. 1999;277:E976-83.

183. Li JM, Mullen AM, Yun S, Wientjes F, Brouns GY, Thrasher AJ, Shah AM. Essential role of the NADPH oxidase subunit p47 phox in endothelial cell superoxide production in response to phorbol ester and tumor necrosis factor-alpha. *Circ Res*. 2002;90.

184. Hwang J, Ing MH, Salazar A, Lassègue B, Griendling K, Navab M, Sevanian A, Hsiai TK. Pulsatile versus oscillatory shear stress regulates NADPH oxidase subunit expression: implication for native LDL oxidation. *Circ Res*. 2003;93:1225-32.

185. Kim KS, Takeda K, Sethi R, Pracyk JB, Tanaka K, Zhou YF, Yu ZX, Ferrans VJ, Bruder JT, Kovesdi I, Irani K, Goldschmidt-Clermont P, Finkel T. Protection from reoxygenation injury by inhibition of rac1. *J Clin Invest*. 1998;101:1821-6.

186. Ellis GR, Anderson RA, Lang D, Blackman DJ, Morris RH, Morris-Thurgood J, McDowell IF, Jackson SK, Lewis MJ, Frenneaux MP. Neutrophil superoxide anion--generating capacity, endothelial function and oxidative stress in chronic heart failure: effects of short- and long-term vitamin C therapy. *J Am Coll Cardiol*. 2000;36:1474-82.

187. Li JM, Shah AM. Endothelial cell superoxide generation: regulation and relevance for cardiovascular pathophysiology. *Am J Physiol Regul Integr Comp Physiol*. 2004;287:R1014-30.

188. Griendling KK, Sorescu D, Ushio-Fukai M. NAD(P)H oxidase: role in cardiovascular biology and disease. *Circ Res*. 2000;86:494-501.

189. Griendling KK, Sorescu D, Lassegue B, Ushio-Fukai M. Modulation of protein kinase activity and gene expression by reactive oxygen species and their role in vascular physiology and pathophysiology. *Arterioscler Thromb Vasc Biol*. 2000;20:2175-83.

190. Wojnowski L, Kulle B, Schirmer M, Schluter G, Schmidt A, Rosenberger A, Vonhof S, Bickeböller H, Toliat MR, Suk EK, Tzvetkov M, Kruger A, Seifert S, Kloess M, Hahn H, Loeffler M, Nürnberg P, Pfreundschuh M, Trümper L, Brockmöller J, Hasenfuss G. NAD(P)H oxidase and multidrug resistance protein genetic polymorphisms are associated with doxorubicininduced cardiotoxicity. *Circulation*. 2005;112:3754-62.

191. Maytin M, Siwik DA, Ito M, Xiao L, Sawyer DB, Liao R, Colucci WS. Pressure overload-induced myocardial hypertrophy in mice does not require $gp91^{phox}$. *Circulation*. 2004;109:1168-71.

192. Wenzel S, Taimor G, Piper HM, Schluter KD. Redox-sensitive intermediates mediate angiotensin II-induced p38 MAP kinase activation, AP-1 binding activity, and TGF-beta expression in adult ventricular cardiomyocytes. *FASEB J*. 2001;15:2291-3.

193. Nakagami H, Takemoto M, Liao JK. NADPH oxidase-derived superoxide anion mediates angiotensin II-induced cardiac hypertrophy. *J Mol Cell Cardiol*. 2003;35:851-9.

194. Grote K, Flach I, Luchtefeld M, Akin E, Holland SM, Drexler H, Schieffer B. Mechanical stretch enhances mRNA expression and proenzyme release of

matrix metalloproteinase-2 (MMP-2) via NAD(P)H oxidase-derived reactive oxygen species. *Circ Res*. 2003;92:e80-6.

195. Luchtefeld M, Grote K, Grothusen C, Bley S, Bandlow N, Selle T, Strüber M, Haverich A, Bavendiek U, Drexler H, Schieffer B. Angiotensin II induces MMP-2 in a p47phox-dependent manner. *Biochem Biophys Res Commun*. 2005;328:183-8.
196. Hill MF, Singal PK. Antioxidant and oxidative stress changes during heart failure subsequent to myocardial infarction in rats. *Am J Pathol*. 1996;148:291-300.
197. Shiomi T, Tsutsui H, Matsusaka H, Murakami K, Hayashidani S, Ikeuchi M, Wen J, Kubota T, Utsumi H, Takeshita A. Overexpression of glutathione peroxidase prevents left ventricular remodeling and failure after myocardial infarction in mice. *Circulation*. 2004;109:544-9.
198. Krijnen PAJ, Meischl C, Hack CE, Meijer CJ, Visser CA, Roos D, Niessen H. Increased Nox2 expression in human cardiomyocytes after acute myocardial infarction. *J Clin Pathol*. 2003;56:194-9.
199. Zelko I, Mariani T, Folz R. Superoxide dismutase multigene family: a comparison of the CuZn-SOD (SOD1), Mn-SOD (SOD2), and EC-SOD (SOD3) gene structure, evolution, and expression. *Free Radic Biol Med*. 2002;33:337-49.
200. Bannister J, Bannister W, Rotilio G. Aspect and structure, function, and application of superoxide dismutase. *Crit Rev Biochem*. 1987;22:111-80.
201. Sandström J, Nilsson P, Karlsson K, Marklund SL. 10-fold increase in human plasma extracellular superoxide dismutase content caused by a mutation in heparin-binding domain. *J Biol Chem*. 1994;269:19163-6.
202. Marklund S. Distribution of CuZn superoxide dismutase and Mn superoxide dismutase in human tissues and extracellular fluids. *Acta Physiol Scand Suppl*. 1980;492:19-23.
203. Sun E, Xu H, Liu Q, Zhou J, Zuo P, Wang J. The mechanism for the effect of selenium supplementation on immunity. *Biol Trace Elem Res*. 1995;48:231-8.

204. Dieterich S, Bieligk U, Beulich K, Hasenfuss G, Prestle J. Gene expression of antioxidant enzymes in the human heart: increased expression of catalase in the end-stage failing heart. *Circulation*. 2000;101:33-9.

205. Baumer AT, Flesch M, Wang X, Shen Q, Feuerstein GZ, Bohm M. Antioxidative enzymes in human hearts with idiopathic dilated cardiomyopathy. *J Mol Cell Cardiol*. 2000;32:121-30.

206. Maier CM, Chan PH. Role of superoxide dismutases in oxidative damage and neurodegenerative disorders. *Neuroscientist*. 2002;8:323-34.

207. Liu D. The roles of free radicals in amyotrophic lateral sclerosis. *J Mol Neurosci*. 1996;7:159-67.

208. Beckman JS, Koppenol WH. Nitric oxide, superoxide, and peroxynitrite: the good, the bad, and ugly. *Am J Physiol*. 1996;271:C1424-37.

209. Byrne JA, Grieve DJ, Cave AC, Shah AM. Oxidative stress and heart failure. *Arch Mal Coeur Vaiss*. 2003;96:214-21.

210. Sam F, Kerstetter DL, Pimental DR, Mulukutla S, Tabaee A, Bristow MR, Colucci WS, Sawyer DB. Increased reactive oxygen species production and functional alterations in antioxidant enzymes in human failing myocardium. *J Card Fail*. 2005;11:473-80.

211. Radi R, Turrens JF, Chang LY, Bush KM, Crapo JD, Freeman BA. Detection of catalase in rat heart mitochondria. *J Biol Chem*. 1991;266.

212. Halliwell B, Gutteridge JMC. *(eds) Free Radicals in Biology and Medicine*. 2000;3rd edit. New York, NY: Oxford University Press.

213. Cao C, Ren X, Kharbanda S, Koleske A, Prasad KV, Kufe D. The ARG tyrosine kinase interacts with Siva-1 in the apoptotic response to oxidative stress. *J Biol Chem*. 2001;276:11465-8.

214. Cao C, Leng Y, Kufe D. Catalase activity is regulated by c-Abl and Arg in the oxidative stress response. *J Biol Chem*. 2003;278:29667-75.

215. Cao C, Leng Y, Li C, Kufe D. Functional interaction between the c-Abl and Arg protein-tyrosine kinases in the oxidative stress response. *J Biol Chem*. 2003;278:12961-7.

216. Cao C, Leng Y, Liu X, Yi Y, Li P, Kufe D. Catalase is regulated by ubiquitination and proteosomal degradation. Role of the c-Abl and Arg tyrosine kinases. *Biochemistry*. 2003;42:10348-53.

217. Sun X, Wu F, Datta R, Kharbanda S, Kufe D. Interaction between protein kinase C delta and the c-Abl tyrosine kinase in the cellular response to oxidative stress. *J Biol Chem*. 2000;275:7470-3.

218. Kruh GD, Perego R, Miki T, Aaronson SA. The complete coding sequence of arg defines the Abelson subfamily of cytoplasmic tyrosine kinases. *Proc Natl Acad Sci U S A*. 1990;87:5802-6.

219. de Haan JB, Bladier C, Griffiths P, Kelner M, O'Shea RD, Cheung NS, Bronson RT, Silvestro MJ, Wild S, Zheng SS, Beart PM, Hertzog PJ, Kola I. Mice with a homozygous null mutation for the most abundant glutathione peroxidase, Gpx1, show increased susceptibility to the oxidative stress-inducing agents paraquat and hydrogen peroxide. *J Biol Chem*. 1998;273:22528-36.

220. Brigelius-Flohe R. Tissue-specific functions of individual glutathione peroxidases. *Free Radic Biol Med*. 1999;27:951-65.

221. Ho YS, Magnenat JL, Bronson RT, Cao J, Gargano M, Sugawara M, Funk CD. Mice deficient in cellular glutathione peroxidase develop normally and show no increased sensitivity to hyperoxia. *J Biol Chem*. 1997;272:16644-51.

222. Cao C, Leng Y, Huang W, Liu X, Kufe D. Glutathione peroxidase 1 is regulated by the c-Abl and Arg tyrosine kinases. *J Biol Chem*. 2003;278:39609-14.

223. Seger R, Krebs EG. The MAPK signaling cascade. *FASEB J*. 1995;9:726-35.

224. Robinson MJ, Cobb MH. Mitogen-activated protein kinase pathways. *Curr Opin Cell Biol*. 1997;9:180-86.

225. Cohen P. The search for physiological substrates of MAP and SAP kinases in mammalian cells. *Trends Cell Biol*. 1997;7:353-61.

226. Tibbles LA, Woodgett JR. The stress-activated protein kinase pathways. *Cell Mol Life Sci*. 1999;55:1230-54.

227. Zhou G, Bao ZQ, Dixon JE. Components of a new human protein kinase signal transduction pathway. *J Biol Chem*. 1995;270:12665-9.

228. Matsuzawa A, Ichijo H. Stress-responsive protein kinases in redox-regulated apoptosis signaling. *Antioxid Redox Signal*. 2005;7:472-81.

229. Xia Z, Dickens M, Raingeaud J, Davis RJ, Greenberg ME. Opposing effects of ERK and JNK-p38 MAP kinases on apoptosis. *Science*. 1995;270:1326-31.

230. Kyriakis JM, Avruch J. Mammalian mitogen-activated protein kinase signal transduction pathways activated by stress and inflammation. *Physiol Rev*. 2001;81:807-69.

231. Sachsenmaier C, Radler-Pohl A, Zinck R, Nordheim A, Herrlich P, Rahmsdorf HJ. Involvement of growth factor receptors in the mammalian UVC response. *Cell*. 1994;78:963-72.

232. Knebel A, Rahmsdorf HJ, Ullrich A, Herrlich P. Dephosphorylation of receptor tyrosine kinases as target of regulation by radiation, oxidants or alkylating agents. *EMBO J*. 1996;15:5314-25.

233. Burdon RH. Superoxide and hydrogen peroxide in relation to mammalian cell proliferation. *Free Radic Biol Med*. 1995;18:775-94.

234. Wang X, Martindale JL, Holbrook NJ. Requirement for ERK activation in cisplatin-induced apoptosis. *J Biol Chem*. 2000;275:39435-43.

235. Guyton KZ, Liu Y, M G, Xu Q, Holbrook NJ. Activation of mitogen-activated protein kinase by H_2O_2. Role in cell survival following oxidant injury. *J Biol Chem*. 1996;271:4138-42.

236. Abe J, Takahashi M, Ishida M, Lee JD, Berk BC. c-Src is required for oxidative stress-mediated activation of big mitogen-activated protein kinase 1. *J Biol Chem*. 1997;272:20389-94.

237. Suzaki Y, Yoshizumi M, Kagami S, Koyama AH, Taketani Y, Houchi H, Tsuchiya K, Takeda E, Tamaki T. Hydrogen peroxide stimulates c-Src-mediated big mitogen-activated protein kinase 1 (BMK1) and the MEF2C signaling pathway in PC12 cells: potential role in cell survival following oxidative insults. *J Biol Chem*. 2002;277:9614-21.

238. Iordanov MS, Magun BE. Different mechanisms of c-Jun NH2-terminal kinase-1 (JNK1) activation by ultraviolet- B radiation and by oxidative stressors. *J Biol Chem*. 1999;274:25801-6.

239. Verheij M, Bose R, Lin XH, Yao B, Jarvis WD, Grant S, Birrer MJ, Szabo E, Zon LI, Kyriakis JM, Haimovitz-Friedman A, Fuks Z, Kolesnick RN.

Requirement for ceramide-initiated SAPK/JNK signalling in stress-induced apoptosis. *Nature*. 1996;380:75-9.

240. Galan A, Garcia-Bermejo ML, Troyano A, Vilaboa NE, de Blas E, Kazanietz MG, Aller P. Stimulation of p38 mitogen- activated protein kinase is an early regulatory event for the cadmium-induced apoptosis in human promonocytic cells. *J Biol Chem*. 2000;275:11418-24.
241. Han SJ, Choi KY, Brey PT, Lee WJ. Molecular cloning and characterization of a Drosophila p38 mitogen-activated protein kinase. *J Biol Chem*. 1998;273:369-74.
242. Cheng A, Chan SL, Milhavet O, Wang S, Mattson MP. p38 MAP kinase mediates nitric oxide-induced apoptosis of neural progenitor cells. *J Biol Chem*. 2001;276:43320-7.
243. Zhuang S, Demirs JT, Kochevar IE. p38 mitogenactivated protein kinase mediates bid cleavage, mitochondrial dysfunction, and caspase-3 activation during apoptosis induced by singlet oxygen but not by hydrogen peroxide. *J Biol Chem*. 2000;275:25939-48.
244. Borsello T, Clarke PG, Hirt L, Vercelli A, Repici M, Schorderet DF, Bogousslavsky J, Bonny C. A peptide inhibitor of c-Jun N-terminal kinase protects against excitotoxicity and cerebral ischemia. *Nat Med*. 2003;9:1180-6.
245. Adler V, Yin Z, Tew KD, Ronai Z. Role of redox potential and reactive oxygen species in stress signaling. *Oncogene*. 1999;18:6104-11.
246. Park HS, Lee JS, Huh SH, Seo JS, Choi EJ. Hsp72 functions as a natural inhibitory protein of c-Jun N-terminal kinase. *EMBO J*. 2001;20:446-56.
247. Fuchs SY, Adler V, Pincus MR, Z R. MEKK1/JNK signaling stabilizes and activates p53. *Proc Natl Acad Sci U S A*. 1998;95:10541-6.
248. Sanchez-Prieto R, Rojas JM, Taya Y, Gutkind JS. A role for the p38 mitogen-acitvated protein kinase pathway in the transcriptional activation of p53 on genotoxic stress by chemotherapeutic agents. *Cancer Res*. 2000;60:2464-72.
249. Di Salvo TG, Mathier M, Semigrain MJ, Dec GW. Preserved right ventricular ejection fraction predicts exercise capacity and survival in advanced heart failure. *J Am Coll Cardiol*. 1995;25:1143-53.

250. Brieke A, De Nofrio D. Right ventricular dysfunction in chronic dilated cardiomyopathy and heart failure. *Coron Artery Dis*. 2005;16:5-11.

251. Gavazzi A, Berzuini C, Campana C, Inserra C, Ponzetta M, Sebastiani R, Ghio S, Recusani F. Value of right ventricular ejection fraction in predicting short-term prognosis of patients with severe chronic heart failure. *J Heart Lung Transplant*. 1997;16:774-85.

252. Malliopoulou V, Xinaris C, Mourouzis I, Cokkinos A, Katsilambros N, Pantos C, Kardami E, Cokkinos D. High glucose protects embryonic cardiac cells against simulated ischemia. *Mol Cell Biochem*. 2006;284:87-93.

253. LeBel C, Ischiropoulos H, Bondy S. Evaluation of the probe 2',7'-dichlorofluorescin as an indicator of reactive oxygen species formation and oxidative stress. *Chem Res Toxicol*. 1992;5:227-31.

254. Berridge MV, Herst PM, Tan AS. Tetrazolium dyes as tools in cell biology: new insights into their cellular reduction. *Biotechnol Annu Rev*. 2005;11:127-52.

255. Gupte S, Kaminski P, Floyd B, Agarwal R, Ali N, Ahmad M, Edwards J, Wolin M. Cytosolic NADPH may regulate differences in basal Nox oxidase-derived superoxide generation in bovin coronary and pulmonary arteries. *Am J Physiol Heart Circ Physiol*. 2005;288:13-21.

256. Li J, Fan L, George V, Brooks G. Nox2 regulates endothelial cell cycle arrest and apoptosis via p21cip1 and p53. *Free Rad Biol Med*. 2007;43:976-86.

257. Miller A, Drummond G, Mast A, Shmidt H, Sobey C. Effect of Gender on NADPH-oxidase activity, expression, and function in the cerebral circulation: role of extrogen. *Stroke*. 2007;38:2142-9.

258. MacCarthy P, Grieve D, Li JM, Dunster C, Kelly F, Shah AM. Impaired endothelial regulation of ventricular relaxation in cardiac hypertrophy: role of reactive oxygen species and NADPH oxidase. *Circulation*. 2001;104:2967-74.

259. Folden D, Gupta A, Sharma A, Li S, Saari J, Ren J. Malondialdehyde inhibits cardiac contractile function in ventricular myocytes via a p38 mitogen-activated protein kinase-dependent mechanism. *Br J Pharmacol*. 2003;139:1310-6.

260. Bennett BL, Sasaky DT, Murray BW, O'Leary EC, Sakata ST, Xu W, Leisten JC, Motiwala A, Pierce S, Satoh Y, Bhagwat SS, Manning AM, Anderson DW.

P600125, an anthrapyrazolone inhibitor of Jun N-terminal kinase. *Proc Natl Acad Sci*. 2001;98:13681-6.

261. Hescheler J, Meyer R, Plant S, Krautwurst D, Rosenthal W, Schultz G. Morphological, biochemical, and electrophysiological characterization of a clonal cell (H9c2) line from rat heart. *Circ Res*. 1991;69:1476-86.
262. L'Ecuyer T, Horenstein MS, Thomas R, Vander Heide R. Anthracycline-induced cardiac injury using a cardiac cell line: potential for gene therapy studies. *Mol Genet Metab*. 2001;74:370-9.
263. Turner NA, Xia F, Azhar G, Zhang X, Liu L, Wei JY. Oxidative stress induces DNA fragmentation and caspase activation via the c-Jun NH2-terminal kinase pathway in H9c2 cardiac muscle cells. *J Mol Cell Cardiol*. 1998;30:1789-801.
264. Fu J, Lin G, Wu Z, Ceng B, Wu Y, Liang G, Qin G, Li J, Chiu I, Liu D. Antiapoptotic role for C1 inhibitor inischemia/reperfusion-induced myocardial cell injury. *Biochem Biophys Res Commun*. 2006;349:504-12.
265. Murdoch CE, Zhang M, Cave AC, Shah AM. NADPH oxidase-dependent redox signaling in cardiac hypertrophy, remodelling and failure. *Cardiovasc Res*. 2006;71:208-15.
266. Meischl C, Krijnen PA, Sipkens JA, Cillessen SA, Munoz IG, Okroj M, Ramska M, Muller A, Visser CA, Musters RJ, Simonides WS, Hack CE, Roos D, Niessen HW. Ischemia induces nuclear NOX2 expression in cardiomyocytes and subsequently activates apoptosis. *Apoptosis*. 2006;11:913-21.
267. Jung YS, Jung YS, Kim MY, Kim E. Identification of caspase-independent PKC epsilon - JNK/p38 MAPK signaling module in response to metabolic inhibition in H9c2 cells. *Jpn J Physiol*. 2004;54:23-9.
268. Rupin A, Paysant J, Sansilvestri-Morel P, Lembrez N, Lacoste JM, Cordi A, Verbeuren TJ. Role of NADPH oxidase-mediated superoxide production in the regulation of E-selectin expression by endothelial cells subjected to anoxia/reoxygenation. *Cardiovasc Res*. 2004;63:323-30.
269. Girotti AW. Lipid hydroperoxide generation, turnover, and effector action in biological systems. *J Lipid Res*. 1998;39:1529-42.

270. McLeod LL, Sevanian A. Lipid peroxidation and modification of lipid composition in an endothelial cell model of ischemia and reperfusion. *Free Radic Biol Med*. 1997;23:680-94.

271. Steenbergen C. The role of p38 mitogen-activated protein kinase in myocardial ischemia/reperfusion injury; relationship to ischemic preconditioning. *Basic Res Cardiol*. 2002;97:276-85.

272. Cook SA, Sugden PH, Clerk A. Activation of c-Jun N-terminal kinases and p38-mitogen-activated protein kinases in human heart failure secondary to ischaemic heart disease. *J Mol Cell Cardiol*. 1999;31:1429–34.

273. Qin F, Shite J, Liang CS. Antioxidants attenuate myocyte apoptosis and improve cardiac function in CHF: association with changes in MAPK pathways. *Am J Physiol: Heart Circ Physiol*. 2003;285:H822-32.

274. Gupte SA, Levine RJ, Gupte RS, Young ME, Lionetti V, Labinsky V, Floyd BC, Ojaimi C, Bellomo M, Wolin MS, Recchia FA. Glucose-6-phosphate dehydrogenase-derived NADPH fuels superoxide production in the failing heart. *J Mol Cell Cardiol*. 2006;41:340–9.

275. Voelkel NF, Quaife RA, Leinwand LA, Barst RJ, McGoon MD, Meldrum DR, Dupuis J, Long CS, Rubin LJ, Smart FW, Suzuki YJ, Gladwin M, Denholm EM, Gail DB. Right ventricular function and failure: report of a National Heart, Lung, and Blood Institute working group on cellular and molecular mechanisms of right heart failure. *Circulation*. 2006;114:1883–91.

276. Huss JM, Kelly DP. Mitochondrial energy metabolism in heart failure: a question of balance. *J Clin Invest*. 2005;115:547–55.

277. Razeghi P, Young ME, Alcorn JL, Moravec CS, Frazier OH, Taegtmeyer H. Metabolic gene expression in fetal and failing human heart. *Circulation*. 2001;104.

278. Barger PM, Brandt JM, Leone TC, Weinheimer CJ, Kelly DP. Deactivation of peroxisome proliferator-activated receptor-alpha (PPARalpha) during cardiac hypertrophic growth. *J Clin Invest*. 2000;105:1723-30.

279. Lin J, Puigserver P, Donovan J, Tarr P, Spiegelman BM. Peroxisome proliferator-activated receptor gamma coactivator 1beta (PGC-1beta), a novel

PGC-1-related transcription coactivator associated with host cell factor. *J Biol Chem*. 2002;277:1645-8.

280. Wredenberg A, Wibom R, Wilhelmsson H, Graff C, Wiener HH, Burden SJ, Oldfors A, Westerblad H, Larsson NG. Increased mitochondrial mass in mitochondrial myopathy mice. *Proc Natl Acad Sci U S A*. 2002;99:15066-71.

281. Sivitz W, Fink B, Donohoue P. Fasting and leptin modulate adipose and muscle uncoupling protein: divergent effects between messenger ribonucleic acid and protein expression. *Endocrinology*. 1999;140:1511-9.